PROCEEDINGS

OF THE

NATIONAL ACADEMY OF SCIENCES

INDIA

1962

Vol. XXXII SECTION – A Part III

NATIONAL ACADEMY OF SCIENCES, INDIA
ALLAHABAD

The *Proceedings of the National Academy of Sciences, India*, is published in two sections: Section A (Physical Sciences) and Section B (Biological Sciences). Four parts of each section are published annually (since 1960).

The Editorial Board in its work of examining papers received for publication is assisted, in an honorary capacity, by a large number of distinguished scientists. Papers are accepted from members of the Academy *in good standing*. In case of a joint paper, one of the authors must be a member of the Academy. The Academy assumes no responsibility for the statements and opinions advanced by the authors. The papers must conform strictly to the rules for publication of papers in the *Proceedings*. A total of 50 reprints are supplied free of cost to the author or authors. The authors may have any reasonable number of additional reprints at cost price, provided they give prior intimation while returning the proof.

Communications regarding contributions for publication in the *Proceedings*, books for review, subscriptions etc., should be sent to the General Secretary, National Academy of Sciences, India, 5, Lajpatrai Road Allahabad-2 (India).

Annual Subscription for both Sections: Rs. 65; for each Section: Rs. 35 (including Annual Number); Single Copy: Rs. 7.50; Annual Number Rs. 5

PROCEEDINGS
OF THE
NATIONAL ACADEMY OF SCIENCES
INDIA
1962

VOL. XXXII SECTION - A PART III

SYMPOSIUM
ON
SPECTROSCOPY

FOREWORD

This volume contains papers presented at the Symposium on Spectroscopy, sponsored by the National Academy of Sciences, India. The meeting took place during the 30th Annual Session of the Academy and was held at Allahabad during February 3-5, 1961. Workers who are engaged in different branches of spectroscopy were requested to present a resume of the recent development in their field of endeavour. Resume on other branches of spectroscopy like microwave spectroscopy, Raman spectra, radio frequency spectroscopy, theoretical aspects of spectroscopy, experimental techniques in spectroscopy could not be included in this volume. We hope to include these in a future volume.

It is my pleasure to acknowledge our indebtedness to those who gave their time and energy to the successful conclusion of the conference, in particular to the members of the Council of the Academy.

Department of Applied Physics
University of Allahabad
Allahabad

S. N. GHOSH
Chairman.

CONTENTS

SPECTRA EXCITED BY SHOCK WAVES

By

W. M. VAIDYA

National Physical Laboratory, New Delhi-12

[Received on 7th April, 1962]

With the advent of supersonic flight of aircraft, rockets and missiles, research on gases subjected to excitation in shock tubes[1] has received considerable impetus. The phenomenon has proved of interest not only from the aerodynamic standpoint but also the luminosity excited by the high temperature of the gas behind the shock front has provided an extremely useful source for spectroscopic investigations. Spectroscopic studies of the glow in shock waves have assisted aerodynamic research and also contributed substantially to our knowledge of the thermodynamic properties of the gases at high temperatures.

A typical experimental arrangement for the excitation and observation of the spectra in shock tubes is shown below. It is constructed from four lengths of two inch copper pipe. One three-foot section is used as the high pressure chamber, which could stand an operating pressure of 450 lbs./sq. in. A pipe union was used to hold the diaphragm, which consisted of a 0.002 inch thick Mylar film made by Dupont. When the pressure in the channel was approximately 10^{-1}mm Hg it was found that one layer of the Mylar film ruptured consistently at a pressure of 50−1 psia in the high pressure chamber. The membrane could be broken either by an excess pressure or by a plunger. For taking observations of the spectra, a quartz window was fixed at one end.

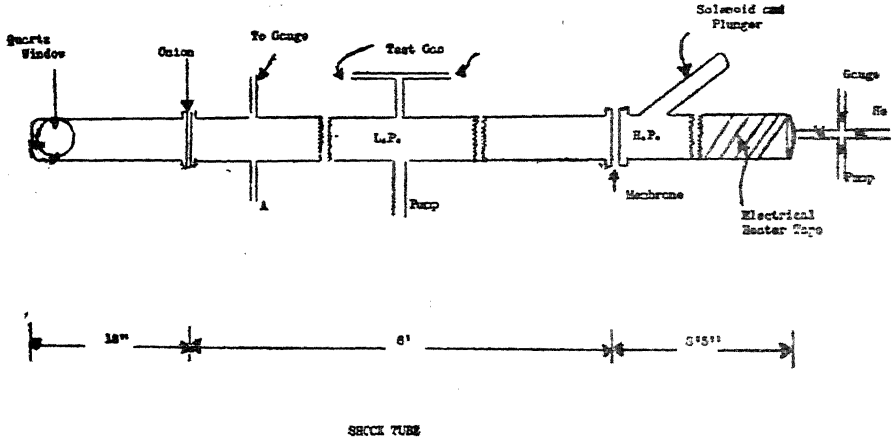

Fig. 1

The intensity of luminosity which causes the excitation of the spectra depends upon temperature attained in the shock tube and this can be calculated from thermodynamic considerations. For this purpose, it is necessary to examine the

space time history of the flow in the shock tube, shown in the x, t diagram Fig. 2 In this diagram (1) and (4) indicate the regions

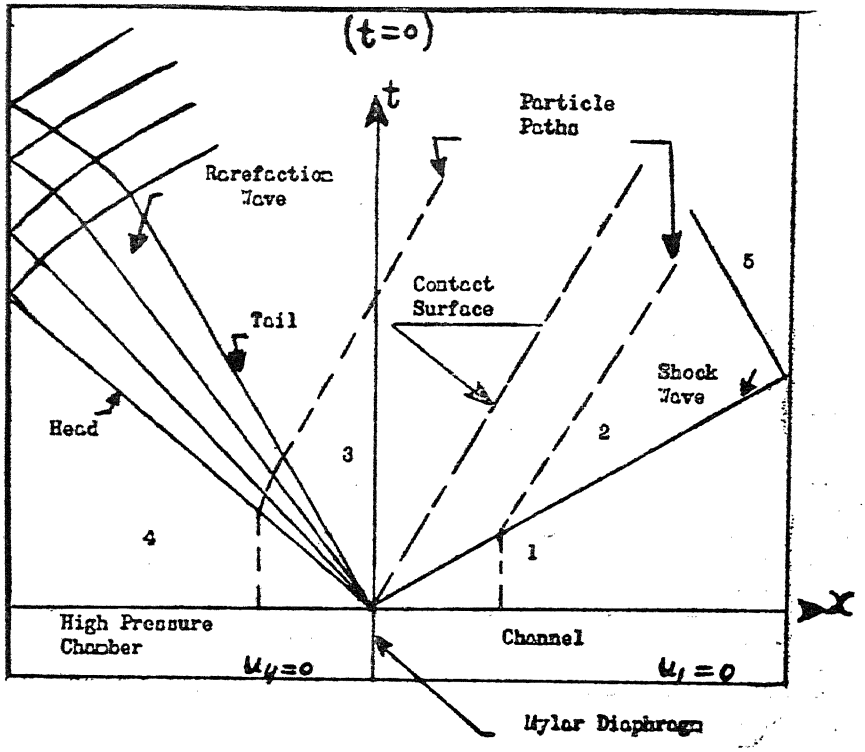

Fig. 2. Diagram of the (x, t) Plane

in the shock tube before rupture of the membrane. Upon rupture of the membrane the gas in the region (4) undergoes an isoentropic expansion and a compression wave, which quickly steepens to a shock wave, moves into the region (1). Simultaneously a rarefaction wave moves into the high pressure chamber. The shock wave is followed by a interface which separates the two gases and is called a Contact Surface, which may be regarded as a piston moving into the low pressure region at the flow velocity. The adiabatic compression of the gas in region (1) by the shock wave produces an increase in the temperature of the gas in region (2) between the shock wave and the contact surface. On reflection of the incident shock wave by the closed end of the tube into this region, the temperature in region (5), behind the reflected shock wave is approximately doubled. This high temperature behind the incident and reflected shock wave causes the gas behind the shock front to be excited to luminosity. The relationship between the various parameters is

$$\frac{P_4}{P_1}=\left[\frac{2\gamma_1}{\gamma_1+1}M_1^2-\frac{\gamma_1-1}{\gamma_1+1}\right]\left[\frac{1}{1-\frac{\gamma_4-1}{\gamma_1+1}\frac{a_1}{a_4}\left(M_1-\frac{1}{M_1}\right)}\right]^{\frac{2\gamma_4}{\gamma_4-1}} \tag{1}$$

$$\frac{T_2}{T_1}=\frac{1}{\alpha_1^2}\left[\frac{M_1^2}{\beta_1}-1\right]\left[\frac{1}{\beta_1\gamma_1M_1^2}+1\right] \tag{2}$$

and

$$\frac{T_5}{T_1} = \frac{1}{\alpha_1^2 M_1^2}\left[2(M_1^2-1)+\alpha_1 M_1^2\right]\left[2(M^2-1)+\alpha_1\right] \qquad (3)$$

$\frac{a_4}{a_1}$: Velocity of sound ratio

$\frac{P_4}{P_1}$ – Initial pressure ratio

$\frac{T_2}{T_1}$ – Ratio of the incident shock temperature to the initial temperature

$\frac{T_5}{T_1}$ – Ratio of the reflected shock temperature to the initial temperature

M_1 – Mach number

It will be seen from (3) that T_5 – the reflected shock temperature and T_2 – shock temperature depend upon the Mach number M_1, which in turn depends upon the pressure ration P_4/P_1 and gas constants, α_1 β and γ. γ is the ratio of the specific heats,

$$\alpha_1 = \frac{\gamma_1+1}{\gamma_1-1}; \quad \beta_1 = \frac{\gamma_1-1}{2\gamma_1}$$

Some of the typical spectra obtained in the shock tube are shown in Fig. 3. In this particular shock wave study, hydrogen was used as the driver gas at from 3–6 atm pressure and with pressures of from 1-20 mm, on the low pressure side, thus giving a pressure ratio of 1000 : 1. The Fig. 3a shows the spectrum of acetylene argon mixture, which shows the C_2 bands strongly superposed on the continuum

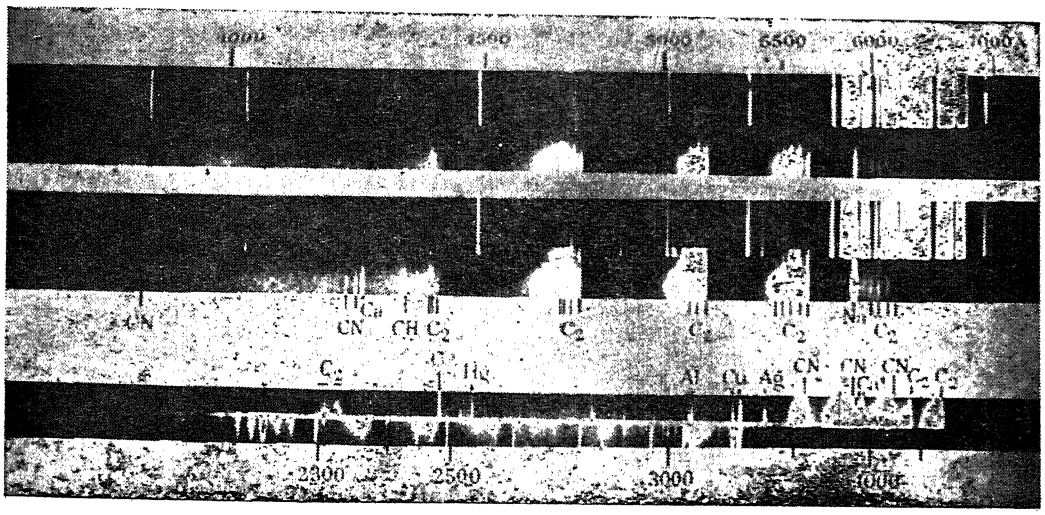

Fig. 3

Weak CN violet bands are also observed, the nitrogen coming from the argon as an impurity. The CH band at 4315 Å appears to be absent. The second spectrum (Fig. 3b) is that of methane argon mixture, which also gives strong C_2 and rather weaker continuum. CN is again present and in this case the CH band at 4315 Å is weakly but fairly definitely present. Carbon monoxide argon mixture (Fig. 3c) gave strong C_2 Swan bands and also the Mulliken band of C_2 at 2313 Å and the carbon line at 2478 Å. The normal discharge tube spectrum of CO, showing Third Positive and Angstrom bands, was not obtained; the Fourth Positive system, the resonance system of CO was not recorded.

In the conventional shock tube studies, the pressure ratio obtainable depends upon the strength of the walls of the tube. The maximum Mach number obtainable under these conditions is of the order of 10, resulting in the temperature of the order of 18000°K. A remarkable increase in the Mach number and consequently the temperature attained was been realised by utilising the controlled fusion reaction. This is essentially dependant upon electromagnetic acceleration of ionised gases. A typical experimental set up is shown in the Fig. 4.

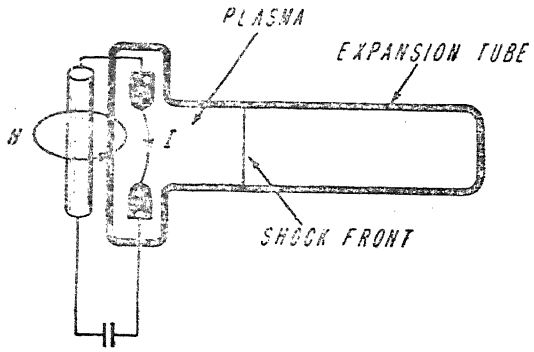

Fig. 4

The Mach numbers attained in electromagnetic shock tubes are of the order of 100–200, yielding temperatures to 30000°-50000°.

A few typical spectra obtained in electromagnetic shock tubes are shown in fig. 5.

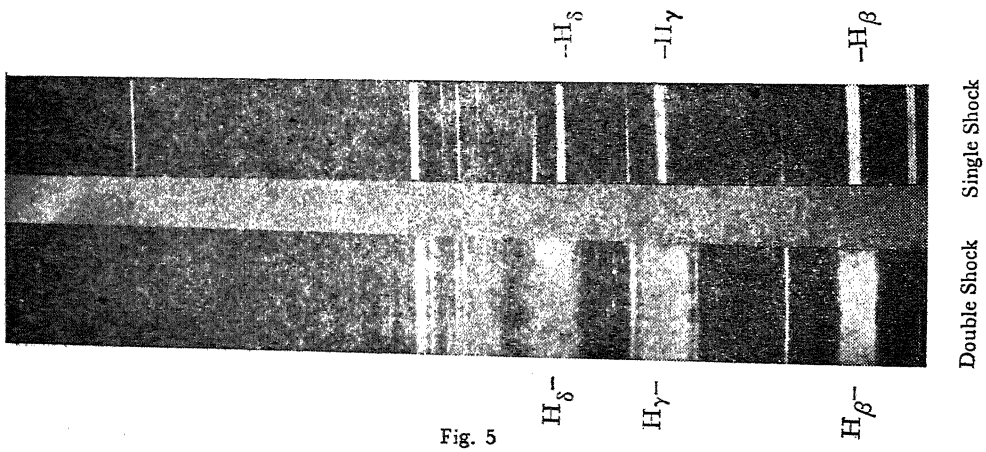

Fig. 5

Apart from the identification of the molecular species emitting the spectra, many interesting studies, regarding temperatures, electron density, time variation of spectra have been undertaken and yielded results of great significance.

REFERENCES

1. Clouston, J. G. & Gaydon A. G., *Proc. Roy. Soc.* **A. 248,** 429 (1958).

Fairbairn, A. R. & Gaydon A. G., *Nature*, **175,** 253 (1955).

Fairbairn, A. R. & Gaydon A. G., *Proc. Roy. Soc.* A. 239, 464 (1957).

Greene, E. F. & Horning, D. F , *J. Chem Phy.* 21, 617 (1953).

Greene, E. F., *J Am. Chem Soc.* **76,** 2127 (1954).

Hollyer. R. N, Hunting, A. G., Laporte, O. & Turner, E. B , *Phy. Rev.* **87,** 911 (1953).

Hollyer, R. N. Hunting, A. G., Laporte, O., & Turner, E. B., *Nature*, **171,** 395 (1953).

Johnson, I & Campbell, C. E., *J. Chem. Phys.* **27,** 316 (1957).

Keck, J, Camm J. & Kivel, B., *J. Chem. Phy.* **28,** 724 (1958).

Parkinson, W. H., & Nicholls, R. W., U. S. Air Force Cambridge Research Centre, Contract No. A. F. **19** (604)—4560. Scientific Report No. 1. University of Western Ontorio, Canada.

Petschek, H. E., Rose P. H., Gleck, H. S. Kane, A., Kantrowitz., A., *J. App. Phy.* **26,** 83 (1955)

Wurtter, W. H., Gleck, H. S. & Treanor, C. E. Q. M—997-A-1, Cornell Aeronautical Laboratory, Buffallo, New York, 1957.

Wurster, W. H. and Glick, H. S., *J. Chem. Phy.* **27;** 1218 (1957).

FLAME SPECTRA

By

W. M. VAIDYA

National Physical Laboratory, New Delhi-12

[Received on 7th April, 1962]

INTRODUCTION

A study of flame spectra is a valuable means of obtaining information about combustion processes and energy content of hot gases generated during combustion, which can occur under a wide variety of experimental conditions, for example-rockets, jet engines, internal combustion engines and so on. In such sources of great inaccessibility, spectroscopy is the only method which can provide data on the nature and behaviour of the radicals produced as a result of chemical reactions. To investigate the characteristics of these radicals appearing in inaccessible sources, it is not necessary to conduct experiments on these difficult sources themselves, since exactly the same radicals can be obtained under simpler conditions in the laboratory. Thus, if one wishes to study OH (Wates-vapour bands) bands appearing in the exhaust flames of jet engines, they can be more simply produced in the ordinary Bunsen flame. This has been a great advantage since it has been possible to understand combustion processes in rockets and jet engines by conducting spectroscopic experiments on simpler sources in the laboratory.

The most familiar example of flames is the Bunsen flame. By separating the two cones, combustion in the outer and inner cones can be followed separately. Such an arrangement is shown in the fig. 1. The flame separator consists of two

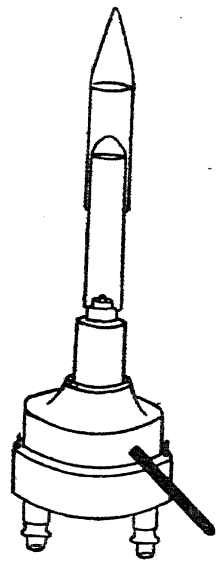

Fig. 1

concentric tubes, F and G, the inner tube, F, being mounted on the outer nozzle, D, of a blow-pipe. The outer tube, G, is made of quartz to permit observations in the ultra-violet. When the gas is introduced and first ignited it burns on the top of the outer tube with a luminous flame. On slowly increasing the air supply, the flame becomes non-luminous, develops two cones and the inner cone descends gradually and settles on the inner tube.

Instead of molecular oxygen as in air, it is possible to use atomic oxygen, obtained by passing a high voltage discharge through molecular oxygen at low pressure. This method follows the procedure originated by Wood[1] to obtain high proportion of atomic hydrogen to extend the Balmer spectrum to higher components in the Balmer series. An experimental set up for producing flames supported by atomic oxygen is shown in fig. 2. The pressure in the discharge is

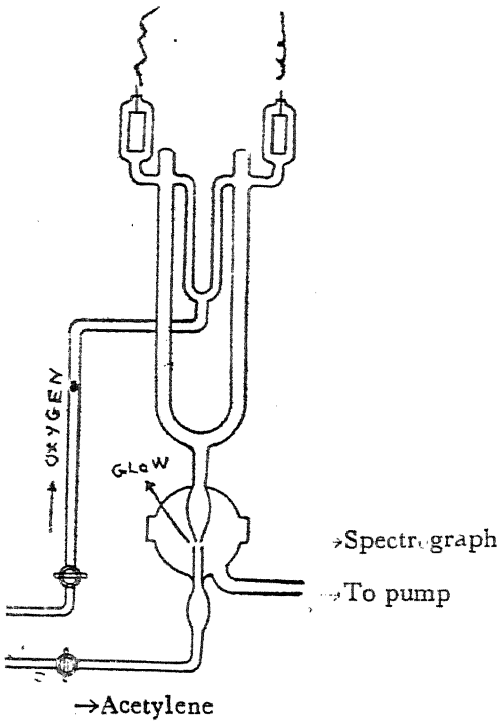

Fig. 2

0·5 mm to 1 mm and the secondary voltage is 5000V-8000V and secondary current 250-500 m amps. For the production of the flame no extra source of ignition is required ; as soon as atomic oxygen stream meets the combustible a glow is formed, which burns steadily.

Another method for the production of flames at low pressures is the technique extensively developed by Wolfard[2] and Gaydon & Wolfard[3]. As the pressure is reduced the quenching diameter increases and hence larger tubes are required

to maintain flames at low pressures. This entails the use of very fast pumps. The diameter of the chamber shown in the fig. 3 is about 10", while the inner tube on

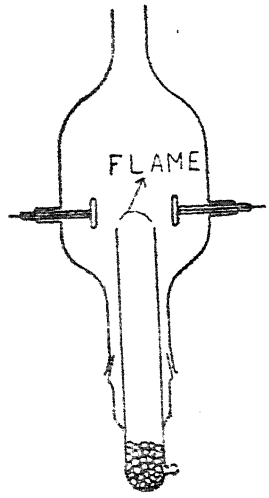

Fig. 3

the top of which the flame is situated can vary from 15 cms — 25 cms. These flames at low pressure have thick reaction zones, which enables detailed examination to be made.

Spectroscopic methods have been applied to flames in the internal combustion engine and exhaust flames of jets. A few typical photographs of flames are shown figs. 4, 5 & 6 and spectra obtained in these different sources are shown in the figs. 7, 8, 9 and 10.

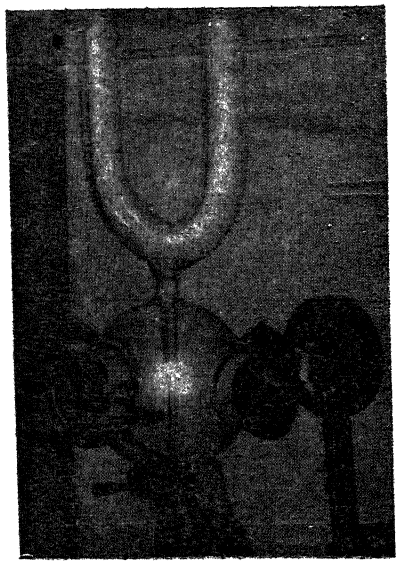

Fig 4. Glow in Atomic oxygen.

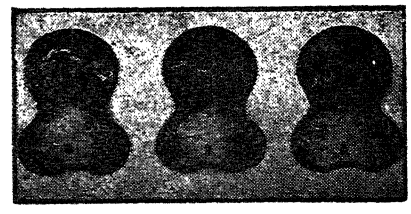

Fig. 5. Various regions distinctly differentiated on individual frames from three different explosions. A, Flame front; B, afterglow; C, non-inflamed charge.

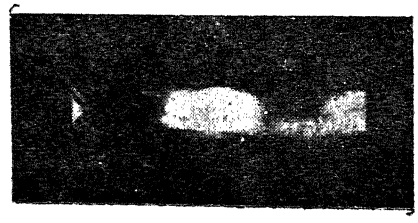

Fig. 6. Exhaust Flame (Rocket).

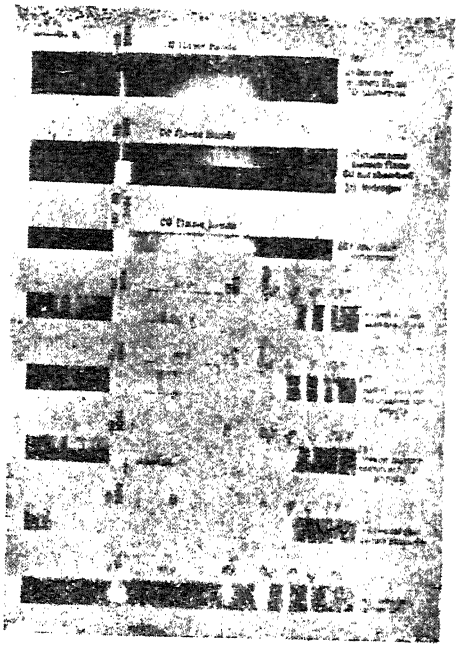

Fig. 7

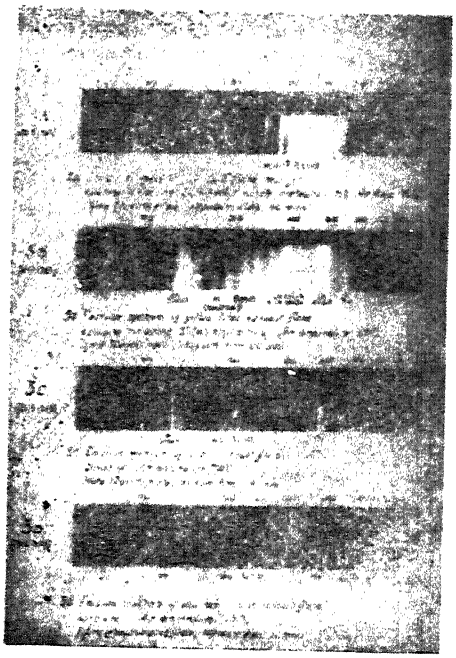

Fig. 9

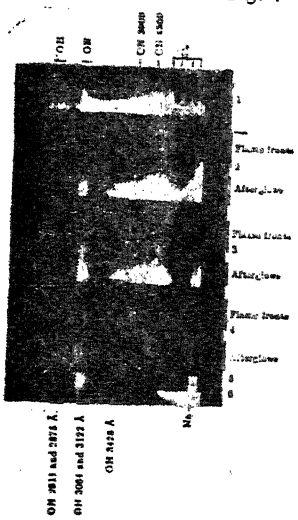

Fig. 8. Comparison of Spectrum of Gas-Air Bunsen Burner Flame with Spectra of several Fuels Burning in Engine under Nonknocking conditions.

1. Bunsen burner.
2. Benzene in engine.
3. Isooctane in engine.
4. Gasoline in engine.
5. Hydrogen afterglow in engine.
6. Hydrogen in engine ; no disk.

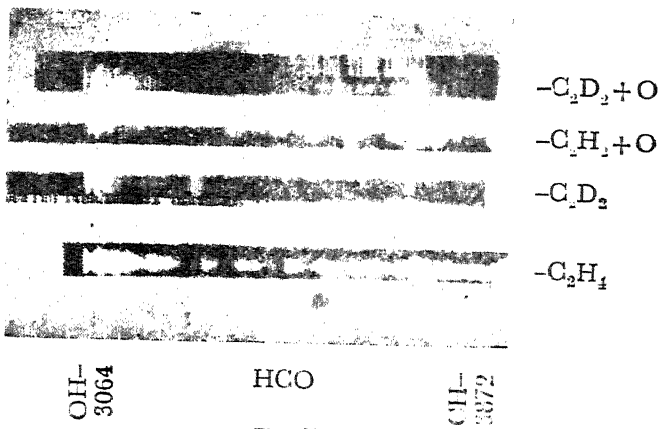

Fig. 10

In the outer cones are found the OH bands and the CO flame bands attributed to CO_2. The OH bands are also found in the inner cones of hydrocarbon flames, glows in atomic oxygen, jet exhaust fiames, flames in internal combustion engine and also the sun and the stars. This is one of the most reactive radicals and plays a prominent part in combustion processes. The important bands are located at λλ3064, 2934, 2811 etc.

Two other band systems, equally well known are the C_2 and CH. The C_2 bands have been recognised since early ninteenth century, but the nature of the emitter was not definitely fixed till the rotational analysis and the isotope effect firmly established the emitter of the bands as C_2 only some 30 years ago. The important band heads of C_2 are at λλ 6191, 5635, 5165, 4737 and 4382 and those of CH at λλ 4315 and 3872.

In addition to the well known bands of C_2, CH and OH found in the inner cones of hydrocarbon flames, they also show another band system, which is provisionally being attributed to HCO. The bands were first noticed in the inner cone of the Bunsen flame by Rassweiler and Withrow[4] in their studies of combustion in engines. It was however found that the bands appeared with much greater intensity and clarity in the inner cone of the ethylene flame burning in a flame separator.[5] From the vibrational analysis and the condition for their occurrence the bands were assigned to HCO. Another approach to the solution of the problem of the emitter was to detect isotope effect by utilising deuterium. This has been successfully done by obtaining the spectrum of deutero-acetylene glow interacting with atomic oxygen. A large number of isotopic bands have appeared in this flame and from the provisional analysis, it appears that the original assigment of HCO appears to be correct.

Spectroscopic methods of determining temperatures

Besides the identification of radicals, another aspect of spectroscopic analysis is the determination of temperatures from band intensity measurements. Thus, the intensity of a band is given by the expression

$$I_{v', v''} = \frac{64}{3} \pi^4 c N_{v'} \nu^4 \bar{R}e^2 \left[\int \psi'_{v'} \psi''_{v''} dr \right]^2$$

where c = the velocity of light

$N_{v'}$ = the number of molecules in the vibrational levels

ν = wave-number of the band

$\bar{R}e$ = average electronic transition moment

$\int \psi'_{v'} \psi''_{v''} dr$ = overlap integral.

[Transitional probability is proportional to the square of the overlap integral.]

Since the sum of the squares of the overlap integrals summed over all values of the vibrational quantum numbers of the upper or of the low state is equal to one,

$$\sum_{v''} \frac{I_{v' v''}}{\nu^4} \propto N_{v'}; \; N_{v'} \propto e^{-Go(v) hc/kT}$$

$$\log \sum_{v''} \frac{I_{v'v''}}{\nu^4} = C_1 - \frac{G'(v')\,hc}{kT}$$

from which T can be calculated.

If the distribution of excited molecules amongst the initial rotational levels for a band in emission is assumed to correspond to thermal equilibrium at an effective temperature θ, the intensity of the lines of one branch, say a R branch are given by

$$Int\ R(J'') = Ci_{R(J'')}\, e^{-B_{v'}J'(J'+1)/0{\cdot}7\theta}$$

where $i_{R(J'')}$ is the appropriate intensity factor.
Hence

$$\log\left(\frac{Int}{i}\right)_{R(J'')} = \log C - \frac{Bv'J'(J'+1)}{0{\cdot}7\theta}$$

If $\log\left(\frac{Int}{i}\right)_{R(J'')}$ is plotted against $J'(J'+1)$, a straight line is obtained, its slope is given by $Bv'/0{\cdot}7\theta$ from which the "effective rotational" temperature θ can be determined, knowing $B_{v'}$ from the analysis of the band structure.

It is possible to derive effective translational temperature by Doppler broadening. For hot gases the random movement of the molecules causes a broadening of the spectrum lines. The half-breadth b is given by

$$b = 2\sqrt{\log 2}\sqrt{2RT/Mc^2} = 0{\cdot}7\ 1{\cdot}10^{-6}\sqrt{\frac{T}{M}}\ \nu\ cm^{-1}$$

where M is the molecular weight, R the gas constant, c the velocity of high and ν, the wave number of the spectrum line. The experimental method involves the use of a Fabry-Perot interferometer crossed with a large spectrograph.

Interference fringes produced in a Jamin or Mach-Zehnder interferometer can also be utilised for the determination of the translational temperature.[7] In such cases, measurement of temperature involves the application of the well known equation

$$n - 1 = k\rho$$

where n is the refractive index and ρ the density and k a constant. If as a result of the passage of a discharge, the refractive index diminishes from n_0 to n, then a fringe shift Δf will be obtained satisfying the relation

$$(no - n)\,t = \Delta f \lambda$$

where t is the thickness of the column of the gas

$$\text{Since } \frac{n-1}{n_0-1} = \frac{\rho}{\rho_0}$$

we obtain

$$\frac{po}{To} - \frac{p}{T} = \frac{\Delta f}{t\,(no - 1)}\lambda$$

Thus, knowing the initial pressure po, temperature T_0 and final pressure p, one can determine T.

From the above it is clear that spectroscopic studies of flame spectra are of great value in elucidating combustion processes and energy content of hot gases generated during such processes.

REFERENCES

1. Wood R. W., *Proc. Roy. Sac.*, Vol. 97, 455 (1920) 102, 1 (1922). *Phil. Mag.*, Vol. 42, 729 (1929) 44, 538 (1922).
2. Wolfhard H. G., *Z. Phys.*, Vol. 112, 107 (1939).
3. Gaydon A. G. and Wolfhard H. G., *Disc. Faraday. Soc.*, Vol. 2, 161 (1947); *Proc. Roy. Soc.*, Vol. 194, 169 (1948).
4. Rassweiler G. W. and Withrow L., *Indus & Eng. Chem.*, Vol. 29, p. 529 (1932).
5. Vaidya W. M., *Proc. Roy. Soc.*, Vol. 147, 513 (1934).
6. Herzberg G. "Spectra of diatomic molecules", 2nd Edn. 1950, 200, 203. Von Nostrand & Cp., N. York.
7. Milatz J. M. W., Vreedenberg H. A. and Braak J. W., *Physica*, Vol. 10, 433 (1943).

RECENT APPLICATIONS OF ULTRASONICS

TO

SOLID STATE PHYSICS

By

G. S. VERMA

Department of Physics, University of Allahabad, Allahabad

[Received on 7th April, 1962.]

The most interesting development in recent years has been the production of Microwave Phonons i.e., acoustic waves at Microwave frequencies. Till 1957 the highest acoustic frequency which could be achieved by tuning the harmonics of the crystal was 500 Mc. In 1957 Baranskii[1], a Russian worker reported that he has been able to produce, 2·0 K Megacycle sound waves. Bommel[2] in collaboration with Dransfeld, produced 4 K Megacycle acoustic waves. Following this Jacobsen[3] of General Electric Research, Schnectady announced that he has produced 10 K Megacycle sound waves.

A cylindrical quartz rod, 25 mm long and 3 mm in diameter, with both end faces polished optically flat and parallel, is extended between two microwave cavities tuned to the same frequency (Fig. 1). Sound waves are generated by

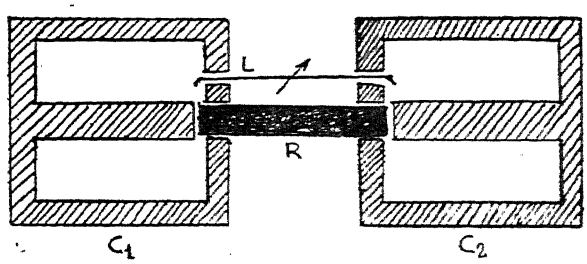

Fig. 1. Schematic diagram of the two cavities coupled acoustically by the quartz rod R and a variable electric coupling L.

surface excitation in the electric field of one cavity and similarly detected in the other. The transmitter cavity is coupled to a pulsed rf power source, and the receiver cavity to a sensitive receiver and oscilloscope. A variable electric coupling between the two cavities provides a means to compare the acoustically transmitted pulse with a calibrated electric leakage signal.

The only crystals in which acoustic waves of such high frequency have been produced are Quartz and Germanium. Bommel and Dransfeld have studied

attenuation of such high frequency sound waves in Quartz[4]. Bommel and Dransfeld observed that attenuation remains constant upto 60°K and at 60°K there occurs a very sharp decrease in the attenuation and below 20°K attenuation is almost negligible. A similar sharp decrease in attenuation at low temperature was also observed in Germanium by Truell[5] and his associates in 1959.

According to Akhiezer[6] sound waves on passing through a crystal disturb the equilibrium distribution of thermal phonons. The re-establishment of equilibrium in the phonon gas requires an increase of entropy and leads to absorption of sound waves. Till 1960 there was no explanation available for the sharp decrease in attenuation. The only hints which were available were that (1) the sharp decrease in attenuation is similar to the sharp decrease in thermal resistance observed in dielectric crystals and (2) the acoustic wave-lengths at such high frequencies, 10—20 microns, are of the order of mean free path for Umklapp processes. It is well known that Umklapp processes are responsible for thermal resistance at low temperatures. For collision processes of phonons, we may have processes for which total wave vector is conserved i.e., $K_1+K_2=K_3$. The two phonons with wave vectors K_1 and K_2 collide and give rise to third phonon of wave vector K_3. Also we may have processes of the type $K_1+K_2=K_3+G$ where G is a reciprocal lattice vector. In this process total wave vector is not conserved and it gives rise to thermal resistance. Such a process is known as Umklapp process. Assuming that there are two groups of phonons, Group (1) which is characterised by large positive changes of temperature and group (2) which are characterised by small or negative changes of temperature and that heat exchange takes place between the two groups in a relaxation time characteristic for the Umklapp process, attenuation of hypersonic wave can be calculated. The assumption that there are two such phonon groups is based upon the experimental fact that for certain directions $\Delta v/v$ is positive and for others it is negative and as the temperature changes are proportional to the velocity changes, we have two groups of phonons.

Verma and Joshi[7] are the first to give the quantitative explanation for the entire temperature dependence of hypersonic attenuation in Germanium. The excellent agreement between the theory and the experiment (Fig. 2) shows that

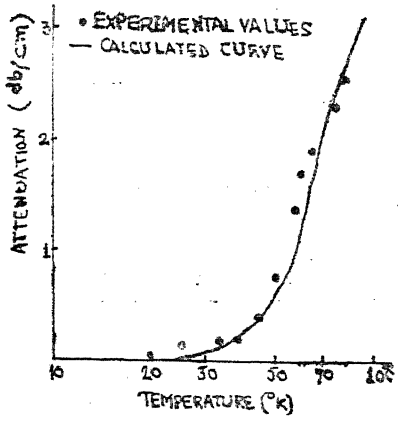

Fig. 2. Temperature dependence of Hypersonic attenuation in Germanium at low temperatures.

phonon-phonon Umklapp processes are responsible for the observed hypersonic attenuation at low temperatures. Attenuation is calculated from the following simplified expression

$$L = \frac{1{\cdot}1\, C T}{\rho v^3}\ \gamma_{av}\ \frac{w^2\tau}{1+w^2\tau^2}$$

where C is the specific heat per cc, v is the longitudinal sound velocity, ρ is the density, γ_{av} is the average Gruneisen constant, w is the angular frequency of the sound wave and τ is the relaxation time for phonon-phonon Umklapp processes. The relaxation time at these low temperatures has been calculated with the help of the relation $K=\frac{1}{3} Cv^2\tau$ where K is the thermal conductivity. Value of the average Gruneisen constant was obtained by choosing its value such that the theoretical value of hypersonic attenuation was equal to the experimental value, say, at 70°K. This value of γ_{av} was used for all subsequent calculations.

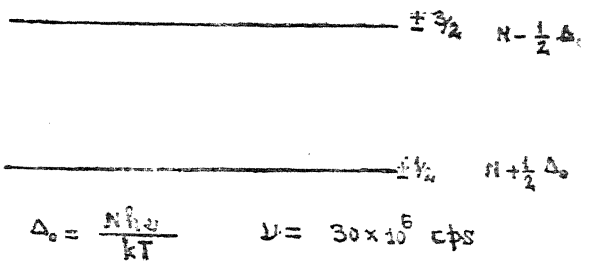

Fig. 3. Two degenerate Quadrupole levels of Cl^{35} separated by 30 Mc. Populations of the two levels are given when the system of nuclear spins is in thermal equilibrium with the lattice.

ULTRASONIC EXCITATION OF NUCLEAR SPIN TRANSITIONS

Since 1955 a series of experiments have been performed which demonstrate that transitions between nuclear spin levels can be induced by ultrasonic waves introduced at the frequency corresponding to the transitions $\Delta m = \pm 1$ or $\Delta m = \pm 2$. The possibility of affecting nuclear magnetisation in solids through the use of Ultrasonics was first suggested by Altschuler[8]. Proctor and Tanttila[9] were the first to perform such experiment at University of Washington, Seattle. $NaClO_3$ is the first crystal in which transitions were introduced between two degenerate quadrupole levels corresponding to 30 Mc.

In $NaClO_3$ crystal, Na is essentially ionically bonded to the ClO_3 radical and the Cl atom is co-valently bonded to three Oxygen atoms. The electric field gradient at Cl nucleus is completely determined by the co-valent bond. The interaction of this field gradient and the electric quadrupole moment of the spin 3/2 Cl nucleus brings about two energy levels. The population of the two levels are given for the case in which the system of nuclear spins is in thermal equilibrium with the thermal lattice vibrations. At thermal equilibrium the nuclei, of course, are constantly making transitions between the two levels but the number of upward transitions per second is equal to the number of downward transitions per second. There are two types of transitions—the direct process transitions and the indirect process or Raman transitions. In terms of quantised lattice vibrations the direct process is one in which a phonon having the energy of the nuclear transition is absorbed as the nucleus goes from the lower state to the upper state and a phonon

is emitted as the nucleus goes from the upper state to the lower state. In the indirect process, a lattice phonon is absorbed, the nucleus makes a transition and a phonon is emitted. The energy of the emitted phonon is equal to the difference in energy between the incident phonon and the change in the nuclear spin energy. At ordinary temperatures the indirect process is dominant since essentially all frequency lattice phonons in the lattice spectrum can contribute to the indirect process, whereas only those phonons having the nuclear transition frequency can contribute to the direct process. The essential idea of the ultrasonic experiments is to enhance the direct process which depends upon the density of lattice vibration of 30 Mc in this case, by ultrasonic waves of 30 Mc frequency. The energy density of 30 Mc phonons is increased to 10^{14} above the thermal equilibrium value.

In $NaClO_3$ experiment no magnetic field was used and transitions were introduced by ultrasonic waves in the quadrupolar levels. Later on magnetic field was used and transitions were introduced in the Zeeman levels of Na^{23} or Cl^{35} nucleus in NaCl crystals by introducing ultrasonic waves of 12·5 Mc/sec corresponding to $\Delta_m = \pm 2$ transitions (Fig. 4). By increasing ultrasonic transition probability it is

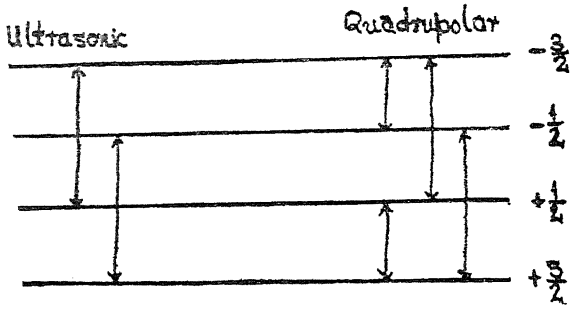

Fig. 4. Transitions between nuclear spin levels of Na^{23} or Cl^{35}.

possible to saturate the spin levels. However, it was realised by everyone working in this field that if it were possible to measure displacements of lattice points under ultrasonic excitation, more reliable values of ultrasonic transition probability could be obtained. This was achieved by Bloembergen and Taylor[10] in 1959. They were able to measure the strain coefficients and obtained results which are in violent disagreement with current theories. They find no angular dependence in the nuclear spin saturation, which implies that $S_{44}/S_{11} = 3/4$. This differs from the Cauchy relation $S_{44}/S_{11} = -1/2$. Also the experimental ratio $(S_{11})Cl/(S_{11})Na = 1{\cdot}8$ whereas the ionic point charge model coupled with an isotropic antishielding factor gives a value 10. The results show inadequacy of the point charge model and indicates the possibility of a considerable amount of covalent character and configurational interaction on the Na^+ ion. It is believed that quantum mechanical calculations of the type Lowdin[11] has done might give some answer to these discrepancies.

Menes and Bolef[12] have measured nuclear resonance acoustic absorption in KI and KBr. A Quartz transducer crystal is bonded to the sample which is prepared to be mechanically resonant. Under the conditions of mechanical resonance the electric impedence of the transducer is a certain function of the acoustic attenuation of the sample. The acoustic attenuation is of the order of 10^{-8}cm.

Utilising the values of nuclear resonance acoustical absorption, Verma and Joshi[13] have calculated the values of γ where γ is the amplification factor by which the quadrupole coupling exceeds that predicted on the basis of a point charge model. They obtain $\gamma=12{\cdot}61$ for ^{127}KI and $\gamma=6{\cdot}34$ for ^{79}KBr. This calculation, however, is based on the assumption that Kessel's[14] theory of resonance absorption of ultrasound in paramagnetic nuclei in a cubic lattice is correct.

MOLECULAR RESONANCE ACOUSTICAL ABSORPTION IN SOLIDS

In 1959 Liebermann[15] showed that in molecular crystals resonance phenomenon resulting in anomalously high acoustic absorption can occur whenever lattice and internal molecular vibrational frequencies overlap. Resonance absorption was calculated in the particular case of Benzene and has been also confirmed experimentally. Verma and Joshi[16] also predicted molecular resonance absorption in solid cyclohexane of a magnitude larger than that of Benzene. It is encouraging to note from the Proceedings of Acoustical Society Meeting at Brown University (1960) that Rassmussen[17] has confirmed our prediction experimentally.

ULTRASONIC SUPPORT TO THE ENERGY GAP MODEL IN BCS THEORY OF SUPERCONDUCTIVITY

The greatest achievement in the last decade in the field of Solid State Physics is the BCS theory[18] of Superconductivity. Although this effect was discovered fifty years back by K. Onnes and a considerable amount of experimental data were amassed during this period, there was no material progress in the understanding of the physical principles underlying the phenomenon. According to BCS theory, which was given in 1957 the electrons close to the Fermi surface form a bound pair state. The two electrons normally should repel each other. However, it has been shown by Frohlich[19] and Bardeen[20] that there occurs a mutual attraction between electrons due to virtual absorption and emission of lattice quanta i.e., phonons just as in a nucleus the protons are held together due to virtual absorption and emission of mesons. Whenever this attraction dominates over repulsive forces, a bound state occurs which results in the decrease of energy. Thus if we assume that there is in metals an effective attraction between the electrons, pairing will occur and the ground state will then be lower than for free electrons by the binding energy of these pair. The electron pairs have integral spins and obey Bose Statistics. It is known that a Bose gas is superfluid at absolute zero and applied to a Bose gas of charged particles, this property manifests itself as superconductivity.

The electronic spectrum consists of an energy gap which is about $3{\cdot}5\ KT_c$ at $T=0°K$, where T_c is the critical transition temperature at which the metal passes from normal phase to superconducting phase. This gap decreases with the increase in the temperature and finally vanishes at $T=T_c°K$. Several experiments such as Absorption edge in Far Infra red by Tinkham[21], Microwave absorption by Biondi, Gurfunkel et al[22], Nuclear Relaxation by Heber and Slitcher[23] etc. have been performed which support the energy gap model. Ultrasonics has given an excellent experimental support to the energy gap model of BCS theory. According to BCS theory

$$\frac{\alpha_s}{\alpha_n}=\frac{2}{e^{\varepsilon_0/KT}+1}$$

where α_s is the attenuation in the superconducting phase and α_n in the normal phase and $2\varepsilon_0$ is the energy gap and thus by measuring ultrasonic attenuation at different temperatures, Morse and Bohm[24] have measured the energy gap at different temperatures and results are in excellent agreement with BCS theory (Fig. 5).

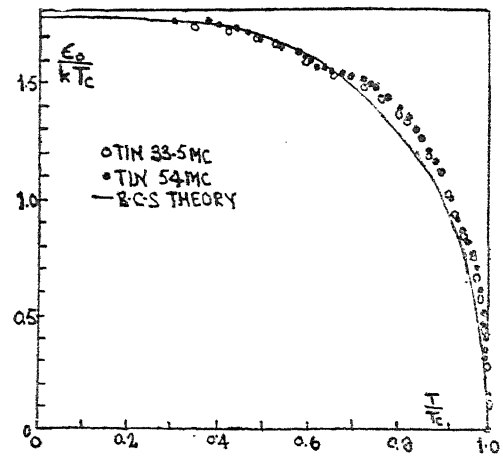

Fig..5. Variations of $\varepsilon_0(T)$ with temperature as observed from the ultrasonic data on tin and compared with theoretical variation assuming the energy gap at 0°K is $2\varepsilon_0 = 3{\cdot}54\ KT_c$.

MOSSBAUER EFFECT AND GRAVITATIONAL 'RED SHIFT' IN ACOUSTICALLY ACCELERATFD SYSTEM

Most recently the Mossbauer[25] Effect has become, in the words of Goudsmit, Editor of Physical Review and Physical Review Letters, one of the 'hottest Topics'. This effect was discovered in 1958 and since then a large number of papers dealing with its applications have started pouring in and most outstanding and dramatic application of Mossbauer effect is the measurement of gravitational red shift by Pound and Rebka[26] which has been reported in April 1 issue of Physical Review letters in 1960. Normally in the process of emission or absorption, a nuclear γ ray loses an amount of energy large compared to the line width. This loss is due to Doppler effect and the energy goes into the recoil motion of the emitting or absorbing nucleus. Mossbauer in 1958 found that under favourable circumstances, namely for an atom tightly bound in a solid at low temperatures emission and absorption can occur without such an energy loss. The recoil energy is taken by the crystal as a whole, without emission of phonons. This effect was first found in Indium.

Pound and Rebka have measured the influence of gravity over a 70 ft height on the frequency of the recoil free 14 Kev γ—ray of 0·1 μsec Fe^{57}. The gravitational effect found agrees with gh/c^2.

Bommel and Dransfeld[27] recently have reported in the November meeting of American Physical Society at Chicago that using the Mossbauer effect they have measured the frequency shift in accelerated system. Two identical piezo-

electric quartz transducers are simultaneously excited to longitudinal vibration at a frequency of few Megacycles. To one surface of each transducer was attached a thin foil of stainless steel, one of them carrying Fe^{57} source, the other one serving as the absorber. Both the transducers are driven at the same amplitude and phase to avoid direct Doppler shift of the γ line. Source and absorber can then be regarded as being in one and the same accelerated system. If the transducers vibrate with amplitude a and angular frequency w and are separated by a distance d, one then expects to find a relative γ-resonance shift given by $\frac{\Delta\nu}{\nu} = aw^2d/c^2$ between source and absorber. Such a shift proportional to 'd' has been observed.

ULTRASONIC INVESTIGATION OF PHOTOCONDUCTORS

Ultrasonic might prove, it is believed, a useful tool for investigation of photoconductors in Solid State Physics. Recently H. Nine[38] (reported in Phys. Rev. Letters April 1960) has observed that the physical acoustical properties of CdS crystals are influenced by photon irradiation. Ultrasonic attenuation and photoconductance in CdS were measured as a function of light intensity and wave length. The effect of light intensity on the ultrasonic attenuation has been proved to be linear. The crystal exhibits the ultrasonic effect over the same range of light wavelengths as the response region of the photoconductance effect—from the band edge for CdS at about 5100 Å upto 8000 Å in the infra red (Fig. 6). The

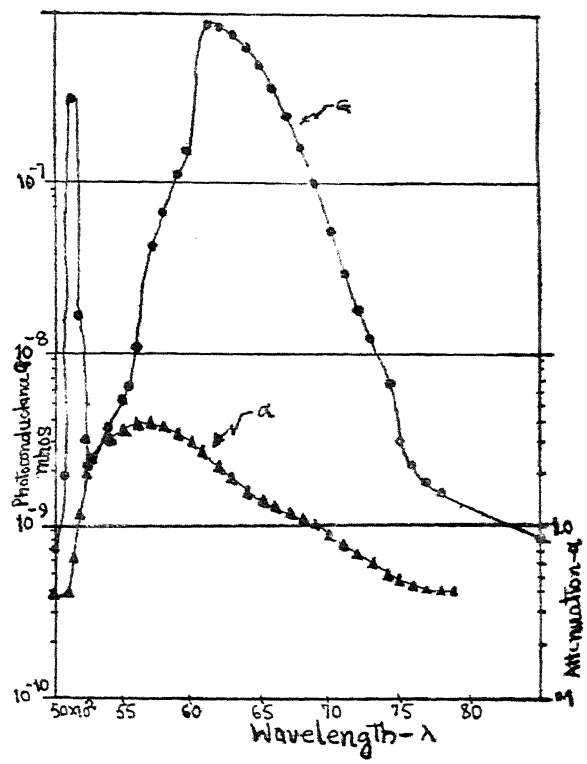

Fig. 6. Photoconductance and Ultrasonic attenuation measured at 45 Mc/sec vs wavelength in angstroms for CdS crystals.

phenomenon of infra red quenching of the photoconductance as well as the ultrasonic attenuation to the dark value by infra red was obtained. Two types of mechanisms are being considered as possible explanations of the ultrasonic attenuation changes (1) relaxation associated with electron or hole trapping at impurity or vacancy sites and (2) changes in thermoelastic attenuation due to heat conduction by photoactivated electrons.

ULTRASONIC ATTENUATION AND ULTRASONIC INVESTIGATION OF FERMI SURFACE OF METALS

The first experimental evidence that electrons in metals could contribute significantly to the attenuation of Megacycle sound waves was uncovered by Bommel[29] and Mac Kinnon.[30] The importance of the electronic system was indicated by the observed change in attenuation upon crossing the superconducting transition. Various theoretical discussions of the contributions of the electrons to the attenuation in normal metals were put forward but the first complete theory was developed by Pippard[31] for the free electron gas.

If the wave is longitudinal the density of positive charge will vary periodically so that in the absence of a compensating variation of $-ve$ charge there will be longitudinal electric field, which will force the electrons into motion. The longitudinal electric field associated with the longitudinal wave is of a different magnitude to keep the charge neutrality such that

$$J_{latt} + J_e = 0$$

In fact only the minutest degree of charge imbalance is needed to keep the electronic current at the same magnitude as the lattice current. If there are collisions between the electron and the lattice, they also help to establish the required electronic current. The electric field which affects the current neutrality is the link between lattice and electrons which is responsible for transferring energy from the former to the latter and so attenuating the wave. The attenuation α is given by

$$\alpha = \frac{Ne^2}{Mu^2 v_s} R\,(E^*, u)$$

Thus the problem of calculating α is reduced to that of calculating E^*, the electric field needed to maintain the current neutrality. Pippard's theory has successfully accounted for the major experimental features of the attenuation.

By this time Bommel[32] had found that the ultrasonic attenuation showed oscillatory dependence upon magnetic field in tin at helium temperature. The fluctuations in attenuation appeared at magnetic fields inconsistent with cyclotron resonance or de Hass-Van Alphen oscillations. Pippard[32] proposed that such oscillations could arise from a matching of the diameters of electron orbits in a magnetic field and the wavelength of the incident sound wave. However, a detailed quantitative theory of the dependence of the attenuation upon the magnetic field was not forthcoming. There was a complete theoretical silence from 1955 to 1960. It was only in early 1960 that Cohen, Harrison and Harrison[33] published a detailed theory in Physical Review.

However, during this period of theoretical silence, a number of experiments were performed which amply confirm Bommel's original experiments and Pippard's suggestion that the oscillations provided new tool for studying the Fermi surface of metals. The principal investigations have been those of Morse and his collabo-

rators[35] on copper and tin, that of Renekar[36] on Bismuth and that of Roberts[37] on Aluminium published in Sept. issue of Phys. Rev. Utilising this low temperature magnetic dependence, Morse and his associates[38] have shown that in Cu, Au and Ag Fermi surface contacts the Brillouin boundary in (111) direction.

REFERENCES

1. K. N. Baranskii, *Dokl. Akad. Nank, USSR*, **114**, 517 (1957).
2. H. E. Bommel and Dransfeld, *Phy. Rev. Letters*, **1**, 234 (1958).
3. E. H. Jacobsen, *Phys. Rev. Letters*, **2**, 249 (1959).
4. H. E. Bommel and K. Dransfeld, *Phys. Rev.* **117**, 1245 (1960).
5. E. R. Dobbs, B. B. Chick and R. Truell, *Phys. Rev. Letters*, **3**, 332 (1959).
6. A. Akhiezer, *J. Phys. USSR*, **1**, 277 (1939).
7. G. S. Verma and S. K. Joshi, *Phys. Rev.* **121**, 395 (1961).
8. S. A. Altschuler, *Dokl. Akad. Nank USSR*, **85**, 1235 (1952).
9. W. G. Proctor and W. Tanttila, *Phys. Rev.* **98**, 1854 (1955).
10. E. F. Taylor and N. Bloembergen, *Phys. Rev.* **113**, 431 (1959).
11. P. O. Lowdin, Thesis, *Uppsala*, 1948 (Unpublished).
12. D. I. Bolef and M. Menes, *Phys. Rev.* **114**, 1441 (1959).
13. G. S. Verma and S. K. Joshi, *Proc. Phys. Soc. (Lond).* **76**, 775 (1960).
14. A. R. Kessel, *J, Exp'. Theo. Phys. USSR*, **36**, 1451 ( ).
    (Translation *Soviet Phys. JETP*, **5**, 1031 (1959).
15. L. Liebermann, *Phys. Rev.* 113, 1052 (1959).
16. G. S. Verma and S. K. Joshi, *Proc. Phys. Soc. (Lond.)* **75**, 935 (1960).
17. A. Rasmussen, *Proc. Acoust. Soc.* Meeting at Brown Univ. (1960).
18. J. Bardeen, L. N. Cooper and J. R. Schrieffer, *Phy. Rev.* **108**, 1175 (1957).
19. H. Frohlich, *Phys. Rev.* **79**, 845 (1950).
20. J. Bardeen, *Rev. Mod. Phys.* **23**, 261 (1951)
21. R. E. Glover and M. Tinkham, *Phys. Rev.* **108**, 247 (1957).
22. Biondi, Gurfunkel and McCoubrey, *Phys. Rev.* **103**, 495 (1957).
23. L. C. Hebel and C. P. Slitcher, *Phys. Rev.* **107**, 901 (1957).
24. R. W. Morse and H. V. Bohm, *Phys. Rev.* **103**, 1094 (1957).
25. R. L. Mossbauer. *Z. Physik* 151, 124 (1958), *Naturwissenschaften* **45**, 533 (1958), *Z. Naturforsch*, **140**, 211 (1959).
26. R. V. Pound and G. A. Rebka, *Ja., Phys. Rev. Letters*, **4**, 337 (1960).
27. H. E. Bommel and K. Dransfeld, *Bull. Am. Phys. Soc. Nov.* 1960.
28. H. D. Nine, *Phys. Rev. Letters*, **4**, 359 (1960).
29. H. E. Bommel, *Phys. Rev.* **96**, 220 (1954).
30. L. Mackinnon, *Phys. Rev.* **98**, 1181 (1955).

31. A. B. Pippard, *Phil. Mag*, **46**, 1104 (1955).
32. H. E. Bommel, *Phys. Rev.* **100**, 758 (1955).
33. M. H. Cohen, M. J. Harrison and W. A. Harrison, *Phys. Rev.* **117**, 937 (1960).
34. A. B. Pippard, *Phil. Mag.* **2**, 1147 (1957).
35. R. W. Morse and J. D. Gavenda, *Phy. Rev. Letters* **2**, 250 (1959).
36. D. H. Renekar, *Phys. Rev.* **115**, 303 (1959).
37. B. W. Roberts, *Phys. Rev.* **119**, 1889 (1960).
38. R. W. Morse, A. Myers and C. T. Walker, *Phys. Rev. Letters* **4**, 605 (1960).

EXCITATION OF SPECTRA BY ION BOMBARDMENT

By

S. N. GHOSH *and* B. N. SRIVASTAVA

J. K. Institute of Applied Physics, University of Allahabad, Allahabad.

[Received on 23rd May, 1962]

INTRODUCTION

The excitation of spectra by ion bombardment, in particular by protons has, of late, been receiving increasing attention. This is mainly due to the fact that protons emanated from the sun excite atleast a part of the aurora. These protons penetrate deep into the atmosphere even upto the auroral heights where on bombarding the constituent gases they excite spectra.

Controlled laboratory experiments for the excitation of gases by bombardment of ions at different energies have recently been carried out mainly by four groups of investigators ; at Yerke's Observatory, Chicago, by Meinel and Fan ; at Harvard University and Geophysical Research Directorate, Boston by Oldenberg, Carleton, Sheridan and Dieterich and at the University of Western Ontario, Canada, by Nicholls, Reeves, Pleiter and Bromley. Recently, Sluyters and Kistemaker have also excited inert gases by Ar^+ ion bombardment.

The work of these investigators is greatly facilitated by the development of stronger ion sources by Moak, Reese and Good (M. R. G. source) and electrostatic lenses. By means of these lenses beams can be collimated to a high degree. Sometimes accelerators were used for obtaining very high energy beam. Furthermore, arrangements can be made so that the spectra may not be contaminated by spectra resulting from secondary electrons emanating from the metal surface of the system by ion bombardment.

Previously, spectra were also excited by bombardment of gases by ions. These were carried out by means of canal rays where gases were bombarded by their own ions. However, in these expriments the spectra might be excited by more than one type of ions. For example, if the discharge tube is filled with N_2, the excited spectra may be due to bombardment of N_2^+, or N^+ or N^{++} ions acting singly or jointly. In the recent experiments, the above uncertainties are eliminated because all the above investigators have mass analysed the ion beams before the gases were bombarded.

At low energies, the excitation of spectra by ion bombardment is caused mainly by the charge exchange process between ions and the bombarded neutral gas molecules. The ions are neutralised and the neutral molecule becomes ionized. During this process the bombarded gas and/or the neutralised ion becomes dissociated and excited. At higher ion energies, the gas molecules are ionized and during the process of ionization, the ions become dissociated and excited.

CHAPTER II

Experimental Arrangements

2.1 Ion Sources

H^+, D^+, He^+, Ar^+, Ne^+, Li^+, H_2^+ and H_3^+ ions have been employed for exciting spectra of gases. In most cases, air was bombarded by these ions. Other gases are also bombarded namely, helium, argon, H_2, N_2 and O_2.

Different types of ion sources were employed by different investigators. Of these sources the one developed by Moak, Reese and Good[1] is very important and has been employed by many investigators. This source, in conjunction with a high voltage accelerator, can produce ionic beam of very high energy with an output current of several hundred microamperes. Briefly speaking, it consists of a specially-designed pyrex glass envelope where ions are produced by an electrodeless discharge (Fig. 2.1). A tungsten wire is fused at one end of the glass envelope and an

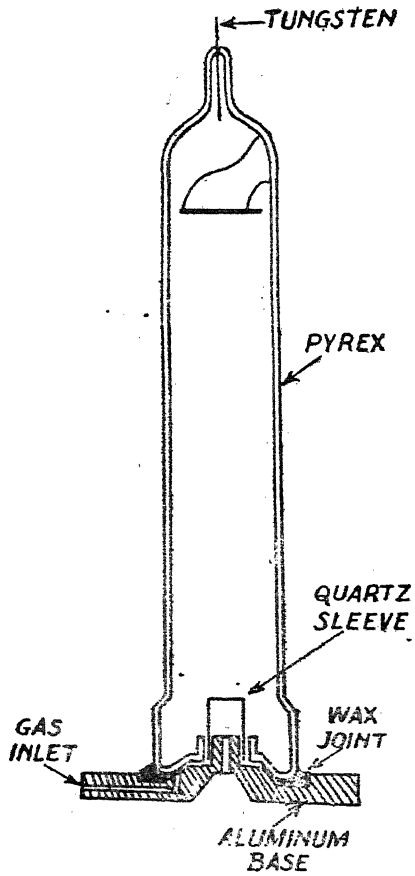

Fig. 2.1 Moak, Reese and Good ion source. Ions are produced in a specially designed pyrex glass envelope by an electrodeless discharge and are extracted through a canal in an aluminium base which is sealed to one end of the pyrex tube.

anode voltage from 2 to 5 Kev is applied. The other end is sealed by an aluminium base having a canal at the centre. Ions formed inside the pyrex glass envelope are extracted through the canal of aluminium base into the accelerator.

Other ion sources[2-13] are also used for exciting spectra in gases. The output current of these sources varies from 0.25 to several hundred microamperes. The energy of the ions used for exciting the spectra varirs from 1 Kev to 1 Mev The characteristic features of these ion sources are given in the following table.*

TABLE 1

Ion sources used for exciting spectra in gases by ion bombardment

Investigator	Type of source with accelerator	Type of beam	Output current	Energy range
Meinel and Fan (1952)[2]	Proton from Kevatron of the Institute of Nuclear Studies, University of Chicago.	H^+	—	230 Kev
Fan and Meinel (1953)[3]	,, ,,	H^+	—	40–230 Kev
		D^+	—	75–320 Kev
		He^+	—	150–450 Kev
		Ne^+	—	400 Kev
Branscomb, Shalok and Bonner (1954)[4]	From the Van de Graaff accelerator of Rice Institute	H^+	—	100 Kev
Fan (1955)[5]	30 Kev ion accelerator of Yarkes Lab.	He^+	Several hundred μa	10 Kev
Nicholles and Pleiter (1956)[6]	A thermionic source with a lithium, Al, Si coated anode	Li^+	—	2–4 Kev
Fan (1956*a*)[7]	Source of (1955)	H^+	—	5–350 Kev
		He^+	—	10–450 Kev
Fan (1956*b*)[8]	M. R. G. source with Van de Graaff accelerator	H^+	Several hundred μa	25–350 Kev
		He^+	,,	10–450 Kev
Dieterich (1956)[9]	M. R. G. source	H^+	10 μa	2 Kev
		H_2^+	5 μa	2 Kev
Carleton (1957)[10]	,,	H^+	20 μa	2–3 Kev
Carleton and Lawrence (1958)[11]	,,	H^+, H_2^+	20 μa	1–4 Kev
Nicholls, Reeves and Bromley (1959)[12]	Thermionic source with Van de Graaff accelerator	H^+	·25–5 μa	0·5–1 Mev
Sluyters and Kistemaker (1959)[13]	Obtained from Amsterdam Electromagnetic Isotope separator	Ar^+	2·0 μa	5–25 Kev
Reeves, Nicholls and Bromley (1960)[14]	Ion beam from 3 Mev Van de Graaff accelerator	H^+, H_2^+, H_3^+	·5–5 μa	0·5–1·5 Mev

* The detailed description of different types of ion sources is given in a review article entitled 'Secondary Electron Emission by Ion Bombardment' by Ghosh and Khare (Under publication).

2.2 Spectrographs

For studying the spectra excited by ion bombardment, different types of grating or prism spectrographs were used. Some of the spectrographs have high resolution, and others have large light gathering power and low dispersion. The spectra have been photographed from 2500A to 9000A. For the ultra-violet and visible region, Eastman Kodak 103-O and 103aF plates and for infra-red region IN plates were used. The spectra were excited at different pressures of gases.

We shall now describe in detail the spectrographs used by the four groups of investigators referred to in the Introduction.

(a) Spectrograph used by Meinel and Fan :

Meinel and Fan (1952), Fan and Meinel (1953), Fan (55, 56a and 56b) carried out observations at Yerkes Observatory and recorded spectra obtained by the bombardment of ions on a nebular spectrograph (grating B spectrograph)[15] of McDonald Observatory. Originally designed by Horace W. Babcock, the nebular spectrograph consisted of an $f/4$ parabolic collimeter mirror of 2″ aperture and 7.65″ focal length, a glass grating of 15,000 lines per inch rulled by H. D. Babcock, and a solid $f/0.65$ UV glass Schmidt camera of 1.33″ effective focal length made by D. O. Hendrix.

(b) Spectrograph used by Carleton :

At Harvard University, Carleton analysed the spectral feature with a Kipp's liquid prism spectrograph[16]. This spectrograph consisted of a liquid prism made of ethyl cinnamate ($C_6H_5\,CH_4CH_4\,COOC_2H_5$) having side walls of crown glass plates. The ethyl cinnamate prism which has a small average refractive index and a large dispersion ($n_D = 1{,}560, n_F - N_C = 0{\cdot}0286, v = 19$) was placed on a cast iron base. The side of the prism, which has a refractive angle of 65°, is 15 mm long and 95 mm high, so that full beam of light can pass through it. The prism was placed in the position of minimum deviation for the green light for which the refractive index is 1·570.

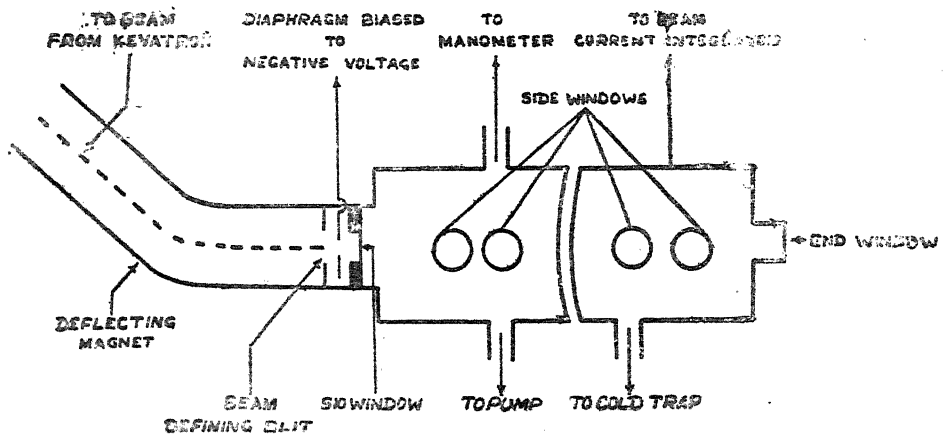

Fig. 2.2 The modified collision chamber used by Fan and Meinel for exciting spectra in gases by ion bombardment.

The spectrograph was mounted inside a metal case. At one end of the case the collimator tube was fixed having a lens of 65 mm diameter and 600 mm focal length. In front of the collimating lens, a unilateral slit of 20 mm height was mounted.

A prism which can be removed if required, was fixed before the slit for taking comparison spectra. The front of the slit was made quite plane in order that a step reducer could be fastened before the slit for securing a perfect projection of the stop reducer on the photographic plate. The diaphragm in the collimator tube prevented stray light from falling on the prism.

Kipp spectrograph has a *f*/2 camera. The lens of the camera has a diameter of 65 mm and a focal length of 140 mm. It can be adjusted for focussing the far infra-red region of the spectrum. An additional shutter was placed between the plate holder and the camera lens, which prevented light from falling on the photographic plate. The length of the spectrum for different spectral region is given below :

Spectral range	*Length of spectrum*
8000 A —6000A	4 mm
6000 A —5000A	6 mm
5000 A —4000A	11 mm

The height of spectrum is 3·5 mm and the dispersion ranges from 100-900 A/mm from violet to infra-red region.

An eye piece (magnifying power 10) can be fastened behind the camera and can be moved along a rail in order to bring the different parts of the spectrum in the field of view. Thus, it can be used as a spectroscope. Instead of a photographic plate, a vacuum thermocouple may be mounted for direct intensity measurement of the spectrum.

(*c*) *Spectrograph used by Reeves et al* :

Reeves *et al*[17] constructed a simple and inexpensive prism spectrograph mounted on a heavy iron base and having a large aperture *f*/1·1. They employed a unilateral Hilger slit and a collimating lens of 58 cm focal length, a 60° dense flint glass prism (μ 5460 = 1·753) of 4·5 cm height and 5·5 cm side and a 35mm Canon camera fitted with Zunow *f*/1·19 element 50 mm lens. The camera could be easily removed for loading and was actuated by an external cable release. The plywood case of the spectrograph was fitted with an additional shutter between the slit and the collimating lens. The dispersion is given below :

130 A/mm at 4050 A,

360 A/mm at 5050 A, and

1400 A/mm at 1000 A.

Identification of various spectral features could readily be made within 2A around 4300A by the use of photometer tracing. Estimated resolving power measured from microphotometer traces of the spectra are $2{\cdot}13 \times 10^3$ at 4246A and $1{\cdot}117 \times 10^3$ at 5025A for a slit width of 10μ.

In a later experiment, Reeves, Nicholls and Bremley[14] used a *f*/4 Hilger Spectrograph for recording spectra resulting from the bombardment of 1 Mev H^+ in N_2 at a pressure of 58μ. A 1·5 meter Baush and Lomb grating spectrograph and a photon counting grating spectrometer were used. The spectrometer had a collimator, a plane grating and a telescope system together with an RCA 1P28 photomultiplier tube cooled by dry ice.

(d) Spectrograph used by Sluyters et al :

To study the lumuinescence produced by collision of high energy Ar^+ions with gases, Sluyters and De Hass designed a grating vacuum monochromator for the spectral range 1000–6500 A. For the ultraviolet region below 1800 A, the entire optical system was enclosed in an evacuated chamber, and the grating was mounted in a Paschen–Runge mounting where the entrance slit, grating and the reflected spectrum lie on a circle whose diameter is the radius of curvature of the grating. As in the vacuum ultraviolet region, aluminium is the best material with the highest reflectivity, these investigators used a one-meter aluminium grating (30×20 mm^2) with 600 lines/mm made by the Nobel Institute of Stockholm. The widths of the two slits (one for incident light entrance and the other for reflected light) are continuously being adjusted from 20μ to 2mm and can be moved in any plane. The exit slit can be replaced by a curved film holder. The spectrograph was evacuated by a diffusion pump to about 10^{-5} mm of Hg.

An E.M.I. 6256 photomultiplier with quartz window was used for detecting different spectral features. To reduce the dark current pulses, the tube was cooled with liquid air to –80°C. The exit slit and the photomultiplier tube were driven by a synchronous motor with a speed of 10 r.p.m.

In table II the speectrographs and film used for studying the emitted light are given.

TABLE II

Investigator	Spectrograph used	Spectral range	Film used
Meinel and Fan (1952)[2]	McDonald Observatory Nebular spectrograph with a solid Schmidt camera. Dispersion 400A/mm at H_α, 385A/mm at H_β and 335A/mm at H_γ.	3500-5000A, the ultraviolet spectrum beyond 3700A was heavily absorbed.	Eastman Kodak 103 aF (3) plate
Fan and Meinel (1953)[3]	,, ,,	3500-6800A	
Branscomb *et al* (1952,54)[4,15]	Quartz spectrograph	2800-5000A	103-0 plate

TABLE II—(*contd.*)

Investigator	Spectrograph used	Spectral range	Film used
Fan (1955,56*a*, 56*b*)[5,7,8]	Same as used by Meinel and Fan (1952).	3700-9000A	Eastman 103 aF (3) for 3700-6800A & IN hyper sensitised for 6300-9000A.
Dieterich (1956)[9]	Kipp liquid spectrograph with an *f*/2 camera having dispersion 100-900A/mm.	4000-8000A	
Carleton (1957)[10]	Same as used by Dieterich and also auroral spectrographs with a *f*/1 Schmidt camera and a dispersion of 140A/mm in the first order and of 40/mm in the third order violet.	4200-8900A	Eastman IN, 103aF and process plate.
Nicholls and Pleiter (1956)[6]	Prism spectrograph with a camera aperture of *f*/2 and a reciprocal dispersion of 130A/mm at 4000A and 1400A/mm at 8000A.	Ultraviolet to 9000A.	
Nicholls, Bromley and Reeves (1959)[12]	Prism spectrograph with camera aperture of *f*/1·1 and a reciprocal dispersion of 130A/mm at 450A.	3800-8000A	Kodak HIR 402 film (IN emulsion).
Sluyters, Kistemaker (1959)[13]	Vacuum Spectrograph with a concave aluminium grating with 600 lines/mm (dispersion 17A/mm).	1000A-6500A	EMI 6256B photomultipier tube is used.
Reeves, Nicholls and Bromley (1960)[14]	(*a*) Prism spectrograph used by Nicholls *et al* (1959). (*b*) A Hilger *f*/4 spectrograph. (*c*) A 1·5 meter Bausch and Lomb grating Spectrograph. (*d*) A Photon counting grating spectrograph.	3500A-9000A	Kodak IN Plate. RCA 1P28 Photomultiplier tube is used.

2.3 Instrumentation

The experimental arrangements for exciting spectra of gases by ion bombardment as used by the four groups of investigators are given below :

In the early stage of observation Meinel and Fan[2] used a 26 cm. long collision chamber attached to an ion accelerator. A differential pressure below 1 mm of Hg was maintained between the accelerator and the collision chamber by inserting a thin nylon window at the place where the ions entered the collision chamber. The nylon window was coated with aluminium deposited in vocuum. The pressure of air inside the collision chamber could be varied from 0.1 to 0.3 mm of Hg, spectra were excited mostly at 0.3 mm pressure by 230 Kev proton bombardment.

Subsequently, Fan and Meinel[3] modified the chamber so that the spectra excited by ion might not be contaminated by the spectra arising from electrons which are produced at the slit of the collision chamber. The collision chamber which was 4 inches in diameter and 36 inches long (Fig. 2.2), was attached to the Kevatron of the Institute of Nuclear Studies, University of Chicago. High energy ions (H^+, D^+, He^+, Ne^+) were allowed to pass through a diaphragm with a 1/4 inch hole at the centre. Finally, before entering the collision chamber, ions passed through a SiO window of 1/16 inch diameter and coated with a thin aluminium for preventing damage from heating. The size of entrance slit was slightly smaller than that of the window so that ions which passed through the slit, could enter the collision chamber. To prevent secondary electrons being ejected from the window (backward ejection) and also from the slit (forward ejection), the diaphragm was negatively biased with respect to the ground. A pressure of 0.3 mm. was maintained in the collision chamber and several spectra were excited at different ion energies ranging from 40 to 400 Kev.

Later Fan[5] excited several spectra in air at a pressure of 10^{-3} mm of Hg by He^+ ion bombardment. After being magnetically analyzed, the monoenergetic He^+ beam was fired through a 1/16 inch hole into the collision chamber. At a later stage, Fan[7,8] maintained a difference of pressure between collision chamber and the rest of the system by means of differential pumping instead of using a window (Fig. 2.3). The collision chamber was insulated from the

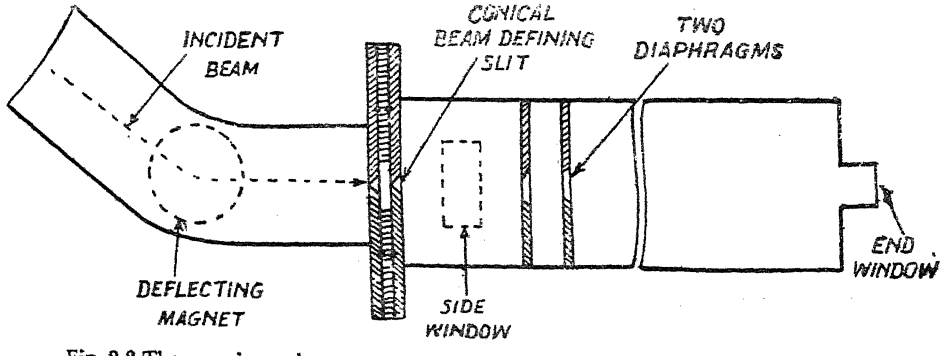

Fig. 2.3 The experimental arrangement used by Fan. The collision chamber was insulated from the accelerator and two diaphragms were inserted to prevent secondary electrons from being ejected from side walls.

accelerator so that for the measurement of beam current, it could be considered as a Faraday cup. He also used a set of two diaphragms to prevent the

econdary electrons from being ejected from sidewalls. The spectra were excited by H^+ and He^+ ion bombardments in air at 1.0 and 0.1 micron pressure. Further experiments[9] were carried out with the M. R. G. source of Oak Ridge Laboratory (Fig. 2.4). Air pressure in the range of 0.1 to 10 mm Hg was

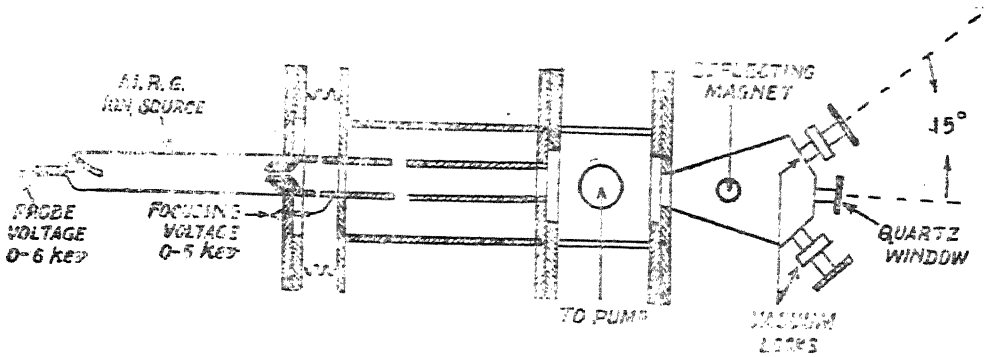

Fig. 2.4 The experimental arrangement used by Fan for exciting spectra in air by H^+ bombardment by using a M. R. G. source of Oak Ridge Laboratory.

maintained by means of differential pumping. Precautions were also taken so that spectra might not be excited by secondary electrons produced at the sidewalls of the collision chamber.

Instead of using an accelerator, Carleton[10] and Dieterich[3] used a M.R.G. source followed by electrostatic lenses (Fig. 2.5) and excited spectra by low energy proton bombardment. As mentioned previously, in this type of source ions were produced by an r.f. discharge and were accelerated towards an exit of 1/16 inch diameter by a d.c. bias of 1–5 Kev (Dieterich used 2.5 Kev bias). The beam

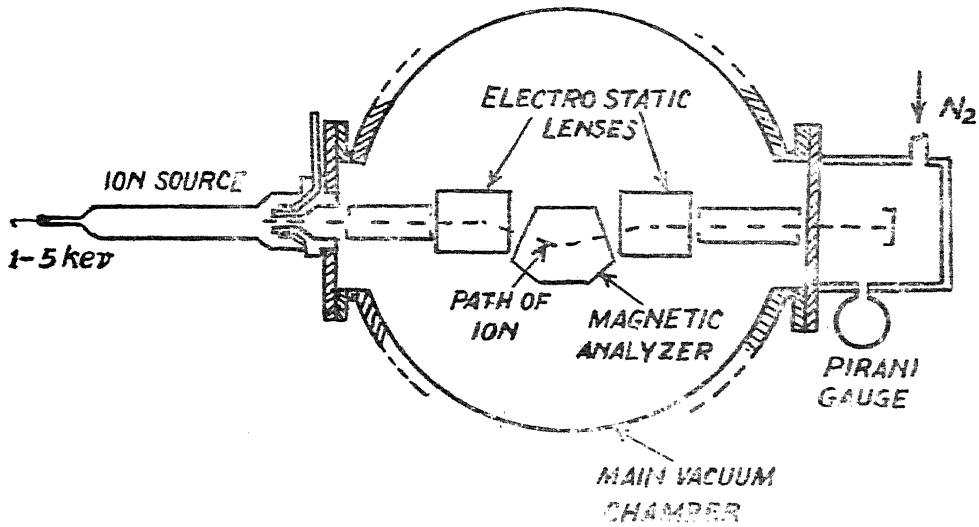

Fig. 2.5 The experimental arrangement used by Carleton and Dieterich. The ion beam produced from a M. R. G. source was collimated into a parrallel pencil of 1/4 inch diameter by an electrostatic lens. It was afterwards mass analysed by a combination of electric and magnetic fields and was again focussed by a second electrostatic lens before entering the collision chamber.

was then collimated into a parallel pencil of 1/4 inch diameter by an electrostatic lens of special design[13]. Thereafter, it was mass analysed by a combination of electric and magnetic fields and was focussed into a 1/16 inch aperture by a second electrostatic lens placed before the collision chamber. The pressure inside the collision chamber could be varied from 0.5 to 50μ, whereas within the ion source the pressure was from 10 to 20 microns. A pressure of 2×10^{-5} mm was maintained by a differential pumping between the portion of the apparatus connecting the ion source and the collision chamber.

In the arrangements used by Nicholls and Pleiter[12] protons from Van de Graff accelerator were fired into a 50 cm long collision chamber through a thin titanium foil of thickness 0.001 inch. The collision chamber was a part of a dynamic vacuum system where gases were leaking at a controlled rate. They[8] observed spectra excited by Li^+ ions in N_2, O_2, air and argon at a pressure 5–40 microns. In a latter experiment,[13]. Nicholls *et al* excited spectra in N_2 and O_2 by monoenergetic proton beam of 0.5–1 Mev energy. Spectra in N_2 were excited by 1 Mev proton at three sets of pressures, 63 to 150 microns, 5 to 20 mm and at atmospheric pressure. Spectra were also excited by 1/2 Mev proton in N_2 at 150μ pressure For oxygen, the spectra were excited only at atmospheric pressure by 1 Mev protons.

In a later experiment, Reeves, Nicholls and Bromley[14] excited spectra of N_2 by H^+, H_2^+, H_3^+. (.5 to 1.5 Mev.) at pressure below 100μ. In order to obtain higher beam intensity (5μa) than those used in previous experiments, a differential pumping system was used. Previously a metallic window was used to separate the collision chamber from the accelerator system.

A small amount of work was carried out at Rice Institute, Houston, Texas by an arrangement shown in Fig. 2.6. The spectra of nitrogen produced by proton

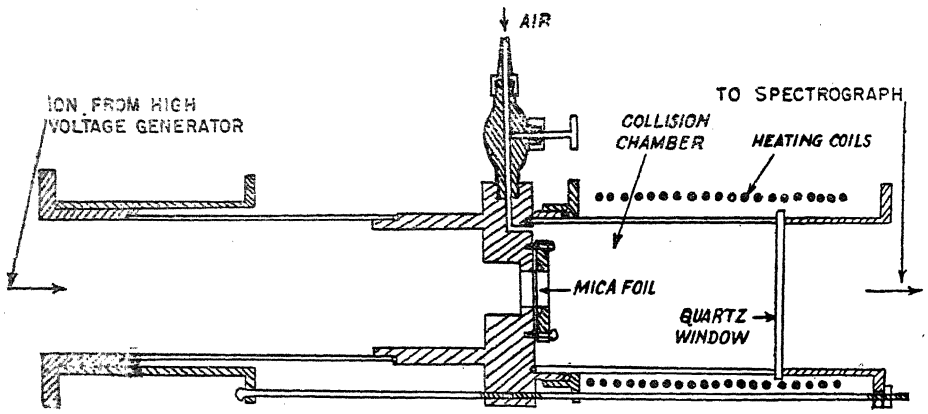

Fig. 2.6 The experimental arrangement employed by Shalek and Bonner for exciting spectra of nitrogen by bombardment of protons in air.

bombardment in air at 15 cm. of Hg and also at 4, 1.7 and 0.8 cm of Hg by Shalek and Bonner[4] were analysed by Branscomb.

Sluyter *et al* [13] investigated the excitation of inert gases by A_r^+ ion bombardment. A monoenergetic beam of Ar^+ ions (current 0·1 μa/mm and energy 5 – 24

Kev) was obtained from Amsterdam Isotope Separator. These ions pass through an entrance slit (5 × 5 sq mm) of a chamber containing two rectangular diaphragms of dimension 4 × 4 sq mm maintained at positive potentials with respect to the slit and as a result secondary electrons were suppressed. The beam was then allowed to enter a collision chamber containing an electrode system mounted on a steel support. A voltage across the Faraday cage, which was placed at the end of the collision chamber prevents reflected particles to reach the measuring section. A vacuum spectrograph described in section 2·2 was mounted prependicular to the collision chamber. A concave aluminium grating entrance slit and exit slit lie on a circle of one meter diameter Paschen Runge mounting. The angle of incidence of light on the grating was 13°. The entrance slit and grating were fixed. The exit slit and the E. M. I. 6256 B photomultiplier tube were mounted at the end of a steel lever arm, which was made to rotate around the center of the circle by a synchronous motor with a speed of 10 r. p. m. Several scanning speeds between 0.1 – 12 r/sec were employed. The signals from the multiplier tubes were amplified by a d. c. amplifier and then recorded. The radiation from the collision chamber was photographed through a thin LiF window of 0·5 mm thickness mounted between spectrograph and the collision chamber. To increase the limit of spectral observation from 1600 to 1000 A sodium salicylate fluorescent screen was placed between the tube and the exit slit.

CHAPTER III

Experimental Results

As already mentioned in the Introduction that four groups of investigators are presently engaged in excitating spectra by ion bombardment. The interest of two groups of the investigators, namely of Meinel and Fan[2,3,5,7,8] and Carleton [10,11] was to elucidate the mechanisms for the excitation of auroral spectra. On the other hand, the third group headed by Nicholls[6,12,14] and Sluyters *et al* are interested in finding characteristic of the spectra excited by ion bombardment. Carleton obtained spectra of N_2 excited by low energy proton bombardment, because he thought that although protons are emanated from the sun with high energy, when these come down to auroral heights they would have lost a large part of their energy so that low energy protons may excite auroral spectra.

The spectra excited by Meinel and Fan consisted of 1st and 2nd positive systems of N_2, 1st negative and Meinel systems of N_2^+, Balmer lines of H and also ionized and neutral atomic nitrogen lines. As in the spectra obtained by Meinel and Fan, Carleton obtained 1st and 2nd positive systems of N_2, 1st negative and Meinel systems of N_2^+, Balmer lines of H and neutral atomic nitrogen lines, but no NII lines. Nicholls, Reeves and Bromley obtained 1st and 2nd positive systems of N_2, N_2^+ 1st negative and Meinel bands, but no NI and NII lines or Balmer lines of H. On bombarding O_2, they observed only neutral and ionized atomic oxygen lines but no O_2 band systems or Balmer lines of H.

We shall now describe in detail the spectra obtained by these four group of workers and also consider the spectra excited by canal rays.

3·1 *Work at Yerkes Observatory*

Meinel and Fan[2,3] anl Fan[5,7,8] took several spectra of air at pressures ranging from 0·3 to 10^{-4} mm of Hg excited by proton bombardment of energy

5—350 Kev. They also observed spectra of air excited by He^+ of 10-450 Kev ion energy, D^+ of 75-320 Kev ion energy and by 400 Kev Ne^+ ion bombardment. The characteristics of these spectra will be presently discussed.

In 1952, Meinel and Fan[3] began their investigation on the excitation of spectra in air by proton bombardment. In the first two years, they bombarded air at a pressure of 0·3 mm of Hg with 40-230 Kev protons and observed spectra in the range 3500 - 6800 A. They recorded Balmer lines H_α, H_β and H_γ, some bands of N_2 1st positive system, second positive system of N_2, first negative system of N_2^+ and certain singly ionized nitrogen lines (λ5003, λ 5680, λ 6482) (Fig. 3·1). The

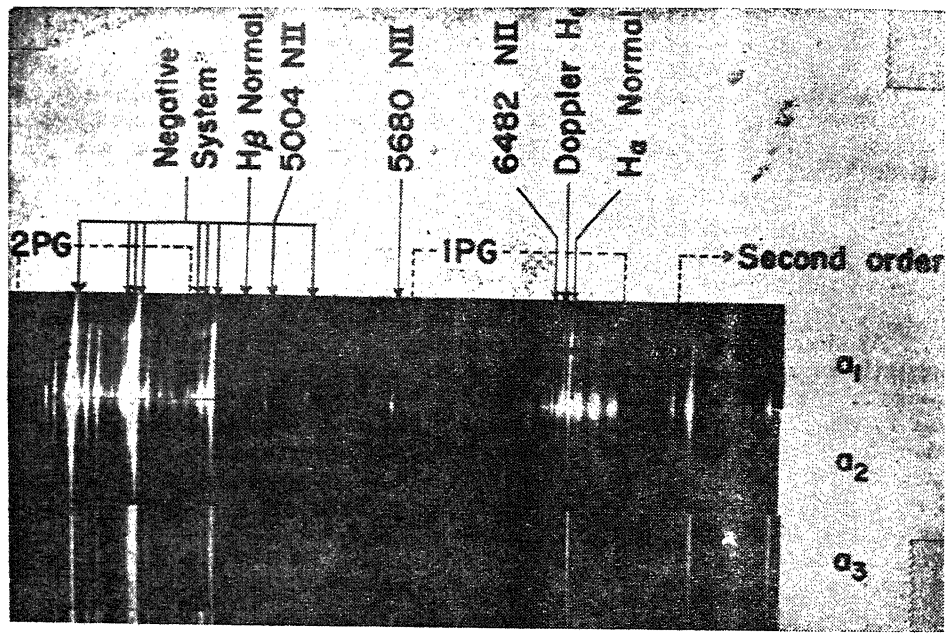

Fig. 3.1 Three early spectra in air (0.3 mm of Hg) obtained by Meinel and Fan by proton (energy 5-350 Kev) bombardments. Within the observed range 3500—6300A, they recorded Balmer lines $H\alpha$ $H\beta$, $H\gamma$, some bands of 1st positive system of N_2, 2nd positive system of N_2, 1st negative system of N_2^+ and certain NII lines.

intensity of 2nd positive bands was very low compared to that of 1st negative system which has the strongest feature in the spectra excited in air produced by bombardment by high energy protons. They could not observe neither N_2^+ Meinel system nor O_2^+ 1st negative system, because due to the low energy electrons which are produced as secondry electrons by the bombardment of ions on the window and walls, strong 1st positive band system of N_2 are excited. Hence, N_2^+ Meinel and O_2^+ 1st negative bands are obscured by the 1st positive system which appear in the same spectral region.

Later on in 1956, Fan[7,8] modified the experimental arrangements in order to reduce the emission of secondary electrons and observed N_2^+ Meinel and O_2^+ 1st negative system in addition to those observed previously. (Fig. 3·2) (In the exten-

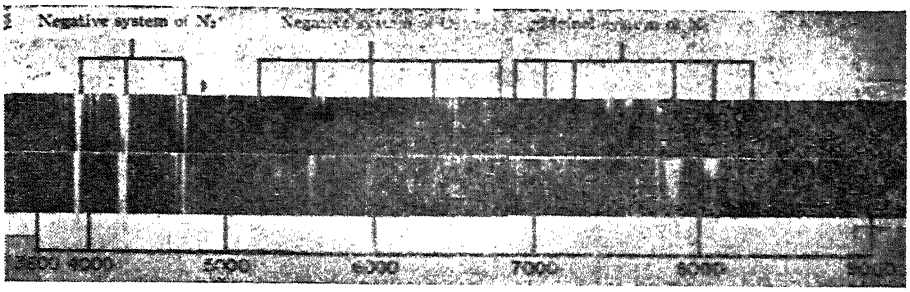

Fig. 3.2 The spectra obtained by Fan after modifying the experimental arrangments in such a way that the emission of secondary electrons is reduced. Note that N_2^+ Meinel and O_2^+ 1st negative systems appear in addition to those observed previously. (The upper spectrum was excited by 20 Kev and the lower by 300 Kev proton bombardments.)

ded spectral range neutral and atomic nitrogen lines λ8188, λ8681, λ8712 and singly ionized atomic oxygen lines were also observed.)

From the apparent difference in lateral intensities, Fan[8] observed many O_2^+ 1st negative bands, and indentified two additional O_2^+, λ6684 (2,4) and λ6777 (1,3) bands which are not observed by Singh and Lal[20] in the spectra produced by discharge in O_2.

Comparing the spectra excited by 20 Kev protons with that by 300 Kev proton in air (Fig. 3·2), it is found that the ratio of intensity of N_2^+ Meinel system to that of N_2^+ 1st negative system is very low by low energy proton relative to the high energy proton bombardment.

Hydrogen lines H_α and H_β are present in every spectra obtained by Fan and Meinel[2,3,5,7,8]. H_γ is only detectable in the spectra excited by high energy proton bombardment. Lines at λ5004, λ5680 and λ6482 of ionized nitrogen atoms are the strongest features in every spectra of H^+—air. Meinel and Fan also observed some neutral nitrogen lines in the infra-red region viz. λ8188, λ8681 and λ8712. Lines at λ7774 and λ8466 of neutral atomic oxygen lines are easily detectable. The intensity of λ7774 OI line by high energy proton bombardment is comparable to the intensity of λ7828 (2,0) of N_2^+ Meinel bands, and is higher compared to those of neutral nitrogen atomic lines in the infra-red region.

For spectra of He^+–air, Fan and Meinel[3] and Fan[8] observed all the bands and lines present in spectra excited by proton bombardment. In earlier experiments, Fan observed only λ5878 and λ6678 of He I normal and Doppler shifted lines

(Fig. 3.3). In 1956, he also identified the line λ3889 HeI line in the spectra in air

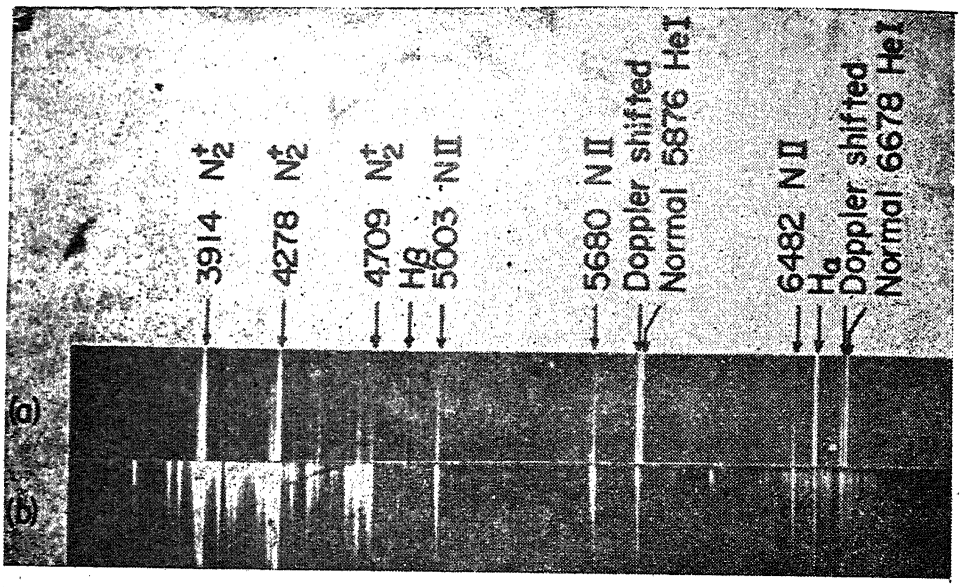

Fig. 3.3 The spectra excited by Fan by bombarding air by 10 Kev He^+ ions. The upper spectrum was taken at air pressure about 10 mm and the lower one at about 10 mm. Note the presence of λ5876 and λ6878 lines of HeI and associated Doppler shifted lines.

excited by 196 Kev He^+ ion bombardment (Fig. 3.4). In some of the spectra,

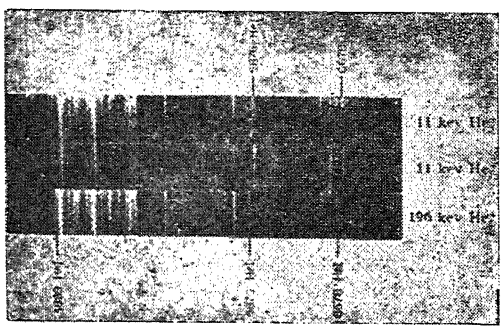

Fig. 3.4 The spectra obtained by Fan by bombarding air by 196 Kev He^+ ion. Note the presence of λ3889 HI line. The upper two spectra are the same as given in Fig. 3.3.

they also observed H_α and H_β lines, which may be due to the presence of minute amount of hydrogen in air. The intensity of bands excited by He^+ ion bombardment is nearly twice that obtained by proton bombardment of same velocity. At a pressure less than 1 micron, stationary HeI lines were not excited.

The spectra excited by the bombardment of 400 Kev Ne^+ ions and of D^+ ions of energy 75-320 Kev in air at 0.3 mm of Hg were observed in the ultraviolet and visible regions (Fig. 3.5). All the prominent bands of N_2 1st and 2nd positive,

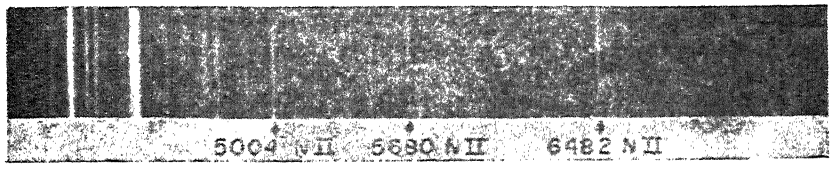

Fig. 3.5 The spectrum obtained by Fan and Meinel by bombarding air (0.2 mm) by 400 Kev N_2^+ ions. It is to be noted that N_2 2nd positive, N_2^+ 1st negative and certain NII lines (λ5004, λ5680 and λ6482) are present in the spectrum. No Ne line it recorded.

N_2^+ 1st negative and λ5004, λ5680 and λ6482 NII lines are present. No Ne line was observed.

3.2 Work at Harvard University

Since 1952, laboratory study for the excitation of N_2 bands by proton bombardment has been in progress at Harvard University. The first work was carried out by Branscomb *et al*[4,18] who were interested in the excitation of N_2 bands by the incoming protons from the sun. These protons should have energy between 100-150 Kev in order that they may penetrate to the auroral height (around 100 Km). In the earlier experiment,[18] they excited spectra of N_2 at a pressure of 15 cm of Hg and observed in the spectral range between 2500 and 5000A, all the prominent members of the second positive system of N_2 and (0,0) band of the first negative system of N_2^+. Later on the experiment was repeated[4] at a few millimeter air pressure and spectra were excited by proton as well as by neutral H atom bombardment. In the range 2500-5000A, they identified the presence of 27, second positive system of N_2 and 7 first negative system of N_2^+ (Fig. 3.6). No atomic lines or O_2 spectra were observed.

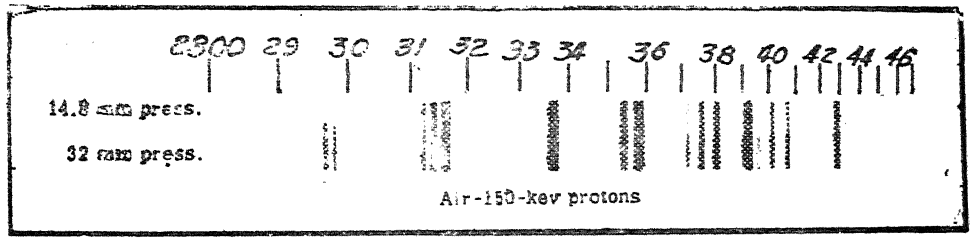

Fig. 3.6 The spectra obtained by Shalek and Bonner by 150 Kev proton and H atom bombardments in air at pressures 14.8 mm and 32 mm respectively. On analysing the spectra, Branscomb found that these spectra contain 2nd positive system of N_2, 1st negative system of N_2^+, but no atomic lines or O_2 bands.

By bombarding *He* with 2 Kev proton and H_2^+, Dieterich[9] observed only H_β line. In one of the plates, he identified λ5876 HeI line. For 2.4 Kev H^+ or H_2^+ ion bombardment in N_2 at a pressure from 10 to 50 micron of Hg, Cerleton[10]

observed 1st and 2nd positive systems of N_2, 1st negative system and Meinel systems of N_2^+, permitted NI lines and Balmer series of hydrogen atom (Fig. 3.7a). The

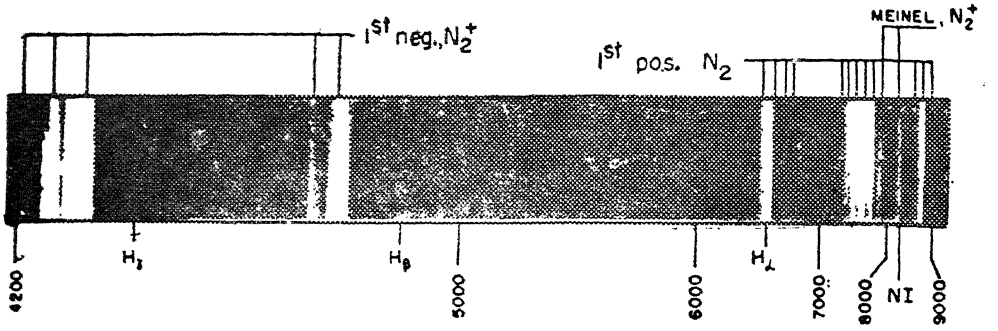

Fig. 3.7*a* The spectrum obtained by Carleton by bombarding N_2 at 20 micron pressure by 2.4 Kev proton. Note that 1st negative band system appears with great intensity.

most intense band is that of 1st negative system of N_2^+. Next in order of intensity are 1st positive system of N_2. Balmer series of H, Meinel N_2^+ system, NI lines and 2nd positive system of N_2. Cross sections for excitation of 1st negative band and Meinel systems of N_2^+ first positive system of N_2 and NI lines around λ8210 for proton bombardment are given in Fig. 3.7b.

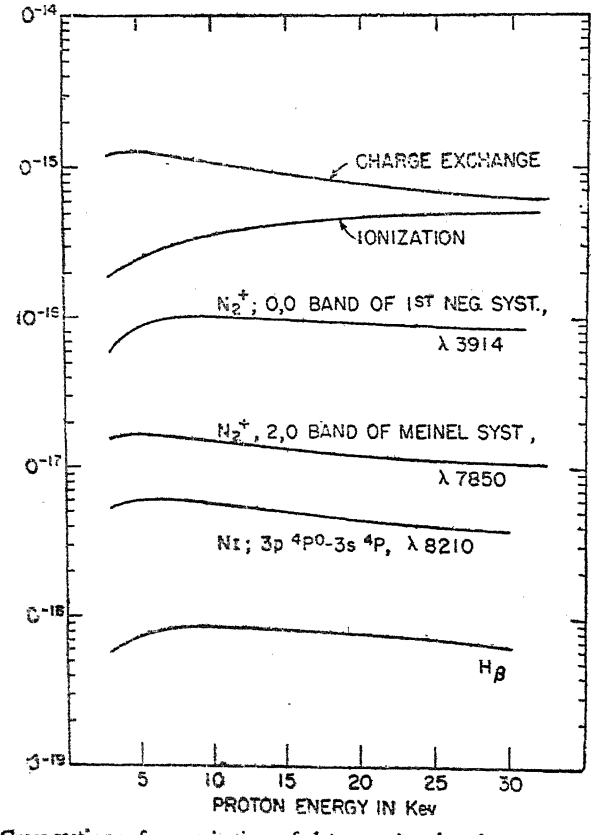

Fig. 3.7*b* Cross-sections for excitation of 1st negative band and Meinel systems of N_2^+, first positive system of N_2 and NI lines around λ8210 for proton bombardment.

In the spectrum taken by Carleton[21], NI lines were not fully resolved from the nearby Meinel band of N_2^+. NI lines were identified by indirect process, viz. by comparing the spectra obtained by ion bombardment with those of glow discharge spectrum taken on Hilger spectrograph. At the suggestion of Prof. Oldenberg, Carleton excited a glow discharge in the collision chamber at slightly higher than usual pressure with the beam cut off. Spectra of the discharge recorded with a Kipp spectrograph, showed the NI lines in the same position and unresolved in the same way as for ion bombardment. But on recording the spectra of the glow ischarge on Hilger spectrograph, he was able to identify two clearly resolved nes λ8181 and λ8681 and also observed H_α, H_β and H_γ lines.

3.3 Work at the University of Western Ontario

In 1956, Nicholls initiated laboratory study for the excitation of different gases by ion bombardment at the University of Western Ontario. He and his associates bombarded N_2, O_2, air and argon by 2–4 Kev Li^+ ions[6]. For N_2 and air they observed NI, NII and NIII lines and N_2^+ 1st negative system. The absence of positive systems* of N_2 which has been observed by others by proton and He^+ ion bombardment in air clearly shows that by the bombardment of Li^+ ions of 2–4 Kev energy in air or nitrogen, no ionization is produced. By bombarding O_2 and air by Li^+, neutral atomic oxygen lines were observed. On bombarding argon, Nicholls et al observed AI and AII lines. Neutral Li atomic lines are present in every spectra. Sodium lines are also present as impurity in nitrogen spectrum.

Nicholls et al[12] bombarded nitrogen by 0.5 and 1 Mev proton at different pressures and observed N_2^+ 1st negative, N_2 1st positive, N_2 2nd positive and N_2 G.G. system. No HI, NI or NII lines were recorded (Fig. 3.8).

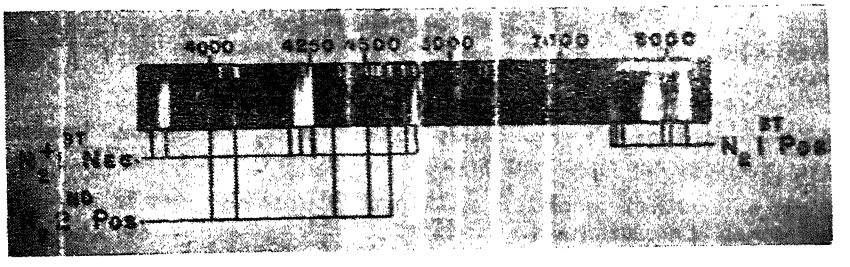

Fig. 3.8 Spectrum obtained by Nicholls *et al* by bombarding N_2 at 150μ pressure with 1 Mev proton.

Reeves et al[14] also bombarded N_2 by 0.5 to 1.5 Mev H^+, H_2^+, and H_3^+ at pressures below 100μ and observed N_2^+ (1st Negative and Meinel), N_2 (1st and 2nd pcsitive) bands. Several lines of NI and NII were also observed in some

* It has been observed by Fan that N_2 1st and 2nd positive systems are mainly excited by secondary electrons produced by ionisation of N_2 by ion bombardment. For Li^+ bombardment, no positive system was observed which indicates the absence of production of secondary electrons by ionization of N_2.

cases. In ion bombardments very weak H_α and H_β lines were also observed.

Nicholls et al[12] found that compared to the spectrum excited by discharge, a proton-induced spectrum has the following characteristics.

1. The bands arising from $v'=0,1$ level ($B^2\Sigma$) of 1st negative system of N_2^+ and those arising from $v'=0,1,2$, level of N_2 ($C\ 3\pi$) of 2nd positive system are enhanced in proton-induced spectrum.

2. The (8,5) N_2 1st positive bands in the proton-induced spectrum has much lower intensity relative to its neighbour (7,4), (6,3), (5,2) and (4,2) as compared to those produced by discharge.

Nicholls et al[12] also observed that in a proton-induced spectrum, the intensity of N_2 2nd positive bands relative to the adjacent 1st negative bands steadily increases with pressure upto atmospheric pressure. Furthermore they have found that for 1st positive bands of N_2 by 1 Mev proton bombardment in N_2, the intensity decreases between the pressure range 63μ and 5mm of Hg, and afterwards with higher pressure the intensity remains practically unchanged upto atmospheric pressure. No such variation has been observed for 0.5 Mev proton bombardment in N_2.

For O_2 bombardment by 1 Mev proton at atmospheric pressure, Nicholls et al[12] observed only OI and OII lines (Fig. 3.9). These lines are however less in

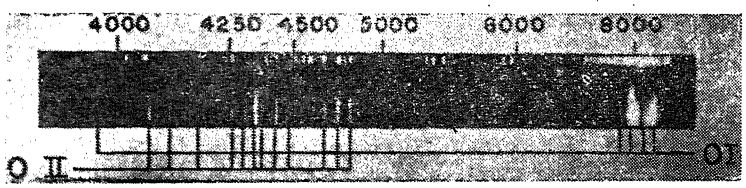

Fig. 3.9 Spectrum obtained by Nicholls *et al* by bombarding O_2 at atmospheric pressure with 1 Mev proton.

intensity compared to nitrogen bands excited in N_2 by proton bombardment. The identified lines and their multiplicities are given in the table III.

Some unidentified weak lines of OI and OII are also present in the blue and infra-red region of the spectrum. No H lines, and bands due to O_2 and O_2^+ are recorded in the spectrum.

The spectra excited by proton bombardments in different gases as observed by the three groups of investigators are summarised in Table IV and the spectra obtained by ions other than proton are listed in Table V.

3.4 Work at F.O.M. Laboratory of Mass spectrography, Amsterdam

In 1959. Sluyters et al[13] excited spectra in inert gases (He, Ne, Ar, Kr and Xe) by bombardment of Ar^+ ions of energy 5-24 Kev at low pressure (10μ) and observed them in the spectral range between 1000 and 6000 A. They identified neutral and ionized lines of argon and those of bombarded gases. The lines identified in different gases by bombardment of Ar^+ are given below :

Gas	*Spectra*
He	AII (52), HeI (6)
Ne	AI (30), NeI (5), NeII (4)
Ar	AI (19), AII (120), AIII (10)
Kr	AI (12), AII (60), AIII (8), KrI (13), KrII (64), KrIII (24)
Xe	AI (12), AII (82), XeI (5), XeII (10), XIII (14).

The number in parentheses denotes the number of identified lines.

TABLE III

The identified lines obtained by 1Mev proton bombardment in O_2 at atmospheric pressure

Wave length (A)	Identification with multiplicity	Wave length (A)	Identification with multiplicity
3947	OI (3)	4590-4596	OII (15)
3954	OI (30)	4641-4661 (5 lines)	OII (1)
4069-4076 (4 lines)	OII (10)	4699	OII (40)
4119	OII (20)	4699-4705	OII (25)
4185-4190 (2 lines)	OII (36)	7156	OI (38)
4275	OII (67)	7254 (3 lines)	OI (20)
4277	OII (68)	7473-7480 (4 lines)	OI (55)
4317-4319	OII (2)	7722-7775 (3 lines)	OI (1)
4347-4351	OII (16)	7943-7952 (4 lines)	OI (35)
4367	OII (2)	7981-7799 (3 lines)	OI (19)
4368	OII (5)	8221-8235 (7 lines)	OI (34)
4415-4417	OII (5)	8446-8447 (3 lines)	OI (4)
4465-4469	OII (94)		

TABLE IV

Investigator	Proton-energy (Kev)	Bombar-ded gas	Pressure (mm. of Hg)	Observed spectral region	Excited spectra
Meinel and Fan (1952)	230	air	.3	3500–5000	N_2^+ (1st Neg) H_β, N_2 (2nd Pos)
Fan and Meinel (1953)	40–230	air	.3	3500–6800	N_2 (1st Neg), NII, N_α, H_β, H_γ, N_2 (1st and 2nd Pos)
Fan (1956a)	5–350	air	$(1-.1) \times 10^{-3}$	3700–9000	N_2^+ (1st Neg)N_2 (2nd Pos) NII, NI, N_2 (1st Pos) N_2^+ (Meinel), H_α H_β H_γ
Fan (1956b)	5–350	air	,,	,,	N_2^+ (Meinel) N_2^+ (1st Neg) N_2 (1st and 2nd Pos) OI (7774, 8446), NI, NII; O_2 (1st Neg), H_α H_β H_γ
Shalek et al (1954)		N_2	8–150	2800–5000	N_2 (2nd Pos), N_2^+ (1st Neg 0.0)
Branscomb et al (1954)	100 to 150	air	a few mm	,,	N_2 (2nd Pos) N_2^+ (1st Neg)
Dieterich (1956)	2	H_2, He	10^{-3}	4000–8000	H_β
Carleton (1957-58)	2.4 15–4.5	N_2	$(.5–50) \times 10^{-3}$	4200–8900	N_2^+ (1st Neg), N_2 (1st Pos), H_α, H_β, H_γ, N_2^+ (Meinel), NI, N_2 (2nd Pos)
Nicholls et al (1959)	1,000	N_2	$(63–150) \times 10^{-3}$, 5, 25 and Atmospheric Pressure	3800–8500	N_2^+ (1st Neg), N_2 (1st and 2nd Pos) N_2 (G. G)
	500	,,	5–20, .15	,, ,,	N_2^+ (1st Neg), N_2 (1st, 2nd Pos)
	1,000	O_2	Atmospheric Pressure	,, ,,	OI, OII (See Table 3
Reeves et al (1960)	500–1,000	N_2	below 100×10^{-3} Pressure	3500–9000	N_2^+ (1st neg & Meinel), N_2 (1st and 2nd Pos), NI and NII lines

Strong neutral nitrogen lines are λ8188, λ8686 and λ8712.
Strong singly ionized nitrogen lines are λ5004, λ5680 and λ6482.
N_2 (G. G) is green Gaydon system of N_2.

TABLE V

The spectra obtained by ions other than proton as observed by three groups of investigators

Investigator	Ion	Ion energy (Kev)	Bombarded gas	Gas Pressure (mm of Hg)	Observed spectral range (A)	Excited spectra
Fan and Meinel (1953)	He^+	150 – 450	air	0·3	3500 – 6800	N_2^+ (1st neg.), N_2 (2nd pos.) NII, HeI
Fan (1955)	He^+	10	air	0·3	3700 – 9000	N_2^+ (1st neg.), N_2 (1st, 2nd pos.), NII, HeI, H_α, H_β, H_γ.
Fan (1956*a*)	He^+	10 – 450	air	$(0.5-100)\times10^{-3}$	3700 – 9000	N_2^+ (1st neg.), N_2 (1st, 2nd pos.), NII, HeI and N_2^+ (Meinel)
Fan (1956*b*)	He^+	10 – 450	air	$(0.1-10)\times10^{-3}$	3700 – 9000	N_2^+ (1st neg.), N_2 (1st, 2nd pos.), NII, HeI, N_2^+ (Meinel), O_2^+ (1st neg.) and OI.
Fan and Meinel (1953)	D^+	5 – 0	air	0·3	3500 – 6800	N_2^+(1st neg.), DI, NII and N_2(2nd pos).
	Ne^+		air	0·3	3500 – 6800	N_2^+(1st neg), NII and N_2 (2nd pos).
Dieterich (1956)	H_2^+	2	He, H_2	10^{-3}	4000 – 8000	HI (5876) and H_β
Nicholls et al (1956)	Li^+	2 – 4	N_2	$(5-40)\times10^{-3}$	3800 – 8500	NI, NII, NIII, N_2^+ (1st neg.), LiI and NaI
	,,	,,	O_2	,,	,,	LiI and OI
	,,	,,	air	,,	,,	NI, NII, NIII, OI, LII and N_2^+ (1st neg).
	,,	,,	A	,,	,,	LiI, AI and AII
Reeves et al (1960)	H_2^+, H_3^+	500 – 1,000	N_2	below 100×10^{-3}	3500 – 9000	N_2^+ (1st neg. and Meinel), N_2 (1st and 2nd pos.), several weak lines of NI and NII and very weak H_α and H_β.

Except for AIII, KrIII and XeIII, most of the spectra were detected in the spectral range between 3000-5800 A. AIII lines were present in the far and extreme, ultraviolet region. The probabilities of different optical transitions as function of energy of the ion beam were measured and the absolute emission cross-section of the corsponding spectral lines were calculated by using the formula,

$$\sigma(E) = \frac{4\pi}{\omega} \frac{s}{INk(\lambda)}$$

where,

ω—solid angle, in which light of the observing section radiates within grating surface

s—output of the multiplier in amperes

I—number of interactiong ions /cm^2/sec.

N—number of atoms in the measuring section

k(λ)—quantum efficiency of the spectrograph in amp. sec/quantum.

Using the above formula, the emission functions of AII lines (λ 4610, λ4658, λ4765 and λ4806) were calculated for Ar^+ ions bombarding He, Ne and Ar. Also, the emission functions of AII (λ4806) and XeII (λ 2475) for Ar^+ ion bombarding Kr and Xe were calculated.

3.5 Spectra Excited by Canal Rays

In canal ray experiments, ions are created by discharge in the same gas whose spectra are excited. In other words, in these experiments within the same tube, the ion source and the collision chamber which contains the bombarding gases are located (Fig. 3.10).

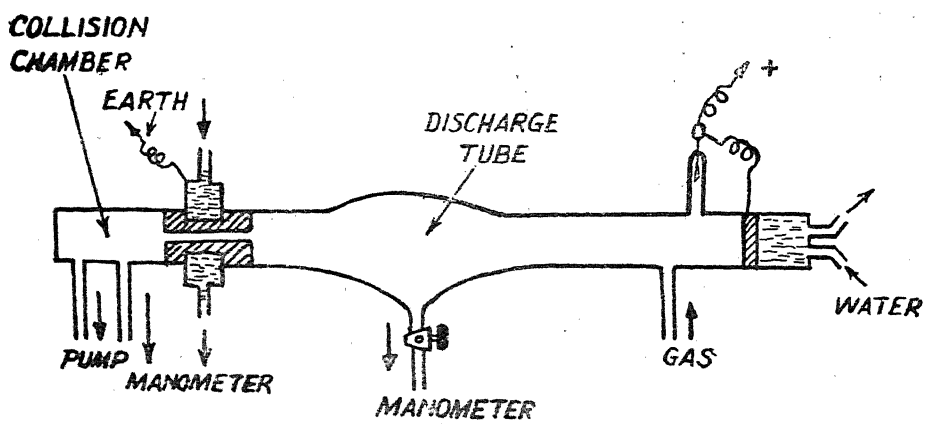

Fig. 3.10 Illustrating the arrangment for exciting spectra by canal rays. Note that within the collision chamber ion source is located.

As early as 1906 Stark and Hermann[23] excited spectra by canal rays in nitrogen. Later on in 1912 at Wurzburg Laboratory, Vegard[28] recorded spectra excited by canal rays in oxygen and nitrogen together with the comparison spectra of oxygen and nitrogen negative glow (swift electron) and nitrogen positive column (slow electron excitation) (Fig. 3.11).

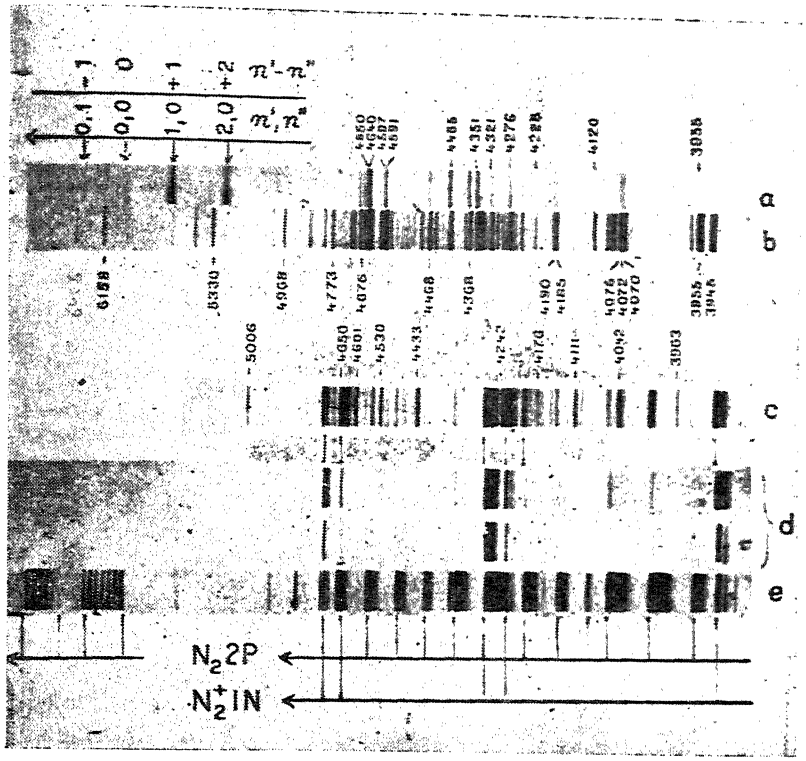

Fig. 3.11
Spectra excited by canal rays in oxygen and nitrogen as obtained by Vegard. Spectra (*a*) and (*b*) are those of O_2; (*c*), (*d*) and (*e*) of N_2.

In 1930, Symth and Arnott[24] throughly studied canal ray excitation in nitrogen in the spectral range 2100-5990A and measured the intensities of N_2^+ 1st negative and N_2 second positive band systems, which are compared with those obtained in discharge and by 700 ev electron bombardment in nitrogen (Fig. 3.12 Spectra of nitrogen discharge glow was also photographed.

With a view to deciding whether the 1st negative band system of N_2^+ in aurora are excited by ion or electron bombardment, Vegard and Raastad[25] in 1950 studied the intensity distribution within the 1st negative band system of N_2^+ produced by bombardment of canal rays in N_2 and those of negative glow (Fig. 3.13) and then compared these with the 1st negative band system of N_2^+ in aurora. They concluded that the auroral intensities for the two sequence v=1 and 2 agree with hose produced by canal rays. For the sequence v=o, the intensity in aurora and tnegative glow agree perfectly well.

Vegard *et al*[25] were also of opinion that some of the bands and lines in aurora might be excited indirectly by transfer of energy from metastable states (collision of second kind). With a view to verify this assumption, they compared the intensity distribution in the discharge in pure N_2 and N_2 mixed with He (metastable

states of He have sufficiently high energy to excite N_2^+ 1st negative bands) and then compared these with that of nitrogen 1st negative bands excited by canal rays of

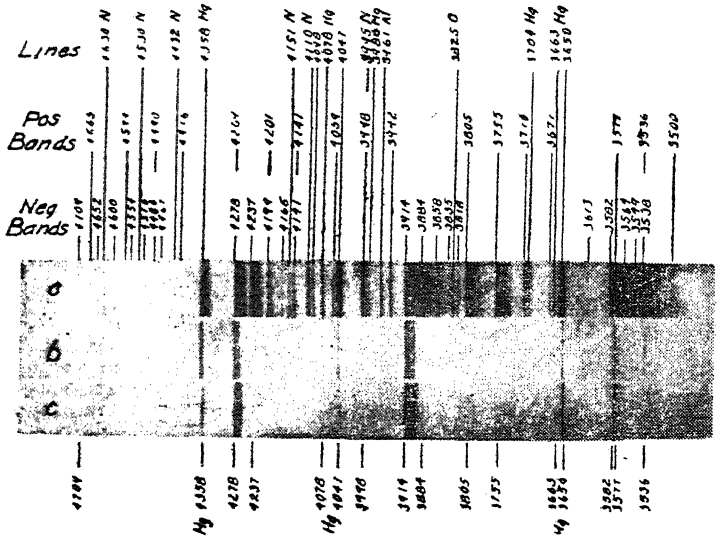

Fig. 3.12. Spectra excited by Smyth and Arnott by canal rays in nitrogen. Spectrum (*a*) is produced by canal rays (5500 Volts), (*b*) by discharge used as the source of canal rays and (*c*) by 700 ev electron bombardment.

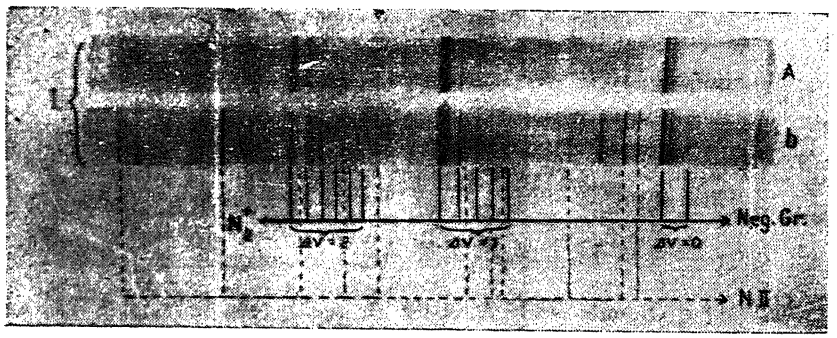

Fig. 3.13. Spectra of negative glow and that produced by canal rays in N_2 in a discharge tube having a potential of 14 Kev and pressume 0.04 mm.

different velocities (Fig. 3.14). They observed that excitation by metastable He

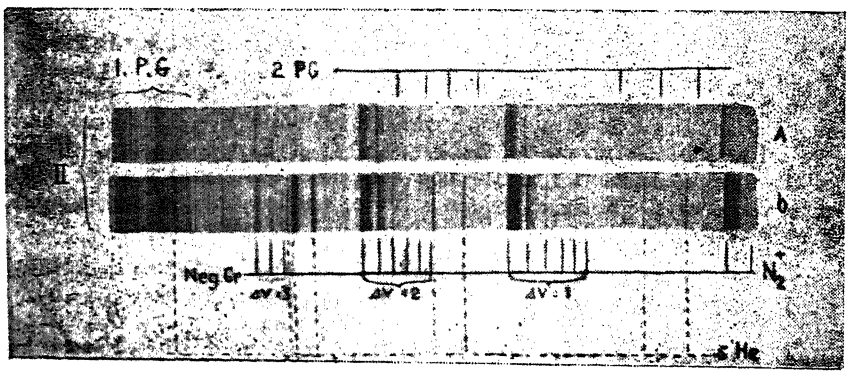

Fig. 3.14. Spectra obtained by Vegard in pure N_2 – He mixture (10% N_2 +90% He). The discharge potential is 3·5 Kev. and pressume is 0·5 mm.

atoms produce an enhancement of band of higher vibrational quantum number compared with that by swift electron (negative glow) in pure N_2. The distribution produced by He^+–collision is similar to that produced by canal rays. They also observed that the relative intensities of bands of higher vibrational quantum number within a sequence increases directly with the energy of canal rays.

In Table VI the characteristics of the spectra excited by canal rays are collected.

3.6 Spectra Excited by High Energy α–particles.

The spectral composition of the feeble light arising from the passage of energetic ions through gases may lead to an understanding of the processes by which ions lose energy during its passage through gases. With this view in mind, certain spectral observations of air bombarded by α—particles have been carried out. Thus, William and Huggins[25] excited spectra in air by α—particles emanated from radium and made observations in the spectral range 3600–4300A and observed N_2 2nd positive and N_2^+ 1st negative band systems. Ortner and Salim[27] also excited air by α–particles from a 4 mc. source of Polonium and identified OI (3948, 3947), OII (4304, 4295, 4076, 79, 85, 89, 83 and 3945), NI and NII lines, N_2 2nd positive, N_2^+ 1st negative system and some continua.

In 1957, Nicholls and Reeves[28] studied the luminescence produced in air by Polonium 210 α-particle. 28 mc α-particle source of Polonium 210 was used and the spectrum was recorded on a 8 mm film with an exposure of ten days.

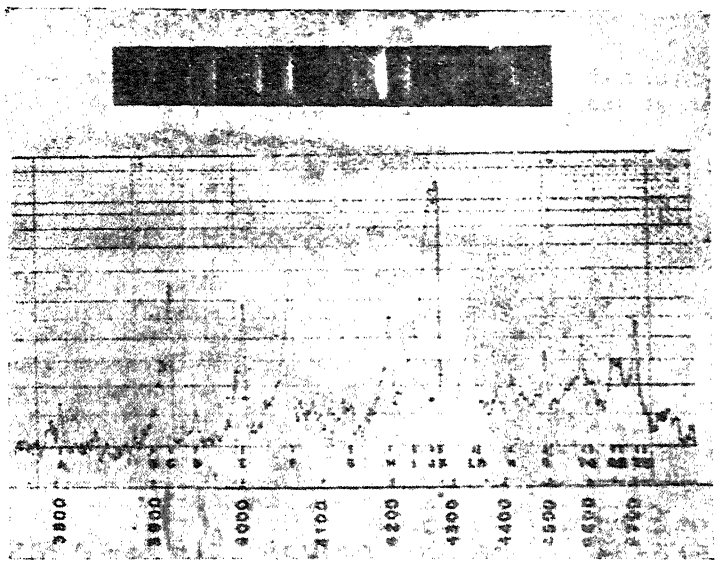

Fig. 3.15
The spectrum with the microphotometer tracing of luminosity produced in air by 28 mc. α-particle source of Polonium 21. The spectrum consists of N_2 2nd positive, N_2^+ 1st negative band systems. No atomic lines (neutral or ionized) of oxygen, nitrogen and helium were observed.

A typical spectrum with the microphotometer tracing is given in Fig. 3.15. In the range 3800–4800A of a typical spectra, the spectrum consists of N_2 2nd positive

TABLE VI

Investigator	Type of canal rays	Spectral range	Excited spectra
Stark and Heemann (1906)	Nitrogen	3500–5500	N_2^+ (1st neg) and N_2 (2nd pos.)
Vegard (1913)	Nitrogen	3550–5200	N_2^+ (1st neg), N_2 (2nd pos), NI (4670, 60, 26, 4344, 4224, 16, 08, 4167, 52, 46, 10, 4100)
			NII (5005, 4678, 4331, 21, 14, 07), OI (4530, 4488, 65, 47, 42, 33, 27, 4242, 37, 28, 4180, 77, 72, 46, 4082, 73, 44, 42, 36, 26, 3995), NIII (4524, 4379).
	Oxygen	,,	O_2^+, (1st neg), OI (6456, 6158, 5436, 5331, 5019, 4968, 4802, 4773, 4368), OII (4861, 4752, 05,00, 4676, 62, 50, 42, 09, 03, 4597, 91, 79, 71, 53, 17, 15, 4379, 51, 49, 47, 4343, 39, 34, 27, 20, 18, 05, 4295, 92, 88, 85, 80, 77, 55, 4190, 86, 83, 55, 19, 4098, 92, 89, 87, 84, 75, 72, 70, 61, 3972, 60, 45).
Smyth and Arnott (1930)	Nitrogen	2100–5990	N_2^+ (1st neg) 31 band, N_2 (2nd pos) 40 bands.
			NI
			NII
			Hg, Al and Cu lines
			Above 4708A, there was very little spectral feature. It is to be noted that the dispersion of E315 quartz Hilger spectrograph which was used for recording is small. Al, Cu lines are present as impurity. Some faints bands in the neighbourhood of λ2500 (possibly from 4th pos. system of N_2).
Vegard and Raastad (1950)	Nitrogen	3900–5700	N_2^+ (1st neg), NII (5699, 5005, 4640, 4528, 4431, 4240, 4175, 4041, 3960) lines. The identification for these lines are given by Vegard.

and N_2^+ 1st negative band systems. No atomic lines of NI, NII, OI, OII, HeI, HeII, were observed. The N_2^+ 1st negative band system has approximately the same intensity distribution as observed in a discharge in He-N_2 mixture. The 0 and 1 level of $C^3\pi$ state of N_2 2nd positive system is enhanced compared to those obtained in a discharge through N_2.

CHAPTER IV

Mechanism for Excitation of Spectra by Ion Bombardment

We have seen in Chapter III that by bombarding air, N_2 and O_2 molecules by ions two types of spectra are excited : (a) that of bombarded gas and (b) that due to bombarding ions. The spectra of the bombarded gas consist of ionized band systems of N_2^+ (1st negative and Meinel), band systems of N_2 (1st and 2nd positive), band system of O_2^+ (1st negative), atomic lines (neutral and ionized) of nitrogen and oxygen. No neutral band systems of O_2 are observed. The spectra due to bombarding ions are the atomic lines resulting from electron capture by bombarding ions.

Before we consider the mechanisms for the excitation of spectra in gases by ion bombardments, we shall briefly discuss the processes which lead to the excitation of gas molecules by ionic impact, namely

(i) Charge exchange with excitation

(ii) Charge exchange followed by dissociation and excitation

(iii) Ionization with excitation

(iv) Ionization followed by dissociation and excitation

(v) Mutual neutralization leading to excited atoms and molecules.

4.1 Collisional Processes Leading to the Excitation of Gases

(a) Charge Exchange.

Several reviews of this process[29-32] are available and may be consulted for fuller information.

Briefly, this process consists in neutralizing an ion and ionizing the collided neutral particle. Such a reaction involving diatomic molecules can be represented as follows :

$$A^+ + B_2 \rightarrow A + B_2^+ \pm \Delta E$$

$$A^+ + B_2 \rightarrow A + B^+ + B \pm \Delta E$$

where A^+ is the incident ion and B_2 is the molecule which is being bombarded by the ions. The products of the reaction may be in excited states.

The above process is of fundamental importance in ion transport phenomena for two reasons, (1) the change of energy envolved in the process is considerably

less than that for pure ionization, and (2) negligible kinetic energy transfer takes place between the incident ion and the ion formed by charge exchange. Whereas in pure ionization the incident particle must possess an amount of kinetic energy at least equivalent to the ionization potential of the struck particle, in charge exchange the energy change is just the difference between the ionization potentials of the two particles (assuming them to be in the ground states). Thus, a charge exchange process may occur when the incident ions have very small kinetic energy. Experiments have shown that ions formed in a change exchange reaction have much less than 1 volt energy even when the incident ions are of very high energy.[33,34] Therefore. the kinetic energy of the neutralized ions (atoms formed by charge exchange) is usually much larger than that of charge exchange ions.

For a large number of charge exchange reactions, it has been found that the cross-section becomes maximum in the region where the adiabatic condition[35] holds, namely

$$a \mid \Delta E \mid / hv \approx 1$$

where,

a—interaction distance (usually 7A)

ΔE—difference between ionization potentials of colliding particles

v—velocity of incident ions.

Fan[3] has shown that for endothermic reactions, the cross-sections for charge exchange reactions is maximum for the energy E_o of the incident ions given by

$$E_o = -QM/m$$

where,

M—mass of the incident ion

m—electronic mass

Q (<0)—the difference of binding energies of electrons in the two states before and after being captured.

Nicholls and Pleiter[6] hold that if, in a charge exchange reaction the time of a collision is comparable to the period of internuclear vibration, a violent perturbation of the internuclear motion occurs thereby producing dissociation and electronic excitation. They further state that charge exchange with dissociation becomes predominant if

$$f(2M/E)^{1/2} \approx 0{\cdot}1$$

where,

f—number of half periods of internuclear vibrations during which ion crosses the molecular diameter.

M—ionic mass in atomic weight unit.

E—ion energy in ev.

Nicholls and Pleiter contend that for $0{\cdot}001 < f < 0{\cdot}01$, only charge exchange (without dissociation) occurs.

A large amount of theoretical and experimental studies of charge exchange cross-sections have been carried out.[37-47] Since we are primarily interested in the interactions between protons with air, N_2 and O_2, we shall briefly describe the results obtained for such reactions.

The charge exchange cross sections for $(H^+ - air)$, $(H^+ - N_2)$ and $(H^+ - O_2)$ reactions have been determined by several investigators from very low energy (10 ev) to 1 Mev and are shown in Fig. 4·1. It will be seen that in the above

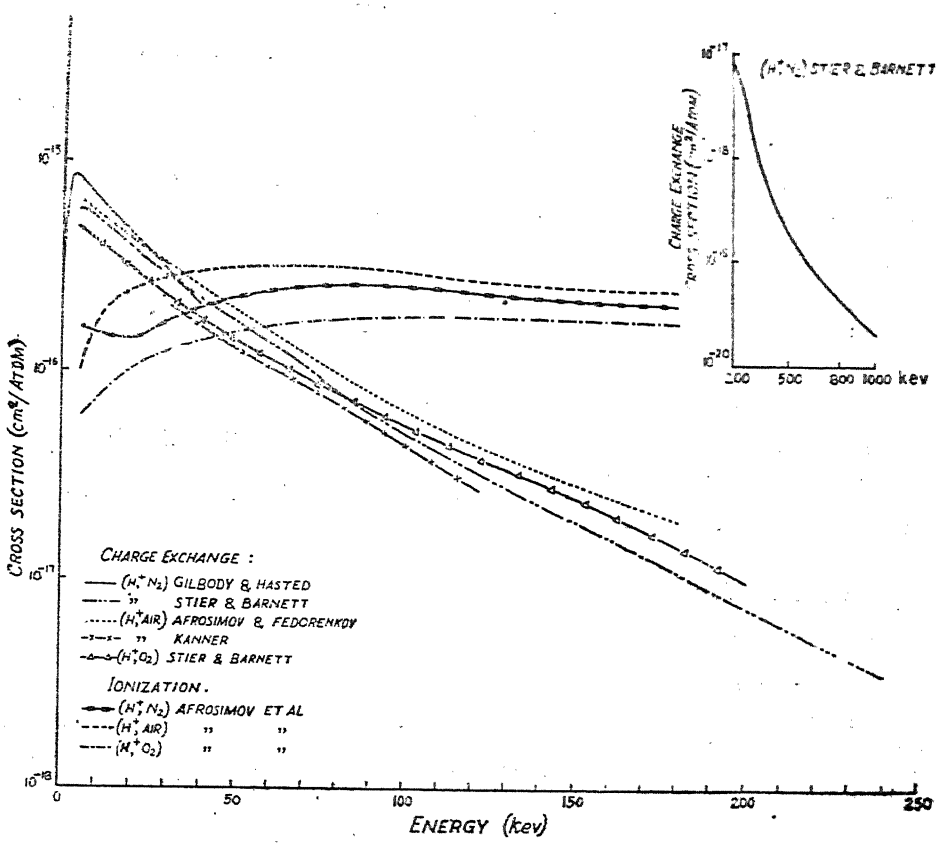

Fig. 4.1 The variations of charge exchange cross-sections for (H+ – air), (H+ — N_2) and (H+ — O_2 reactions from 10ev to 1 Mev as obtained by several investigators. Note that the cross-sections become maximum at a few Kev ion energy. The other three curves illustrate the variations of ionization cross-sections of N_2, O_2 and air by proton bombardments. Note that at high energies of the order of several tens of Kev, where charge exchange cross-sections are low, the cross-sections for ionization become high.

energy range cross-sections vary over several orders of magnitude and that they become maximum at a few Kev ion energy.

(*b*) *Ionization*

We have seen before that the charge exchange cross-section becomes large at comparatively low energy and decreases rapidly with energy when the energy is of the order of several tens of Kev. In the high energy range, the bombarded particles are ionized and we have the following processes for the interactions between ions and gas molecules (diatomic) :

$$A^+ + B_2 \rightarrow A^+ + B_2^+ + e$$

$$A^+ + B_2 \rightarrow A^+ + B + B^+ + e.$$

In these cases also reaction products may also be in excited states.

The cross-sections for ionization of N_2, O_2 and air by proton bombardments shown in Fig. 4·1 confirm the statement stated above.

Table 7[48] gives the energy loss by protons and H atoms while passing through H- atoms in excitation, charge exchange and ionization.

(*c*) *Mutual Neutralization*

In this process positive and negative ions collide producing two excited particles :

$$A^+ + B_2^- \rightarrow A' + B_2' \pm \triangle E$$

$$A^+ + B_2^- \rightarrow A' + B' + B \pm \triangle E.$$

The ionization energy of A minus the electron affinity of B_2 molecule is shared by the neutralized atoms and molecules. It has been shown from theoretical considerations that near about the resonance condition ($\triangle E \approx O$), the probability of such a reaction becomes high.[49]

4.2 Spectra of the Bombarded Gas

(*a*) *Spectra of Nitrogen*

(*i*) N_2^+ *1st negative band system*

After exciting spectra in air at different pressures and energies, Fan and Meinel[3,5] and Fan[7,8] concluded that the 1st negative band system of N_2^+ is excited during the process of charge exchange and direct ionization, and proposed the following reactions for the excitation of this band system :

(i) $A^+ + N_2 \rightarrow A + N_2^{+*} (B^2\Sigma)$ (charge exchange)

(ii) $A^+ + N_2 \rightarrow A^+ + N_2^{+*} (B^2\Sigma) + e$ (direct ionization)

where A^+ is the incident ion or secondary electron. The latter may be produced at the walls of the collision chamber by the bombardment of incident ions.

After altering the experimental arrangements such that the ejection of secondary electrons are reduced (see Chapter II), Fan confirmed the validity of the above two mechanisms.

From the linear plot of light intensity per unit current of proton with N_2 pressure, Carleton observed that N_2^+ 1st negative system is excited by a single collisional process, namely

TABLE VII

Analysis of energy loss contributions in units of ($eV \times 10^{-15}$ cm^2)

$Log_{10}E$ (Kev)	1.00	1.25	1.50	1.75	2.00	2·25	2.50	2.75	3.00	3.25
Process					Proton impact					
Ionization	2.62	4.29	5.15	5.07	4.18	3.04	2.07	1.39	0.887	0.538
Excitation	2.60	2.64	2.32	1.82	1.37	0.959	0.648	0.426	0.274	0.174
Capture excitation (charge exchange)	1.87	1.81	0.939	0.258	4.11×10^{-2}	4.07×10^{-3}	2.86×10^{-4}	1.57×10^{-5}	7.18×10^{-7}	2.93×10^{-8}
Process					Neutral H atom impact					
Single Ionization	1.79	2.52	3.09	3.33	3 11	2.56	1.89	1.32	0.780	0.570
Double Ionization	3.81×10^{-3}	4.65×10^{-2}	0.293	0.902	1.58	1.80	1.55	1.12	0.709	0.429
Single excitation	0.518	0.332	0.198	0.113	6.43×10^{-2}	3.67×10^{-2}	2.04×10^{-2}	1.14×10^{-3}	6.50×10^{-3}	3.61×10^{-3}
Double excitation	2.23×10^{-2}	8.35×10^{-2}	0.144	0.161	0.136	9.52×10^{-2}	6.03×10^{-2}	3.83×10^{-2}	2.21×10^{-2}	1.28×10^{-2}
Simultaneous excitation	2.04×10^{-2}	0.127	0.380	0.603	0.584	0.430	0.278	0.177	9.65×10^{-2}	6.07×10^{-2}
Capture excitation	0.493	0.366	0.252	0.090	0.026	0.00	—	—	—	—

(i) $H^+ + N_2 \rightarrow H + N_2^{+*}$ (charge exchange)

(ii) $H^+ + N_2 \rightarrow H^+ + N_2^{+*} + e$ (direct ionization).

Of the two processes, charge exchange process is favoured for low energy ion bombardment.

The 1st negative band system of N_2^+ can not be excited by secondary electron bombardment, because the excitation mechanism would then be a two-stage process, namely (a) production of electrons by bombardment of ions and (b) the excitation of 1st negative bands by electrons thus produced. The variation of light intensity with N_2 pressure would then be given by a quadratic curve instead of by a linear one.

From the absence of Balmer lines of H atoms in spectra excited by high energy protons in N_2, Nicholls et al[12] concluded that at high energy the charge exchange cross-section is low and hence the 1st negative bands are excited by ionization and excitation of N_2, namely

$$H^+ + N_2 \rightarrow H^+ + N_2^{+*} + e$$

$$N_2^{+*} \rightarrow N_2^+ + h\nu \text{ (1st negative band system).}$$

The secondary electrons thus produced may also excite N_2^+ 1st negative band system at higher pressure (above 80μ). However, the apparent increase in the intensity of 1st and 2nd positive band systems of N_2 with pressure relative to N_2^+ 1st negative band system favours proton excitation for N_2^+ bands.

While corroborating the suggestion given by Fan[7,8]. Branscomb et al[18] have also suggested that the excitation of 1st negative bands of N_2^+ may also be produced by neutral H atom bombardment.

(ii) N_2^+ Meinel band system

Before 1956, Fan excited Meinel band system of N_2 by electron bombardment. In 1956, Fan also excited this band system by secondary electrons produced by 2 Kev electrons. Fan[8] also observed that the intensity ratio of N_2^+ 1st negative system compared to Meinel system is almost constant in spectra excited by primary electrons for energies greater than 25 ev. Furthermore, he found that the ratio of the intensity of Meinel to 1st negative band system is more or less same for ions as for electrons of same velocity, and that, this ratio is much larger in case of 300 Kev proton bombardment compared to that produced by 20 Kev proton bombardment.

For 205 Kev proton bombardment in air, Fan observed that the ratio of intensity of 1st negative system to Meinel system of N_2^+ is about ten times higher than that produced by electrons with an energy of 120 ev. He suggested that this difference might be due to the fact that in the case of ion bombardment, there is an appreciable change of momentum transfer, which causes an increase in the internuclear distance of N_2^+ ions after collision.

Carleton[10] and Carleton et al[11] observed N_2^+ Meinel system by (2-5 Kev.) proton bombardment of N_2. As in the case of 1st negative band of N_2^+, they found that the plot of intensity of N_2^+ Meinel band per unit current of bombar-

ding particles with respect to N_2 pressure is linear suggesting that the excitation mechanism of Meinel system may be as follow :

$$H^+ + N_2 \rightarrow H^+ + N_2^+ (A^2\pi) + e \text{ (ionization)},$$

$$H^+ + N_2 \rightarrow H + N_2^{+*} (A^2\pi) \text{ (charge exchange)}.$$

As remarked in Sec. 4.1 for low ion energy, the charge exchange mechanism is favoured compared to ionization.

Reeves, Nicholls and Bromley[14] on bombarding N_2 with H^+, H_2 and H_2^+ ions (0.5 – 1.5 Mev) observed N_2^+ Meinel band system and proposed that like N_2^+ 1st negative band system, Meinel band system is also excited by direct ionization by ion bombardment.

(iii) First and Second Positive Band Systems of N_2

Excitation of first and second positive systems of N_2 by ion bombarnment has been attributed by different investigators to several secondary processses (not involving primary ions). This is because the excitation to the upper states of these band systems involve a change in multiplicity (inter-combination transition), and therefore these band systems cannot be excited by the primary proton beam. Fan[8] and Nicholls et al[12] were of opinion that N_2 molecules were excited by secondary electrons produced either by reactions between protons and N_2 or from walls by bombardments of ions. On the other hand, Branscomb et al[13] and Carleton[10] hold that these band systems are excited by H atoms produced by charge exchange between protons and N_2 molecules.

Meinel and Fan assumed that 1st and 2nd pasitive band systems of N_2 are excited by secondary electrons.

$$\text{(i) } N_2 + e \rightarrow N_2 (B^3\pi_g \text{ or } C^3\pi_u) + e$$

$$\text{(ii) } N_2^+ + e \rightarrow N_2 (B^3\pi_g \text{ or } C^3\pi_u).$$

Fan[8] verified the process (ii) by comparing three spectra excited by 23 ev and 500 ev electrons, and 20 Kev protons. For spectra obtained by 25 ev electron bombardment only 1st and 2nd positive system of N_2 are excited indicating that N_2 molecules are excited by process (ii). In the spectra excited by 500 ev electrons and 20 Kev protons, the intensities of 1st and 2nd positive systems are negligible compared to that of 1st negative system of N_2 indicating that for high energy electron or proton bombardment, N_2 molecules are ionized and excited.

Branscomb et al[13] have suggested that the 2nd positive system of N_2 produced by 100 Kev proton bambardment is excited by H atoms. These atoms are produced with increasing percentage as the proton beam loses energy by collision with gas molecules and are slowed down to a few Kev or less.

Carleton[10] observed that the intensity of 1st positive system of N_2 varies approximately as the square of N_2 pressure, thereby confirming that this system was excited by a secondary process. He holds that the 1st positive system of N_2 was produced by neutral H atoms formed by charge exchange between protons and N_2 molecules. This is confirmed by his observations[11], namely that the intensity of N_2 1st positive system varies directly with N_2 pressure for unit current of H atoms.

From the above it is clear that the 1st and 2nd positive bands of N_2 are excited by proton bombardment either by high energy H atoms produced by charge exchange or by secondary electrons produced by ionization of gases. This view was corroborated by Bates.[50]

(iv) Excitation of Atomic Nitrogen Lines

As already mentioned in Chapter III, NI and NII lines are excited by ion bombardment of air or N_2. Excitation of these lines can be produced by the following reactions :

(i) $A^+ + N_2 \rightarrow A + N^{+\prime} + N'$ (charge exchange followed by dissociation and excitation)

(ii) $A^+ + N_2 \rightarrow A^+ + N^{+\prime} + N' + e$ (ionization followed by dissociation and excitation)

Fan[5] assumed that direct ionization and dissociation of N_2 (process ii) is responsible for the excitation of these lines by high energy ion bombardment. On the other hand, for low energy ions, charge exchange with dissociation (process i) is preferred.

For excitation of weak lines of NI and NII by H_2^+ and H_3^+ ion bombardments of N_2, Reeves et al[14] proposed an ionization process followed by dissociation.

4·2 (b) Spectra of Oxygen

As already mentioned only a few spectra of oxygen are excited by ion bombardment. In 1956, Fan observed[7,8] some O_2^+ 1st negative band system and a few OI lines by ion bombardment of air. Also, by bombarding O_2 with 1 Mev protons, Nicholls et al observed neutral as well as singly-ionized atomic oxygen lines, but did not notice any band feature.

(i) O_2^+ 1st negative, OI and OII lines

Fan[8] suggested that the exciatation of O_2^+ 1st negative band system is probably caused by the same process which excite Meinel band system by bombardment of N_2, namely that by secondary electrons produced either from walls or by reactions between ions and air molecules.

Nicholls et al suggested the following mechanism for the excitation of OI and OII lines which are produced by bombardments of 1 Mev protons in oxygen at atmospheric pressure :

$H^+ + O_2 \rightarrow H^+ + O^{+\prime} + O' + e$ (ionization followed by dissociation with excitation)

$O' \rightarrow O + h\nu$ (OI lines)

$O^{+\prime} \rightarrow O^+ + h\nu$ (OII lines).

It is to be noted that Balmer lines of H otoms are not excited by high energy proton bombardment of O_2 indicating that charge exchange does not occur for such bombardments.

4.2. Spectra due to Bombarding Ions

Atomic lines of neutralized ions

HI lines

As mentioned before Meinel and Fan[3], and Carleton[10] observed Balmer lines by bombardment of air or N_2 with protons. In addition to the stationary lines, Fan observed Doppler shifted Balmer Lines.

According to both Fan[7,8] and Carleton[10], Balmer lines were excited by the following reactions:

(i) $H^+ + B_2 \rightarrow H' + B_2^+$ (charge exchange)

$H' \rightarrow H + h\nu$ (Doppler shifted Balmer lines)

(ii) $H^+ + B_2 \rightarrow H' + B_2^+$ (charge exchange follwed by excitation of neutralized ions)

$H' \rightarrow H + h\nu$ (Balmer series).

On bombanding N_2 by H_3^+ ions, Reeves et al[14] observed very weak H_α and H_β lines and proposed the following excitation process:

$$H_3^+ + N_2 \rightarrow \left.\begin{matrix} H + H^+ \\ \text{or } H_2^+ \end{matrix}\right\} + H^* + N_2^{+*} + e.$$

4·4. Discussion

From the study of spectra produced by ion bombardment in gases, it can be concluded that gases are excited mainly by charge exchange accompanied by excitation (at low ion energy) and by ionization followed by excitation (at high energy of the order of several tens of Kev). For both these processes the resultant products may by dissociated.

It has been found from mass-spectrometric analysis of N^+ ions produced by bombardment of air by protons of energy 5-180 Kev, that the cross-section for the production of these ions is maximum at 20 Kev. This accounts for strong NII lines (λ5003, λ5686, and λ6482) in 20 Kev proton-induced spectra. Again, from mass-spectrometric analysis it has been found that the cross-section for N^{++} ion formation is maximum in the energy range 30—70 Kev proton bombardment. If N^{++} ions are excited, we may expect to find NIII lines by bombardment of protons of this energy. Likewise OII lines may be observed by proton bombardment in the energy range (10-30 Kev) where cross-section for the formation of O^+ ions is maximum.

It has been observed, that Balmer lines of hydrogen are present in proton-induced spectra only up to 80 Kev proton energy. Such observation has also been reported by Vegard[23] in hydrogen canal ray excitation. The absence of these lines in the high energy proton-induced spectra by Branscomb et al[18] and Nicholls et al[12] can be accounted for by the very low cross-section of charge exchange at high energy.

Nicholls et al[12] performed expriments of O_2 bombardment by high energy protons at atmospheric pressure. If the expriments were performed at low pres-

sure, one would expect to have enhanced lines from metastable states due to low collisional frequency. The lines of ionized state are also expected to be enhanced because of low probability of neutralization of ions with electrons at low pressure. It may be noted that by 1 Mev proton bombardment of O_2, Nicholls et al did not observe O_2 band system (neutral or ionized). Unlike N_2 molecules, O_2 is not excited during ionization by high energy proton bombardment. The O_2 molecules are dissociated and hence account for atomic oxygen lines.

Problems

A few suggestions for future work on the excitation of spectra of gases by ion bombardment are given below:

1. The excitation of spectra of gases by porton bombardment has been carried out only at several discrete energies, namely at 2·4 Kev, 5-350 Kev and 1 Mev. Investigation should be carried out over a wide variation of energy ranging from a few Kev to Mev because the relative importance of different processes (charge exchange, ionization, mutual neutralization etc.) varies markedly with the energy of the bombarding ions.

2. Information regarding the excitation of spectra by bombardment of ions other than protons is very meagre. Data should be collected for other ions having different energies.

3. More work on the excitation of oxygen molecules should be carried out. Unlike N_2, the O_2 bands are not excited by ion bombardment. Also, spectra of other gases should be excited by ion bombardment.

4. Data regarding excitation of spectra by electron bombardment are also not sufficient. Concentrated efforts should be made to excite spectra by electrons.

5. Work for excitation by netural beams should also be carried out. The available data is extremely meagre.

REFERENCE

1. Moak, C. D., Reese, H. and Good, W. M., *Nucleonics*, **9**, 18 (1951).
2. Meinel, A. B. and Fan, C. Y., *Ap. J.*, **115**, 330 (1952).
3. Fan, C. Y. and Meniel, A. B., *Ap. J.*, **118**, 205 (1953).
4. Branscomb, L. M., Shalek, R. J. and Bonner, T. W., *Trans. Am. Geophy. Un.*, **35**, 107 (1954)
5. Fan, C. Y., *Ap. J.*, **122**. 350 (1955).
6. Nicholls, R. W. and Pleiter, D., *Nature* (London), **178**, 1456 (1956).
7. Fan, C Y., Airglow and Aurorae, Pergaman Press, London, 1956, Page 276.
8. Fan, C. Y., *Phys. Rev.*, **103**. 1740 (1956)
9. Dieterich, E. J., *Phys. Rev.* **103**, 632 (1956).
10. Carleton, N. P., *Phys. Rev.*, **107**, 110 (1957).
11. Carleton, N. P. and Lawrance, T. R.. *Phys. Rev.*, **109**, 1159 (1958).
12. Nicholls, R. W., Reeves, E. M. and Bromley, D. A., *Proc. Phys. sec.*, **74**, 87 1959).
13. Sluyters, J. M. and Kistemaker, J., *Physica*, **25**, 1389 (1959).

14. Reeves, E. M., Nicholls R.W. and Bromley, D. A., *Proc. Phys, Sec.*, **76**, 217 (1960).

15. Page, T., *Ap. J.*, **108**, 157 (1948),

16. Instruction Manual of M/s. N. V. Instrumentfabrick Er-Hardel v.h.p.j. Kippt and Zonen-DELFT (Holland).

17. Reeves, E. M. and Nicholls, R. W., *J. Opt. Soc. Amer*, **48**, 358 (1958)

18. Shalek, R. J., Bonner, T. W. and Branscomb, L M., *Phys. Rev.*, **85**, 739 (1954).

19. Carleton, N. P., *Rev. Sci., Instr*, **28**, 9 (1957).

20. Singh. N. L. and Lal, L, *Science and Culture* (Calcutta), **9**, 89 (1943).

21. Sheridan, W. F., Oldenberg, O and Carleton, N. P. 2nd International conference on the Physics of Electronic and Atomic Collisions, University of Colorado, Boulder 1159, 1961.

22. Stark, J. and Harmann, W., *Phys. Zeits.*, **7**, 92 (1906).

23. Vegard L., *Phys. Zeits.*, **14**, 677 (1913).

24. Smyth, H. D. and Arnott, E. G F., *Phys Rev.*, **36**, 1023 (1930).

25. Vegard, L. and Raastad, H., *Geophys. Publ.*, **17**, No. 7 (1950).

26. Huggins, Sir Wm. and Huggins, Lady, *Proc. Roy. Soc., A*, **72**, 196 (1903) ; *ibid* **76**, 488 (1905). **77**, 130 (1906).

27. Ortner, G. and Salim, *S., Nature*, **169**, 1060 (1952).

28. Nichools, R. W. and Reeves, E. M., *Nature*, **180**, 1168 (1957).

29. Massey, H. S W. and Burhop, E. H. S. Electronic and Ionic Impact Phenomena (Clarendon Press, Oxford, 1952).

30. Allison, S. K. and Warshaw, S. D., *Rev. Mod. Phys.*, **25**. 779 (1953).

31. Ghosh. S. N., Sheridon, W. F., Dillon, Jr. J. A. and Edward, H. D., **Geophysical Research** paper no. **48**, 1955.

32. Allison, S. K., *Rev. Mod. Phys.*, **30**, 1137 (1958).

33. Sherwin, C. W., *Phys. Rev.*, **57**, 814 (1940).

34. Keene, J. P., *Phil, Mag.*, **40**, 369 (1949).

35. Massey, H. S. W., *Rep. Prog. Phys.*, **12**, 248 (1949).

36. Fan, C. Y. Conference on Physics of Electronic and Atomic Collisions, **New York, Jan,** (1958).

37. See references given by Allison, S. K , *Rev. Mod., Phys.* **30**, 1137 (1958).

38. Potter, R. F., *J. Chem. Phys.* **22**, 974 (1954).

39. Dillon, J. A., Sheridan, W. F. Edwards, H. D. and Ghosh, S. N., *J. Chem. Phys.*, **23**, 776 (1955).

40. Ghosh, S. N. and Sheridan, W. F., *J. Chem. Phys.*, **25**, 1076 (1956) *ibid.* **26**, 480 (1957), *ibid.* **27**, 1436 (1957).

41. Ghosh, S. N. and Sheridan. W. F., *Ind. J. Phys.*, **61**, 193 (1956).

42. De Heer, F. J., Huizinga, W. and Kistemaker J., *Physica*, **23**, 181 (1957).

43. Moisiewitsch, B. L, *Proc. Phys. Soc.*, **69**, 653 (1956).

44. Fedorenko N. V. and Afrosimov, V. V., *J. Tech. Phys.*, (USSR) **26**, 1941, (1956) Soviet Phys. JETP 1872 (1956).

45. Federenko, N. V., Afrosimov, V. V. and Kaminkar *J. Tech. Phys.* (USSR) **26**, 1926 (1956), Soviet Physics. JETP **1**, 1861 (1956).

46. Il'in, R. N., Afrosimov, V. V. and Fedorenko, N. V. Soviet Physics JETP volume 36 (9), 29 (1959).

47. Sluyters, Th. J. M., De Haas, E. B. and Kistemaker, J. *Physica* 25, 1379 (1959).

48. Dalgarno, A. and Griffing, G. W. *Proc. Roy Soc.*, **232**, 423 (1955).

49. Bates, D. R., Massey, H. S. W. *Proc. Roy. Soc.*, (London) **137**, 261 (1946).

50. The Earth as A Planet ed. by G. P. Kuiper pp. 626 (The University of Chicago Press, Chicago, 1954).

ROCKET SPECTROSCOPY

By

S. N. GHOSH *and* SHARDA NAND

J. K. Institute of Applied Physics, University of Allahabad, Allahabad.

[Received on 7th April, 1962]

1. INTRODUCTION

With the help of rocket-borne spectrographs, the solar spectrum between the wavelength range 3000A to X-rays can be explored. This region in inaccessible to ground-based spectrographs, because these radiations are absorbed in the upper regions of the earth's atmosphere by ozonosphere and also by the sun's atmosphere. Only a portion of this spectral region has been photographed with balloon-borne spectrographs, whereby a part of the ozonosphere can be crossed. A great amount of work in this region of sun's spectrum has recently been carried out with rocket-borne instruments, thereby opening a new branch of spectroscopy which is now called as the 'Rocket Spectroscopy'.

During the period between 1946, when the first rocket-borne spectrograph was flown, and 1952, the region of the solar spectrum between 3000A and 2000A was explored. Several excellent references of the work carried out during this period have already appeared (Baum *et al*, 1946; Hopfield *et al*, 1948; Durand *et al*, 1949). In December 1952, Lyman-α (1215·7A) line was first photographed by Pietenpol and others (1953). Following this discovery, the solar spectrum in the very far ultraviolet region was photographed and more information of X-rays emanated from the sun was obtained. In this article, we shall confine ourselves to investigations carried out after 1952.

The region of the solar spectrum observed after 1952 can be classified under four heads:

(*a*) Region around Lyman-α line
(*b*) Ultraviolet region above Lyman-α upto 2000A
(*c*) Ultraviolet region below Lyman-α
(*d*) X-ray region.

The ultraviolet region was photographed with rocket-borne spectrographs and, furthermore, by means of photon counters with suitable filters, and also with thermoluminescent phosphors, the solar energies in these spectral regions were determined. In the X-ray region, the measurements were mainly confined to the determination of energy by means of photon counters and thermoluminescent phosphors.

Apart from basic information of the sun's spectrum, such investigation yields results of far reaching importance. For example, from the energy measurements, the equivalent blackbody temperature of the sun in the far ultraviolet and X-ray regions were determined and it was found that this temperature differs markedly from that of a sun having a blackbody temperature of 6000°K. Also, these measurements lead to precise information of certain solar-terrestrial relationships, in particular, the radiations which cause the ionized regions of the upper atmosphere.

2. INSTRUMENTATION

As already mentioned, the investigation of solar spectrum between 2000A to X-rays was carried out by (*a*) spectrographs, (*b*) photon counters, (*c*) thermoluminescent phosphors, and (*d*) ion chambers. We shall now briefly describe these apparatus.

(a) Rocket-borne spectrographs

A major difficulty of photographing solar spectrum arises from the fact that the rocket rolls and yaws, thereby preventing the spectrograph to remain pointed towards the sun. As a result, the spectrograph 'looks' towards the sun only for a

short period of the total time of flight which is usually about 5 minutes. In order to overcome this difficulty, the spectrographs having wide field of view were carried in rockets which were stablized by means of servomechanisms with photoelectric sensing devices known as 'sun followers'.

Four types of entrance apertures having wide field of view have been devised. In these types, different methods were employed to admit light and expand the field of view (Fig. 1). The characteristics of these apertures are given by Tousey

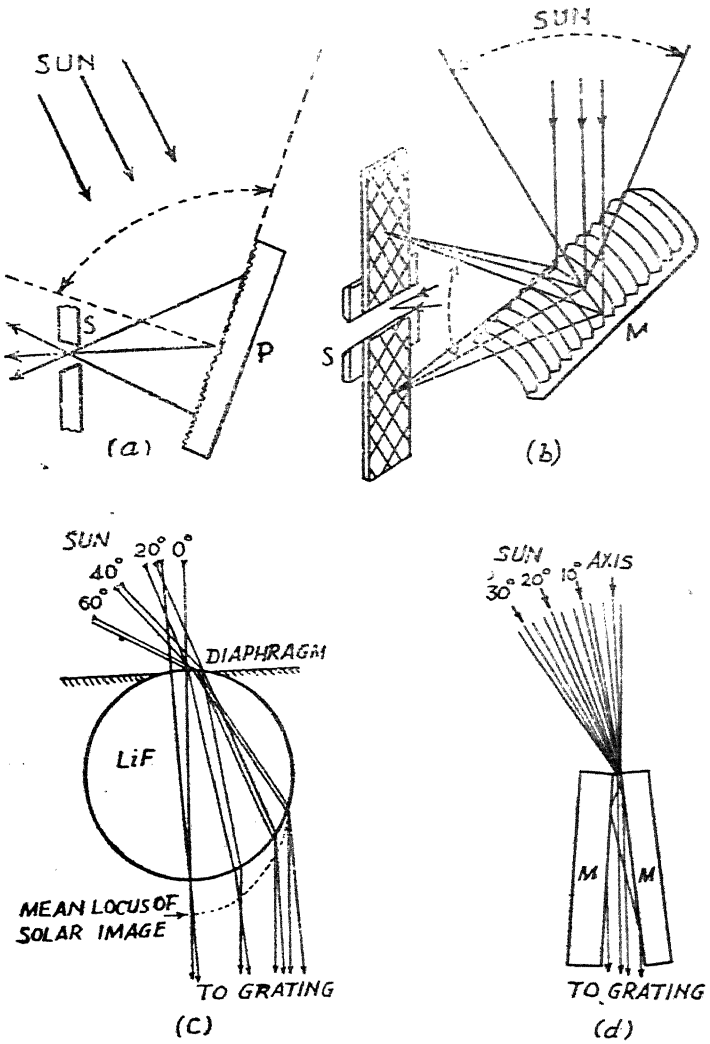

Fig. 1. Wide-field-of-view entrance aperture systems used in rocket spectrographs.
(a) Diffuse reflector and slit; (b) Corrugated cylindrical mirrror and slit; (c) Lithium fluoride sphere; (d) Mirror-jawed slit (Tousey, 1953).

(1953) and are shown in Table 1. The wide field of view aperture is fitted to a rocket spectrograph which usually consists of a grating of 15,000 lines/inch and having a radius of curvature of 40 to 50 cm.

Between the period 1952-1959, several flights with different spectrographs were carried out. The principal features of the spectrographs are given in Table 2. The spectra in the first order at near normal incidence were taken.

TABLE 1

Entrance Aperture for Rocket-borne Spectrographs

Entrance aperture	Description	Remarks
An open slit system S preceded by diffuse reflector P	A rough aluminized glass serves as the diffuse reflector.	The system produces sharp spectra. It is a low speed system, and hence requires a long exposure to record the spectrum. Because of the changing spectral reflection of the diffusing surface with angle, calibrations of relative intensities over the spectrum is difficult to obtain.
A cylindrical mirror with aluminized surface	It acts as one dimensional diffusing plate.	By such device sun light over a 70° field of view is focussed into a long narrow strip.
Polished sphere of LiF	The sphere is 2 mm in diameter. The spectral lines of about 0·6 mm in height are produced by the astigmatism introduced by grating arrangement.	Useful field of view is a cone of 140° diameter. The wavelengths upto the transmission limit of LiF (1100A) can be photographed. Since it forms a high speed system, many spectra during a rocket flight can be recorded. Both relative and absolute intensities can be established by calibration. The spectrum shifts position when the sun moves within the field of view during an exposure. Whenever a long exposure is required, a blurred spectrum is produced.
Mirror-jawed slit	An open slit is provided with jaws in the form of mirrors. The jaws are of aluminized glass and are set at an angle of 10°. This device expands the field of view in the plane at right angles to the slit to about 60°. The spectrograph is mounted with the rocket axis in the plane of Rowland circle.	It yields a sharp spectra and can be calibrated for intensity. The spectrograph records wavelengths below 1100A. It is specially used with a one-axis sun follower which corrects for rocket roll.

Note,—To photograph the spectrum in the extreme ultraviolet region the mirror-jawed slit system is commonly used in conjunction with the biaxial pointing control. The spectrograph is set at grazing incidence for photographing the sun's spectrum below 500A. This region is practically out of range of a grating set at normal incidence for which the reflectivity is very low. To increase the speed of grazing-incidence spectrograph, a toroidal mirror system is used (Rense and Violett, 1959).

TABLE 2

Rocket	Time of flight	Description of spectrograph	Film	Height reached by rocket (km)	Region explored (A)	Remark	Ref
Aerobee fired at Holloman Research and Development Centre, New Mexico	1938 UT Dec. 12,52	A grating spectrograph ruled on soft glass coated with aluminium was employed. The grating constants were, 6000 lines/cm, radius 49·8 cm, and dispersion 13A/mm at 1216A and 19A/mm at 3000A. The spectrograph was set at an angle of incidence of 85°.	Eastman 103 UV – sensitized 16 mm.	81	Fraunhofer lines from about 2000 to 5000A and Lyman-α line were photographed.	The solar activity of the day was above the average. A very active centre in the western hemisphere of the sun was probably responsible for auroral display on Dec, 12 and magnetic storm on Dec. 13. Two small flares occurred shortly after the flight. One of them was of dark flare type.	(a)
Aerobee Holloman Air Force Base, New Mexico.	Feb. 21,55	The grating spectrograph was mounted on a Rowland circle. The dispersing element was a concave diffraction grating of 6000 lines/cm and 40 cm radius of curvature, and was set at an angle of incidence of 2·3°. The spectrograph used in this firing is shown in Fig. 2.	Eastman SWR and IV-0-UV	115	1892-977 ; about 45 emission lines Ly_{α}, and Ly_{β} were photographed.	...	(b)
Aerobee fired at Holloman Air Development Centre, New Mexico.	0947 MST March 29, 55.	The spectrograph built by McPherson Precision Instrument Co. was of normal incidence type and having a grating of 40 cm radius and 15000 lines/inch with an average dispersion of 41·5A/mm. The slit width was 20 microns.	Eastman SWR	112	3000-9000. The Lyman-α line was photographed. Lyman-β was not detected.	...	(c)

TABLE 2—(*continued*)

Rocket	Time of flight	Description of spectrograph	Film	Height reached by rocket (km)	Region explored (A)	Remark	Ref.
Intermediate Aerobee fired at Holloman Air Force Base, New Mexico.	0830 MST Aug. 6,57	An aluminized replica concave grating with a radius of curvature of 39 cm and 6000 lines/cm mounted on a Rowland circle and set for an angle of incidence of 49.5°, was employed. The linear dispersion at 1200A was 0·042 mm/A and at 1800A was 0·047 mm/A. The slit width was 5·9μ.	Eastman SWR	Exposures were taken between altitude range 95-150 km.	1900-1000. About 30 emission lines were photographed and absolute intensity were determined. Five spectra at altitudes 95, 110, 130, 140, and 150 km were photographed with exposure times 1·5, 5·2, 28·1, 12·1, and 89·2 sec. respectively.	...	(d)
Aerobee–Hi fired at Holloman Air Force Base, New Mexico.	0554 MST June 4,58	The grating spectrograph mounted on Rowland circle and set for an angle of incidence of 85° was employed. John Hopkins original grating with ruled area 1 × 2 cm on aluminium and having 49·81 cm radius and 6000 lines/cm was used. The dispersion at 1200A was 12·6A/mm, and at 600A and 300A was respectively 9·3A/mm and 6·6A/mm. Slit width was 10μ.	Eastman Kodak SWR	Over 200	1216-839. About 150 solar omission lires were photographed.	At the time of flight there was considerable solar activity. Intense plage areas were present. Although no flare occurred at the time of the flight, flare activity was very high for the day. The zenith angle of the sun was about 80°.	(e)

Aerobee-Hi fired at Holloman Air Force Base, New Mexico.	0815 MST March 30, 59.	Similar spectrograph as employed on June 4,1958, was used with the following modifications: The grating was a Bausch and Lomb uncoated replica on a red glass blank with radius 49·81 cm and 6000 lines/cm. The ruled area was 1·8 × 3·6 cm. Slit width was 6 μ.	Eastman Kodak SWR	Over 200	1216-83·9. About 150 solar emission lines were photographed.	During the time of flight solar activity was above the average, with no outstanding single event or extensive plage areas. A high speed dark flare of class I occurred during flight. The zenith angle of the sun at the time of flight was 60°.	(e)
Aerobee-Hi IGY-NN3.24F White Sands, New Mexico.	0845 MST March 13, 59	A tripartite replica diffraction grating coated with Al_2O_3, blazed for ab out 1000A, with 40 cm radius, and 600 lines/mm was employed The slit width of 15 μ was illuminated with a 40 cm radius concave mirror. The collector mirror was a crystal quartz. The dispersion was 40A/mm.	Eastman SWR 35 mm.	198	1817-500. Seven lines of Lyman series and He I (584·3A) line were photographed. Lyman–γ was absent.	...	(g)

a—Pietenpol *et al* (1953) : Rense (1953)

b—Johnson *et al* (1958)

c—Jursa *et al* (1955)

d—Abound *et al* (1959); Behring *et al* (1958)

e—Violett and Rense (1959)

g—Purcell *et al* (1960)

(b) Photon Counters

For detecting ultraviolet and X-ray radiations, different types of photon counters were designed. Broadly speaking, there are two types of counters, namely

(1) Ultraviolet photon counters,

(2) X-ray photon counters.

The details of both types of photon counters are described by Friedman, Lichtman, and Byram (1951).

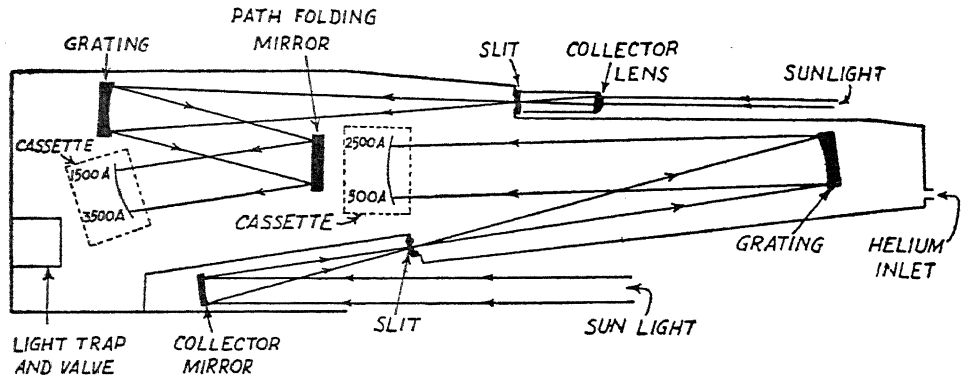

Fig. 2. Rocket-borne spectro-graph flown on Feb. 21, 1955 (Johnson et al, 1958).

Ultraviolet photon counters :

The function of this type of counter is the same as that of a self-quenching Geiger counter which is used for detecting X-rays and γ-rays. The electrons ejected by photoelectric process from the surface of the cathode wall trigger the Townsend avalanches of the discharge. The presence of even traces of electronegative gases in the Goiger tube increases the photoelectric work function of the counter whereas, a depression of the threshold wavelength is observed when halogen gases (Cl_2 or Br_2) or halogenated hydrocarbons such as methylene bromide are introduced into the counter. Also, for studying limited regions of the spectrum (bandwidth of only a few hundred angstorm), suitable filters such as lithium fluoride, sapphire, quartz, potassium chloride, and vycor glass are used. Fig 3 shows the spectral response of three types of photon counters (Friedman et al, 1951). The conversion from the counting rate to the flux of incident energy is obtained by comparision with the response of photomultiplier tube (coated with sodium salycilate or vacuum pump oil), which has been previously calibrated against a mercury lamp at 2536A.

X-ray photon counters:

Unlike the photon counting action of ultraviolet photon counter, the X-ray photons transmitted through the window are almost completely absorbed by the gas present in the X-ray counter. Assuming that each photon produces discharge in the tube, the couting efficiency is taken to be equal to the product of window transmission and the percentage of photons absorbed by the gases in the tube. This assumption is true for the majority of gas mixtures which use a rare gas in combination with a hydrocarbon quenching gas. A certain fraction of the absorbed quanta fails to produce discharge if an impurity of electronegative gas is pre-

sent. This is particularly observed when a halogen gas is mixed with the rare gases. For counters used in rockets, it was found that only 1/5 th of the quanta transmitted through the window were effective in triggering counts.

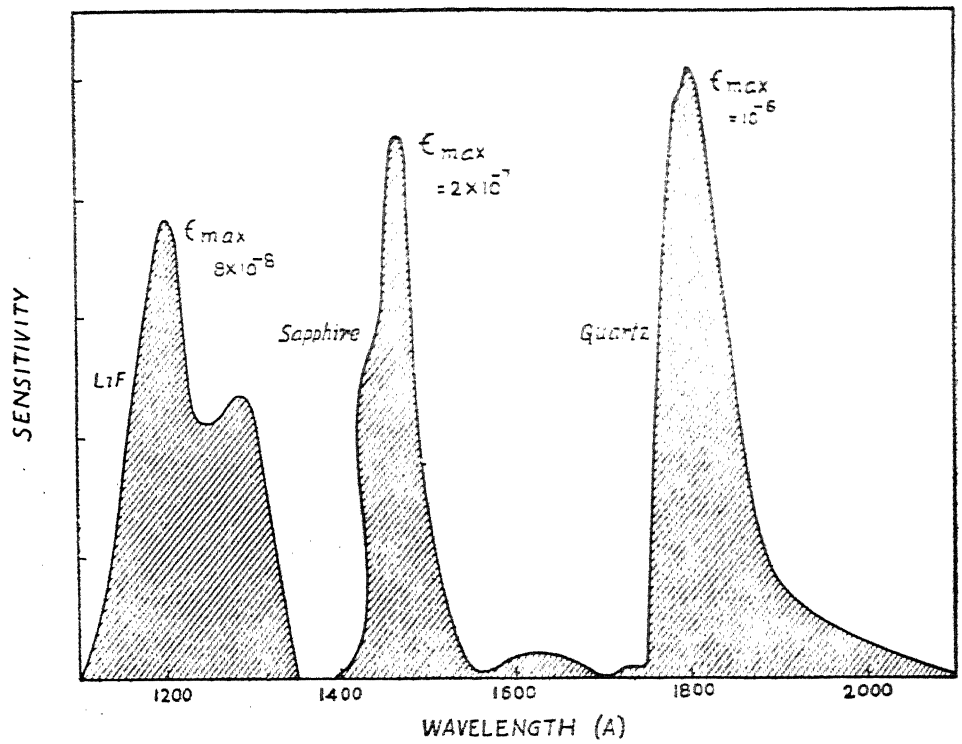

Fig. 3. Response curves for ultraviolet photon counters carried in rockets. ε_{max} (counts/quantum) represents maximum photoelectron yield. (Friedman et al, 1951).

(c) Thermoluminescent phosphor

The phosphor used for detecting ultraviolet radiation and X-rays is prepared by the method described by Watanabe (1951). $CaSO_4$ is mixed with a few percent of $MnSO_4$ in dilute sulphuric acid. The mixture is allowed to stand for a few hours and then evaporated to dryness and finally the residue is heated to redness. The powder thus prepeared is white. Phosphor strips are prepared by pressing the powder into 100 mesh nickel screens and then binding the powder in place with a mixture of 5 percent Duco cement and 95 percent acetone. The properties of $CaSO_4$. Mn phosphor have been discussed by Watanabe (1951).

To measure the solar radiation in the extreme ultraviolet and X-ray regions, thermoluminescent phosphor ($CaSO_4$. Mn) is excited by the radiation. The stored energy in the phosphor is quickly released by heating and the luminescence so produced is measured with a photomultiplier tube. The details of instrumentation

are given by Tousey, Watanabe, and Purcell (1951). Fig. 4 shows the response of the phosphor.

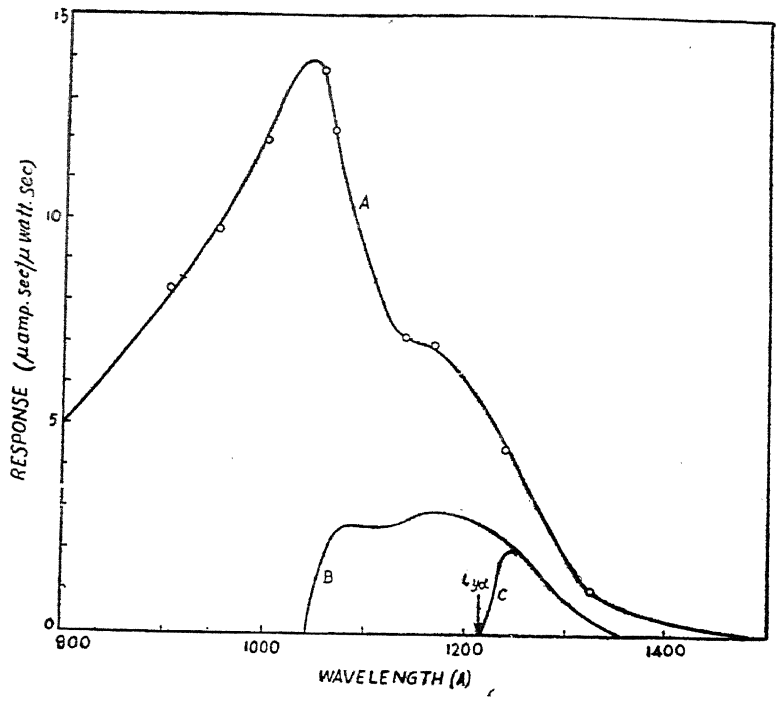

Fig. 4. The spectral response curves of $CaSO_4$. Mn phosphor calibrated against a thermocouple (curve A) with LiF filter (curve B), and CaF_2 filter (curve C) after Tousey, Watanabe, and Purcell (1951).

For studying limited wavelength bands, the filters given in Table 3 are used.

TABLE 3

Filters	Thickness (mm)	Wavelength region (A)
CaF_2	1—3.4	1230—1340
LiF	1—2	1040—1340
None		0—1340
Be	1—0.1	0—8
LiF minus CaF_2		1040—1230
None minus (Be + LiF)		8—1040

The total response of the phosphor, R, may be given by the expression

$$R = \int_{\lambda_1}^{\lambda_2} H_\lambda S_\lambda T_\lambda \, d\lambda \int A(\theta, \phi)\, dt$$

where

H_λ—solar spectral intensity,

S_λ—sensitivity of the phosphor,

T_λ—filter transmission,

and A (θ,ϕ)—area of the phosphor normal to the solar rays.

(d) Ion chambers

Ion chambers are employed for the measurement of solar radiation in the extreme ultraviolet region, especially the Lyman-α radiation. The chambers are filled with nitric oxide gas. The gas is photoionized by Lyman-α radiation transmitted through the lithium fluoride window. For computing the quantum efficiency of the chamber, the cross-section of nitric oxide determined by Watanabe (1954) and window transmission are utilized. The ion chambers used in rockets are calibrated by direct comparison with a standard nitric oxide chamber. The response of ion chamber for Lyman-α radiation is shown in Fig. 5. The details of ion chamber photometry are discussed by Chubb et al (1957).

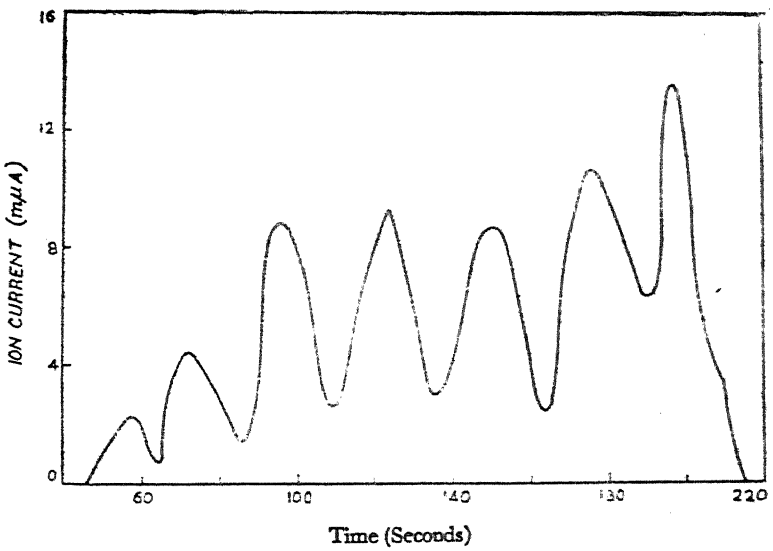

Fig. 5. Response of nitric oxide ion chamber for Lyman-α radiation (Chubb et al, 1957).

3. EXPERIMENTAL RESULTS

(a) Region around Lyman-α line

After detecting in the solar spectrum the Lyman-α line which passes through a deep well in the O_2 absorption spectrum, attempts were made to measure its energy. It was first measured by means of photon counters and thermoluminescent phosphors ($CaSO_4$.Mn). Recently, photographic and ion chamber techniques,

which give more accurate energy measurements, have been employed. These measurements show that Lyman-α is the strongest emission line below 2000A.

Measurement of energy:

The solar radiation between the wavelength region 1180-1300A, which penetrates upto 74 km, was first detected in 1952 by Byram et al (1952) with the aid of photon counters. For measuring the intensity of Lyman-α line, Byram et al (1953) employed photon counters which were sensitive in the range 1180-1300A. The sensitivity of the counters was fairly constant over a range of several angstroms in the neighbourhood of Lyman-α line. The intensity of Lyman-α line at the top of the atmosphere was found to be 0.1 ± 0.02 erg cm^{-2} sec^{-1}. By thermoluminescence technique, Tousey et al (1951) obtained its value as 0.4 erg cm^{-2} sec^{-1}. On the other hand, using photographic method Pietenpol et al (1953) reported its intensity to be 0.3 erg cm^{-2} sec^{-1}. It was shown subsequently that the value obtained by ion chamber is around 6 erg cm^{-2} sec^{-1}. The energy of the continuous solar emission background in the neighbourhood of 1200A is less than 0.01 erg cm^{-2} sec^{-1} $100A^{-1}$ which is equivalent to a black body temperature less than 4600°K (Byram et al, 1953).

The measurements of Lyman-α radiation from photographs give better results than those obtained from thermoluminescent phosphors and photon counters. Again, the ion chamber (with LiF window) measurements are more accurate and reliable. With the aging of the ion chamber, the caliberation changes only in one direction, thereby, attributing too high an efficiency to the chamber. The ion chamber values may therefore, be taken as the minimum values.

The results of ion chamber measurements of energy of this radiation carried out during the period 1955-1958 and the earlier results obtained by photon counters, thermoluminescent phosphors are given in Table 4. It is evident from the table that the values of Lyman-α intensity obtained by ion chambers are consistently high. Byram, Chubb, Friedman, Kupperian and Kreplin (1958) interpreted the low values as due to the minimum phase of the solar cycle and higher values to maximum phase. However, consistent values around 6 erg cm^{-2} sec^{-1} were obtained with ion chambers during the period 1955-58. In order to make a definite statement regarding the consistency and variation of energy, it is necessary to wait till observations are taken at least during the declining phase of the current solar cycle.

Photometry of 1215-1350A:

From the spectrogram obtained from rocket-borne experiment, it is difficult to obtain the absolute intensity of spectral lines, although their relative intensities can be determined. However, by choosing suitable filters it is possible to obtain the absolute intensity by ion chamber photometry in different bandwidths. We shall discuss below the ion chamber photometry for 1225-1350A region (Byram *et al*, 1958).

Ion chamber photometry in conjunction with CaF_2 window can be utilized to measure the absolute intensity of solar radiation in the region 1225-1350A. From the measurement of the integrated flux the absolute intensity of this band can be determined, which in turn can be utilized to find out the individual intensities of the spectral lines from their relative intensities obtained from spectrogram.

TABLE 4

Measurements of Lyman-α intensity

Rocket launch time	Sun's condition	Intensity at the top of the atmosphere (erg/cm^2 sec)	Apparatus used	Wavelength region (A)	Reference
1600 MST Sept. 29,49	Quiet	1–10	Photon counter	1100–1350	Friedman et al, (1953)
1101 MST Feb. 17,50	—do—	0.4	Thermolum-inescent phosphor	1050–1240	Tousey et al, (1951)
0659 MST April 30,52	—do—	0.15	Photon counter	1180–1300	Byram et al, (1953)
0644 MST May 5,52	—do—	0.1±0.02	—do—	1180–1300	Byram et al, (1953)
1938 UT Dec. 12,52	—do—	0.5	Spectrograph	...	Rense (1953)
0830 MST Feb. 2,54	—do—	1.6	—do—	...	Johnson et al, (1958)
0830 MST Feb. 21,55	—do—	0.6	—do—	...	Johnson et al, (1958)
1550 MST Oct. 18,55	—do—	5.7 (−1, +3)	Ion chamber	1100–1350	Byram et al, (1956)
1715 MST Oct. 21,55	—do—	4.0 (±0.8)	—do—	1100–1350	Byram et al, (1956)
0830 MST Nov. 4,55	—do—	9.2 (±3.0)	—do—	1100–1350	Byram et al, (1956)
Dec. 13,55		3.0	Spectrograph	...	Miller et al, (1956)
1915 UT July 17,56	Quiet	6.1 (±0.3)	Ion chamber	1050–1350	Chubb et al, (1957)
1917 UT July 20,56	Late in class I flare	6.1 (±1.4)	—do—	1050–1350	Chubb et al, (1957)
2113 UT July 25,56	Quiet	6.7 (±0.3)	—do—	1050–1350	Chubb et al, (1957)
1600 CST July 29,57	—do—	6.1 (±0.3)	—do—	1050–1350	Byram et al, (1958)
1208 CST March 23,58	—do—	6.3 (±0.3)	—do—	1050–1350	Byram et al, (1958)

Following the above method and using the relative intensity data of the spectral lines as given by Johnson et al (1958) and ion chamber flux measurement obtained with IGY Aerobee NN 319F rocket fired on March 23, 1958, the absolute intensities of spectral lines were determined. These values which are listed in Table 5 represent the upper limits of intensities because contributions from continuum or weaker lines were not taken into consideration.

TABLE* 5

Spectral lines (Johnson *et al*, 1958)	Wavelength (A)	Intensity (erg cm^{-2} sec^{-1})
N V	1238.8	0.01
S II	1259.5	0.003
Si II	1260.7	0.012
Si II	1265.0	0.020
O I	1302.2	0.039
O I	1304.9	0.052
O I	1306.0	0.064
Si II	1309.3	0.013
C II	1334.5	0.12
C II	1336.7	0.15

This type of ion chamber photometry can be applied to other wavelength intervals.

(b) Ultraviolet region above Lyman-α upto 2000A

This region as well as the region below Lyman α (Section 3-*c*) have been explored mainly by rocket-borne spectragraphs. The characteristic features of different rocket-borne spectrographs have already been given in Table 2. We shall present here the important results which reveal the main features of the spectrum in the region below 2000A.

A good spectrogram of solar spectrum in the extreme ultraviolet region was obtained from a rocket on February 21, 1955 at 115 km altitude (Johnson et al, 1958). The spectrum (Plate 1) shows 45 emission lines in the region 1892A to 977A. From the analysis of the spectrum, it has been concluded that the lines of highest excitation potential arise from O VI, N V, C IV, and Si IV. The resonance lines of C II, C III, C IV, N V, O VI, Si III, and Si IV predicted by Woolley and Allen (1950) were observed in this spectrum, Only lines N II (λ 1086) and N III (λ 990) did not

* Byram, Chubb, Friedman, Kupperian, Jr., and Kreplin (1958)

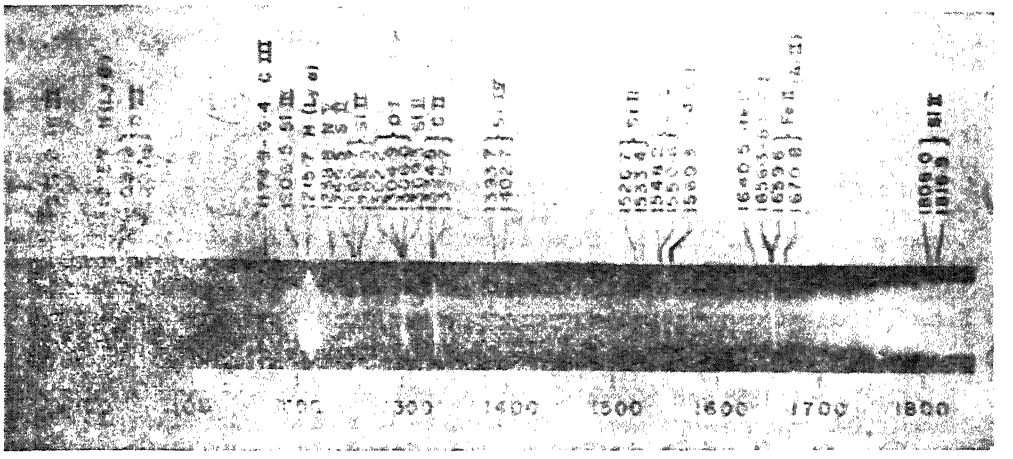

Plate I The solar spectrum obtained on Feb. 21, 1955 at an altitude of 115 km (Johnson et al, 1958).

appear although predicted to be of the same intensity as the 977A line of C III. Besides emission lines of hydrogen, helium, carbon, nitrogen, oxygen, aluminium, silicon, phosphorus, sulphur, iron, Fraunhofer lines are present. The solar continuum was photographed in this spectrum to approximately 1550A where it disappears into the background of focussed stray light (Fig. 6). The irregular structure in the

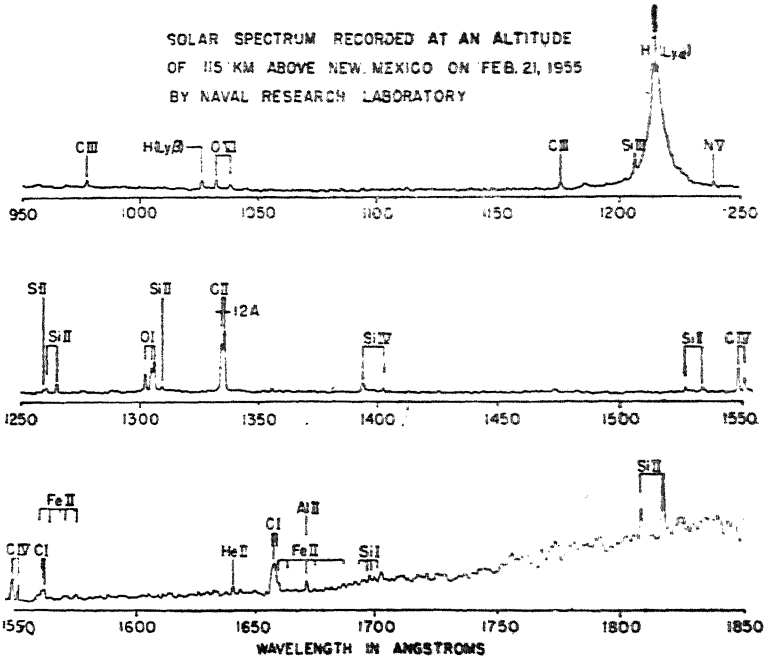

Fig. 6. The logarithmic densitometer trace of the spectrum obtained from 115 km altitude on Feb. 21, 1955 (Johnson et al, 1958).

spectral region from 1850 to 1550A is caused by Fraunhofer absorption. Below 1550A the irregularities become less and are due only to the granularity of the film. In addition to Lyman-α, Lyman-β line was photographed.

Intensities of 24 solar emission lines in the range 1206-1817A were estimated from photometric analysis of rocket spectrograms obtained on August 6, 1957 between altitude range 130 – 150 km (Abouni et al, 1959). Above Lyman-α line (intensity 3.4 erg cm^{-2} sec^{-1}), two lines of Si II of energy 1.05 (λ 1808 0) and 1.65 (λ 1816.9) erg cm^{-2} sec^{-1} are most intense. The emission lines and their intensities above Lyman-α are given in Table 6. From inspection of the table it is obvious that upto 1817A, other lines are weak compared to Lyman-α line. The identification of emission lines in the range 1032-1893A has been reported by Behring, McAllister, and Rense (1958).

(c) Ultraviolet region below Lyman-α

On June 4, 1958 and March 13 and 30, 1959, the solar spectrum in the region below 1000A was photographed from Aerobee-Hi rockets. On March 13, 1959, the solar spectrum was obtained upto 550A (Plate 2) from an altitude of 198 km. This spectrum shows many new emission lines of which the most important are the

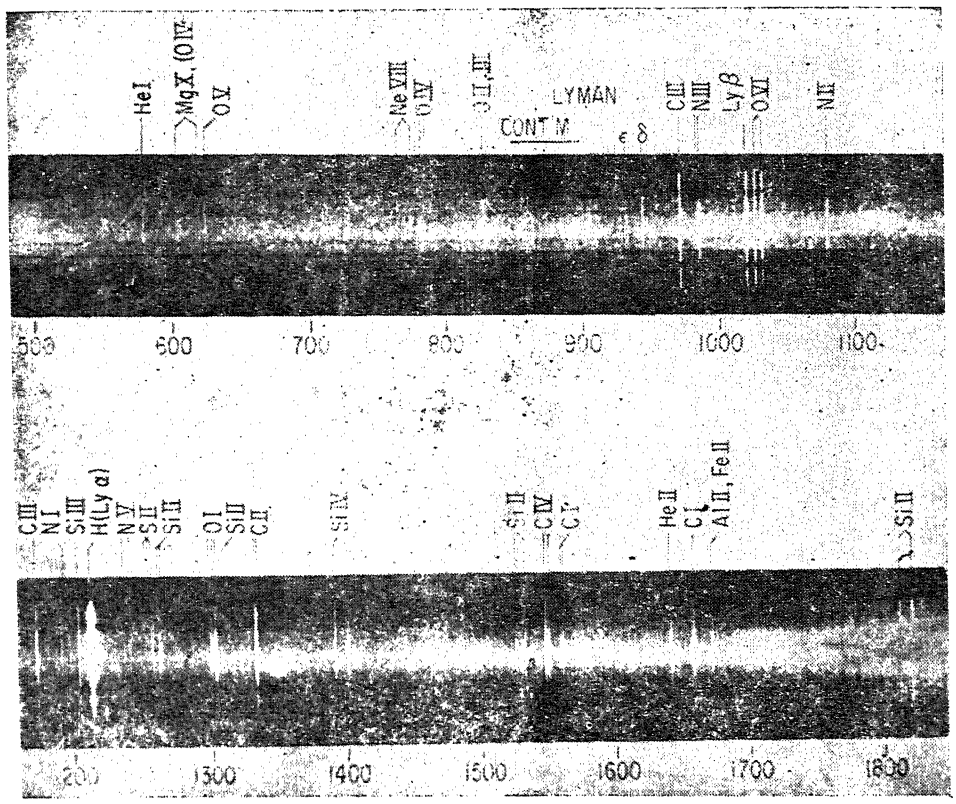

Plate II The solar spectrum obtained on March 13, 1959 at an altitude of 197 km. Note that the continuous background is due to stray light for $\lambda < 1500$A and from 920A to 830A, the background density is increased by Lyman-continua (Purcell et al, 1960)

TABLE 6

Intensities of Emission Lines

Spectral lines	Wave length (A)	Intensity (erg cm^{-2} sec^{-1})	Excitation potential (ev)
Si III	1206.5	0.23	34.61
HLα	1215.7	3.43	10.15
He II	1215.1	0.17	75.28
Si II	1265.0	0.02	17.91
O I	1302.2	0.04	9.48
O I	1304.9	0.04	9.48
O I	1306.0	0.04	9.48
Si II	1309.3	0.04	17.57
C II	1334.5	0.31	20.45
C II	1335.7	0.33	20.45
Si IV	1393.7	0.24	66.56
Si IV	1402.7	0.17	66.50
Si II	1526.7	0.03	16.20
Si II	1533.4	0.06	16.20
C IV	1548.2	0.55	91.12
C IV	1550.8	0.31	91.11
C I	1560.3	0.04	7.91
C I	1561.4	0.08	7.91
He II	1640.4	0.27	72.64
C I	1656.3	0.28	7.46
C I	1658.1	0.20	7.45
Fe II	1670.8	0.21	15.60
Si II	1808.0	1.05	14.94
Si II	1816.9	1.65	14.94

resonance lines of He I, N I, II, III, and V ; O II, III, IV, and V; S VI ; N_e VIII ; and Mg X. Also many higher members of Lyman series (Lyβ, 1025.71 ; δ, 949.75 ; ε, 937.80 ; ζ, 930.75 ; η, 926.32 ; θ, 923.15 ; ι, 820.96 ; χ, 919.35) and the Lyman-continuum are present in the spectrum. Lyman-γ (λ 973) is absent because of absorption of N_2. The microphotometer tracing of the spectrum (Plate 2) is given in Fig. 7. The observed emission lines with possible identifications are given by Purcell, Packer, and Tousey (1960).

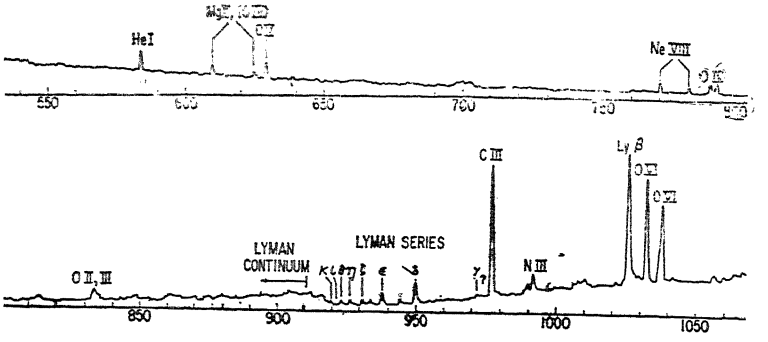

Fig. 7. A microphotometer trace of the spectrum obtained from 197 km altitude on March 13, 1959 (Purcell et al, 1960).

The solar spectra photographed on June 4, 1958 and March 30, 1959 from an altitude of over 200 km have been analysed by Violett and Rense (1959). About 150 emission lines with their relative intensities and identifications in the range between 1216A (Lyα) and 83.9A have been reported. The spectrograms show the Lyman series and the helium resonance lines (He I, 584.33A and He II, 303.8A). These spectrograms also show the emission lines of beryllium, carbon, nitrogen, oxygen, neon, magnesium, aluminium, silicon, phosphorus and sulphur.

Purcell, Packer, and Tousey (1960) compared the spectrum of the sun photographed on March 13, 1959 with that obtained by Violett and Rense (1959). The observed emission lines in the region 1216A to 584.3A are discussed. The spectrum taken on March 13, 1959 shows seven higher members of Lyman series and two resonance lines of S VI (933.38A and 944 52A) but Lyman-γ (λ 972.9) is absent, whereas the spectra obtained on June 4, 1958 and March 30, 1959 show the presence of Lyman-γ line and seven lines of intensity 10 (the unit of intensity being 1/1000th the intensity of Lyman-α), of which one is identified as N I line (λ 964.5). There are many lines obtained by Violett and Rense (1959) which are not present in the spectrum obtained by Purcell et al (1960), but which are of greater intensity than nearby lines that appear in both spectra. For example, lines 614.9A of intensity 20 and 617.2A of intensity 25 are not present in the spectrum photographed by Purcell, Packer, and Tousey, although 625.1A of only intensity 5, is prominent.

Further experiments are required to explain the spectrum below 1000A. It is desirable to obtain spectra from higher altitudes where absorption by telluric bands is absent.

(d) Soft X-rays below 100A emitted by the sun

Since 1949, the energy of X-rays emitted by the sun was measured by rocket-borne experiments. These measurements were carried out both during quiet sun

conditions as well as during flare time. During the former condition, solar X-rays penetrate only upto about 100 km altitude and during the latter time, when shorter wave-lengths are emitted, X-rays penetrate deep into the atmosphere and are detected even upto the altitude of 44 km. These energy measurements were carried out mainly by means of photon counters with Be, Al, mylar, and glyptal windows which transmit radiations 2-8A, 8-20A, 44-60A, and 44-100A respectively. A few measurements were also carried out with thermoluminescent phosphors.

With a view to measure solar X-rays energy in different wavelength intervals rocket experiments were performed. We shall now briefly describe some of the experiments carried out after 1955.

In July 1956, rocket experiments were carried out to measure X-rays during flare by using photon counters. X-rays of wavelengths less than 8A were measured with a Geiger counter with Be window. To measure any hard X-ray flash that might be encountered during a flare, a partially shielded scintillation counter with a Na I (Tl) crystal 1-1/8 inches diameter and 1/2 inch thick, combined with a 6199 photomultiplier, was employed as an X-ray pulse amplitude spectrometer. To determine the intensity and to analyse the characteristics of the incident flux of solar X-rays, it is necessary to correct the observed responses of the counters for the variation in angle between the sun and the plane of view. This latter variation is obtained by two photocells sensitive to visible light (Chubb et al, 1957). The large angle between the direction of the sun and the detector view plane which occurs during most of the flights result in a shift in spectral sensitivity curve of the counter as shown in Fig. 8. The X-ray intensities measured during flare times indicate high state of coronal excitation.

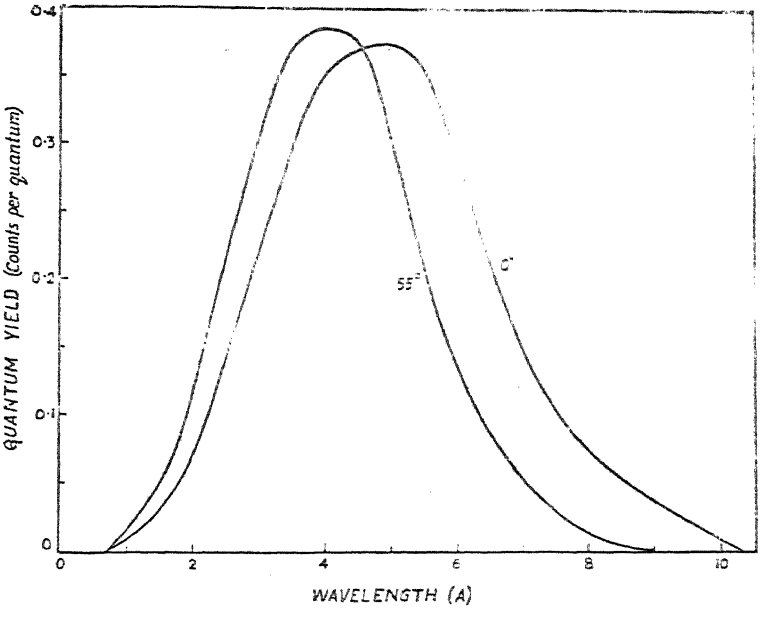

Fig. 8. The spectral response of Be X-ray Geiger counter calculated from window and gas absorption coefficients for normally incident X-rays and X-rays incident at an angle of 55°. (Firing occurred during flare time on July 20, 1956) [Chubb et al, 1957].

Similar rocket experiments were performed by Naval Research Laboratory in August-September, 1957, in order to measure X-rays emanated from the sun during flare time. The rockets were equipped with X-ray photon counters sensitive to wavelengths from 1 to 8A. In these flights attempts were made to time the rocket firing to coincide with the maximum phase of the flare. These measutements showed that X rays of short wavelength are produced in sufficient intensity during flares (Friedman, 1959).

In summer 1959, a series of rocket experiments were carried out with a view to measure solar X-rays during solar flares and also during non-flare conditions. The data show that during non-flare conditions at sunspot maximum, the X-ray counting rates for 8-20A were increased forty times (Chubb et al 1960) than the rates measured at solar minimum. In the 2-8A region, the relative increase was much greater. It was noted that solar maximum in the 2-8A region measured in 1959 agree remarkedly with the value obtained in 1949. These firings have provided seven data, three in non-flare conditions and four during class 2^+ solar flares. Each flare was accompanied by a large sudden ionospheric disturbance. The results of these flights together with results obtained on previous flights are summarised in Table 7.

The existence of readily measurable X-ray emission below 0.6A constitutes the most striking phenomenon accompanying all the three sudden ionospheric disturbance producing flares. In two most intense flares, X-rays of energies upto 70 Kev (less than 0.2A wavelength) were observed. The flux of high energy quanta penetrates the atmosphere below 43 km.

The penetration of different wavelengths through the earth's atmosphere is shown in Fig. 9. The solid curves (Friedman, 1959) represent the penetration of solar radiations into the atmosphere for vertical incidence obtained from rocket-borne experiments. The dot-dash curves (Byram, Chubb, and Friedman, 1954) show the penetration of certain radiations computed from absorption coefficients (Compton and Allison, 1953). Dotted line curves represent the transmission of solar radiations observed from V-2#49 rocket using photon counters.

It will be seen from the above curves that, in general, radiations penetrate deeper into the atmosphere as the wavelength decreases. There are, however, certain departures. Wavelengths 1475A, Lyman-α, 1200A, and Lyman-β penetrate much deeper into the atmosphere. In the dot-dash curves, wavelength 30A penetrates to a lesser depth compared to wavelengths 35A, 60A, and 100A. Also, it may be noted that Lyman-α and 2.5A, and wavelengths 10A and 32A have the same penetrating characteristics.

From the nature of these transmission curves, one can easily conclude that different amounts of energy corresponding to different wavelengths are absorbed at different altitudes of the atmosphere. Wavelengths from 200A to 850A are absorbed above 125 km, whereas those between 5A and 100A are absorbed in the region 90–125 km. The Lyman-α radiation (Byram et al, 1953) penetrates upto 74 ± 2 km. Also, Lyman-β is absorbed between altitudes 90 and 125 km. Wavelength 2.5A penetrates below 70 km and 1A well below 60 km. A significant feature of these curves is that X-rays (100–10A) are absorbed in the narrow altitude range of the E-layer.

4. APPLICATIONS OF OBSERVED DATA TO SOLAR AND GEOPHYSICAL PROBLEMS

The data obtained from rocket-borne spectrographs, photon counters, thermoluminescent phosphors and ion chambers were utilized to obtain information about the sun and the earth's atmosphere, in particular the following:

(1) The temperature of the sun,

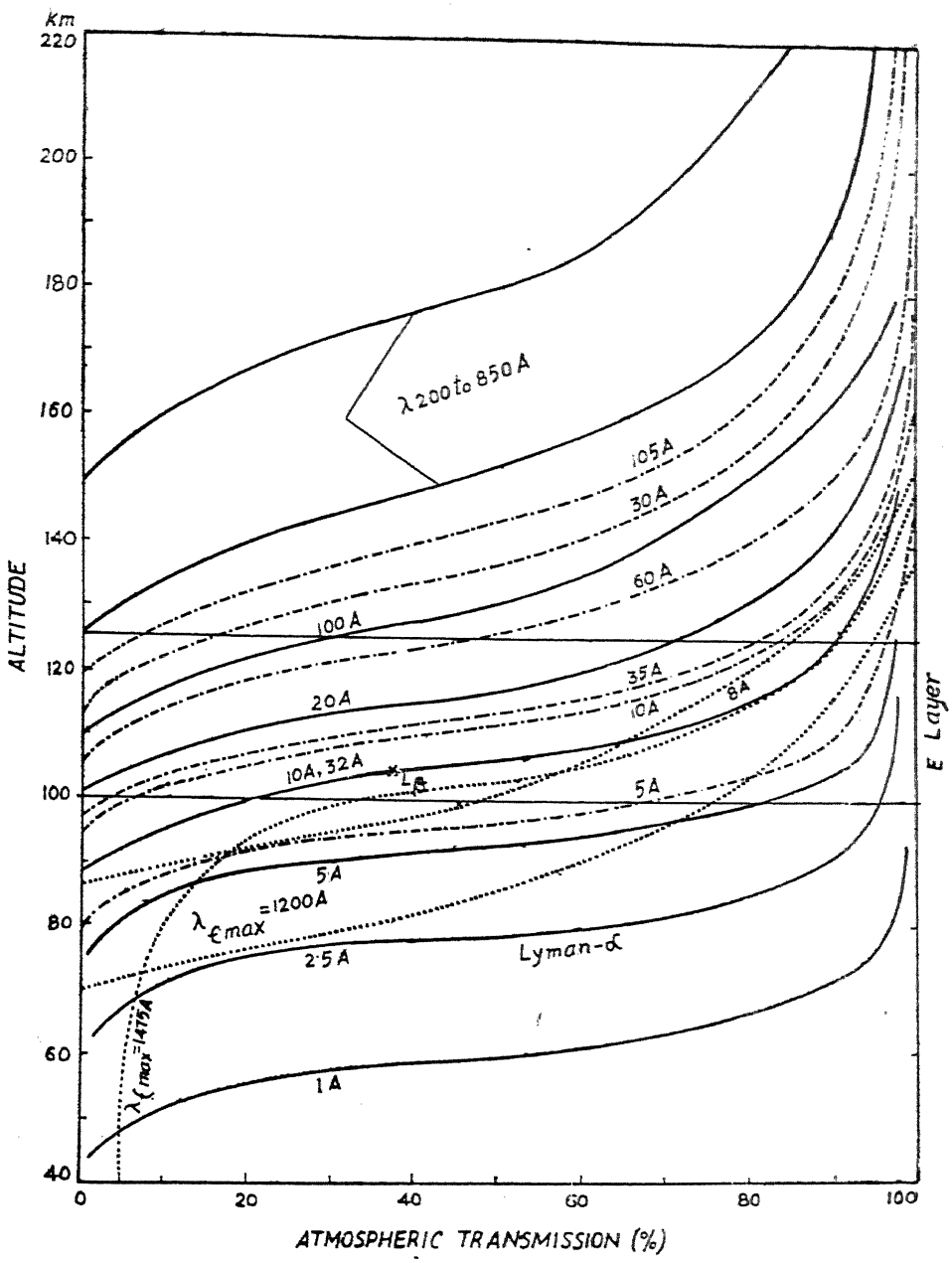

Fig 9. Atmospheric transmission for different wavelengths in the X-ray and ultraviolet regions. The solid curves (Friedman. 1959) are obtained from rocket-borne experiments. Dotted line curves (Friedman, 1951) are also obtained using photon counters in V-2 #49 rocket. Dot-dash curves are computed from absorption coefficients given by Compton and Allison (1953)

TABLE 7

Rocket	Time of flight	Sun's condition	Be counter response at the top of atmosphere	Al counter response at the top of atmosphere	Energy			Reference
			2–8A (counts/cm² sec)	8–20A (counts/cm² sec)	2–8A (erg/cm² sec)	8–20A (erg/cm² sec)	Other wavelength intervals (erg/cm² sec)	
V–2#49	1730 UT Sept. 29, 49	160 minutes after class I flare	1.0×10^4	...	0.0015	...	...	Chubb et al (1957)
A–9	1459 UT May 1, 52	Quiet	495	...	0.0017	...	...	Chubb et al (1957)
A–10	1344 UT May 5, 52	–do–	<125	...	<0.0005	...	...	Chubb et al (1957)
Viking 9	Nov., 52	High solar activity	...	...	...	0.6	...	Havens et al (1954)
Viking 9	2138 UT Dec. 15, 52	Quiet	$<1.5 \times 10^3$	2.9×10^6	<0.0006	0.2	...	Chubb et al (1957)
A–14	2240 UT Nov. 15, 53	–do–	<40	$<3.1 \times 10^4$	$<6.7 \times 10^{-6}$	<0.0015	...	Chubb et al (1957)
A–15	1546 UT Nov. 25, 53	–do–	332	$<2.6 \times 10^4$	2.9×10^{-6}	<0.0013	...	Chubb et al (1957)

A–16	1529 UT Dec. 1, 53	–do–	...	4.5×10^{4}	...	0.0004	...	Chubb et al (1957)
Aerobee 16	Dec., 53	Low coronal activity	...	...	...	0.0017	0.03 ($\lambda\lambda$ 44-60) 0.02 ($\lambda\lambda$ 60-100)	Havens et al (1954)
A–34	2250 UT Oct. 18, 55	Quiet	...	1.4×10^{5}	...	0.0012	...	Chubb et al (1957)
D–8	1915 UT July 20, 56	Late in class I flare	1.2×10^{5}	...	0.005	...	...	Chubb et al (1957)
Nike-Deacon NN7 , 42F	0949 Z Aug. 20, 57	1+ weak SWF	...	...	...	...	3.0×10^{-3} ($\lambda\lambda$ 2.5- ?)	Friedman (1959)
Nike Deacon NN7 , 45F	1412 Z Aug. 29, 57	Class 2 1/2hr SWF	...	...	...	...	2.0×10^{-2} ($\lambda\lambda$ 3-8)	Friedman (1959)
Nike-AS NN7 , 49F	1054 Z Sept. 18, 57	Class 3 2 hr SWF	...	...	...	...	1.2×10^{-4} ($\lambda\lambda$ 1.5- ?)	Friedman (1959)
8–69	1600 UT Aug. 14, 59	Quiet	1.3×10^{4}	2.0×10^{6}	5.5×10^{-4}	1.8×10^{-2}	0.6 ($\lambda\lambda$ 20-100)	Chubb et al (1960)
8–73	2253 UT Aug. 31, 59	Class 2+	$>7 \times 10^{5}$	$>1.0+10^{7}$	$>3.0 \times 10^{-2}$	$>9.0 \times 10^{-1}$	4.5×10^{-6} (below λ 0.6) <4.0 ($\lambda\lambda$ 20-100)	Chubb et al (1960)

TABLE 8

Equivalent blackbody temperatures of the sun obtained from rocket-borne experiments in the x-ray and ultraviolet regions

Wavelength region (A)	Condition of the sun	Energy (erg $cm^{-2}sec^{-1}$)	Equivalent blackbody temperature (°K)
Below 8	Late in class I flare	5×10^{-3}	$6{\cdot}8 \times 10^{5}$
6 – 10	160 minutes after class I flare	$10^{-4} - 10^{-3}$	$3{\cdot}5 \times 10^{5}$
8 – 12	Quiet	3×10^{-3}	$3{\cdot}0 \times 10^{5}$
8 – 18	High coronal activity	0·6	$2{\cdot}6 \times 10^{5}$
8 – 20	– do –	0·1	$2{\cdot}3 \times 10^{5}$
8 – 20	Quiet	$1{\cdot}5 \times 10^{-3}$	$2{\cdot}1 \times 10^{5}$
8 – 20	Quiet	$1{\cdot}3 \times 10^{-3}$	$2{\cdot}1 \times 10^{5}$
8 – 20	Quiet	$1{\cdot}2 \times 10^{-3}$	$2{\cdot}1 \times 10^{5}$
8 – 20	Quiet	$0{\cdot}4 \times 10^{-3}$	$2{\cdot}1 \times 10^{5}$
10 – 60		1·0	$1{\cdot}1 \times 10^{5}$
44 – 60	Minimum solar activity	$1{\cdot}4 \times 10^{-2}$	$6{\cdot}8 \times 10^{4}$
44 – 100	– do –	$3{\cdot}5 \times 10^{-2}$	$5{\cdot}2 \times 10^{4}$
44 – 100	– do –	$2{\cdot}9 \times 10^{-2}$	$5{\cdot}2 \times 10^{4}$
1050 – 1240	Normal	0·4	5300
1200	– do –	$6{\cdot}2 \times 10^{-2}$	(6000)*
1216	No unusual solar activity	6·3	7730
1150 – 1340	– do –	1 – 10	5630
1230 – 1340	– do –	0·2	4840
1500	– do –	$5{\cdot}4 \times 10^{-3}$	(4500)*
2050	– do –	3·7	(5000)*

*For figures marked with asterisk, the amounts of energy have been calculated from temperatures.

(2) Ionized regions of the earth's upper atmosphere,

(3) Distribution of neutral particles of the earth's atmosphere with the height.

(a) The temperature of sun for the X-ray and ultraviolet regions-energy at the top of earth's atmosphere

As already mentioned, the solar energy at the top of the earth's atmosphere corresponding to different wavelengths from ultraviolet to X-rays were obtained from rocket-borne experiments. From these energy values and considering the sun as a blackbody radiator, the coronal temperatures corresponding to the emission of X-rays and ultraviolet radiations were computed following the method of Nicolet (1952) as follows:

If $\rho(\nu)$ be the density of radiation emitted by the sun, we obtain from Planck's formula,

$$\rho(\nu)=\frac{8\pi h\nu^3}{c^3}\ (e^{h\nu/kT}-1)^{-1}$$

where the symbols have their usual significance. The radiation density $\rho'(\nu)$ at the top of the atmosphere is given by the relation

$$\rho'(\nu)=\beta_s\,\rho(\nu)$$

The dilution coefficient β_s is given by

$$\beta_s=\frac{R^2}{4r^2}=\frac{(\text{sun radius})^2}{4\,(\text{sun-earth distance})^2}=5{\cdot}41\times10^{-6}.$$

The temperatures thus calculated are given in Table 8 (Ghosh and Sharda Nand, 1960). These values fairly agree with other available data given in Table 9.

TABLE 9

Equivalent blackbody temperature of quiet sun in the x-ray and ultraviolet regions obtained by Nicolet

Wavelength (A)	Equivalent blackbody temperature (°K)
4	5×10^5
10	3×10^5
14	2×10^5
20	$1{\cdot}6\times10^5$
21·5	$1{\cdot}5\times10^5$
29·6	$1{\cdot}2\times10^5$
50	$7{\cdot}5\times10^4$
75	5×10^4
200	2×10^4
228	$1{\cdot}9\times10^4$
250	$1{\cdot}8\times10^4$
500	7×10^3
910	5×10^3
1000	5×10^3

The variation of temperature of the sun with wavelengths in the X-rav region is shown in Fig. 10. It may, however, be pointed out that the emission from the

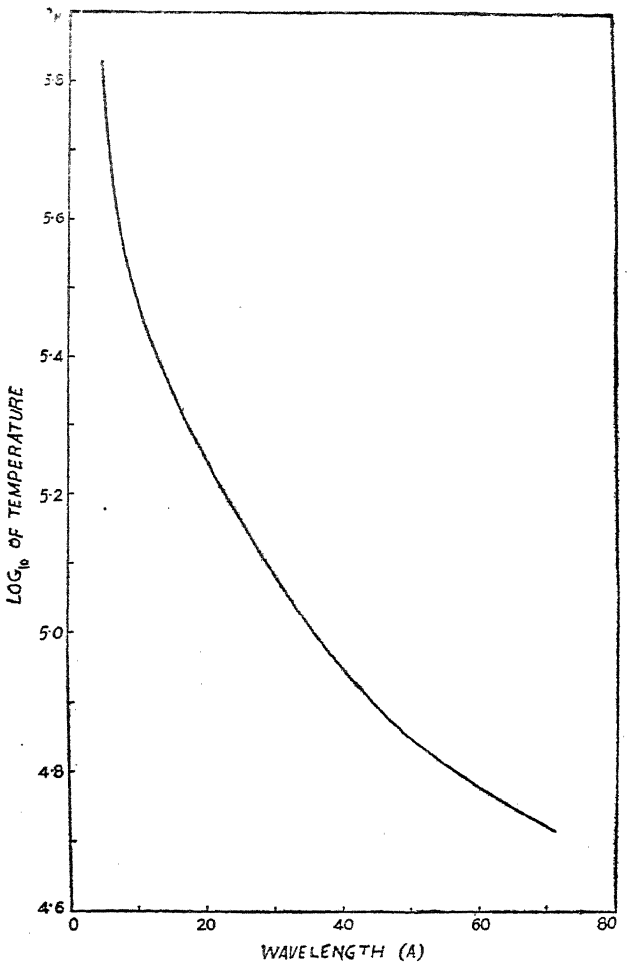

Fig. 10. Variation of temperature of the sun with wavelength in the X-ray region obtained from rocket data (Ghosh and Sharda Nand, 1960).

sun may be of grey body type (Byram, Chubb, and Friedman, 1956). If such be the case, the actual temperature will be higher than those given in Table 8.

(b) Ionized regions of the earth's upper atmosphere

With the direct measurements of solar energies in the extreme ultraviolet and X-ray region and their penetration through the earth's atmosphere as obtained from rocket-borne experiments, it is now possible to investigate more thoroughly the formation of ionized layers in the atmosphere. These investigations are given below.

D-region

Among the various processes proposed for the production of D-layer, which lies between altitudes 60 and 100 km (Ghosh and Sharda Nand, 1961), the process proposed by Nicolet (1945), namely, that the normal D-layer is formed by the photoionization of nitric oxide

$$NO + h\nu\ (> 9.5\ ev) \rightarrow NO^+ + e$$

has the strongest support. Watanabe, Marmo, and Pressman (1955) considered various hypotheses and showed that the most probable process for this layer formation is the photoionization of NO by ultraviolet radiation between wavelength region 1100-1340A. From rocket spectrograms, Rense (1953) and Jhonson, Purcell, and Tousey (1954) showed that the most of the energy in this spectral region is concentrated in the Lyman-α line. Therefore, the normal D-layer may be produced by the following process

$$NO + L_\alpha\ (1216A) \rightarrow NO^+\ (v = 0, 1, 2, 3) + e$$

The vibrational levels of NO^+ are obtained from laboratory data (Watanabe, 1954).

According to Nicolet (1954), the enhancement in the D-layer ionization during fade-outs is due to the flare activity causing the increase of Lyman-α intensity and hence of the rate of photoionization of nitric oxide. However, rocket-borne experiments equipped with ion chambers showed no large increase in Lyman-α intensity during strong flares (de Jager, 1959). Friedman and Chubb (1955) pointed out that soft X-ray may be responsible for the enhancement in D-layer ionization. Such X-rays are not observed under quiet solar conditions but are emitted with sufficient intensity during flares (Friedman, 1959).

Following the suggestion of Friedman and Chubb (1955), the enhancement in the ionization of D-layer produced by solar X-rays ($\lambda < 10A$) has been studied by Ghosh and Sharda Nand (1961). They calculated the rate of ion production due to X-rays and found its average value to be 100 and 133 ions $cm^{-3}\ sec^{-1}$ in the altitude ranges 80-100 km and 60-80 km respectively.

The rate of ion production is also calculated from the formula

$$q = \alpha N_e^2 \quad \ldots (1)$$

If the value of α is assumed to be $2.7 \times 10^{-7}\ cm^3\ sec^{-1}$ (Nicolet and Aikin, 1960) and $2.2 \times 10^{-6} cm^3\ sec^{-1}$ (Mitra and Jones, 1954) for the altitude ranges 80-100 km and 60-80 km respectively, the calculated values of the rate of ion production agree with the values obtained from the above expression provided $N_e = 2 \times 10^4$ and $7.7 \times 10^3\ cm^{-3}$ in the ranges 80-100 km and 60-80 km respectively.

E-region:

E. O. Hulburt (1938) proposed that soft X-rays may produce the E-region Hoyle and Bates (1948) supported Hulburt's proposal. In considering auroral phenomena, Vegard (1923, 1938) also suggested that X-rays are a major contributor to the ionization at high altitudes. Also, from solar energy measurements by rocket-borne experiments, it appears that ionization of E-layer is due to soft X-ray emissions from solar corona. Recently, Friedman (1959) suggested that E-region is produced by X-rays and Lyman-β (1025.7A). Ghosh and Sharda Nand (1960) hold that although Lyman-β radiation is absorbed in E-layer, it does not produce ionization because it requires radiations of wavelength less than 1019A*.

*The first ionization potential of O_2 obtained by Watanabe, Marmo, and Inn (1953) and also by Watanabe (1954) is 12.07 ± 0.01 ev (1027A). If we accept this value instead of 12.2 ev given by Herzbreg (1950), Lyman-β can ionize O_2 molecules.

From the transmission curves (Fig. 9) for solar radiations in the X-ray and ultraviolet regions through the earth's atmosphere obtained from rocket data, it has been shown by Ghosh and Sharda Nand (1960) that only X-rays between the wavelength region 5-100A are absorbed in the region of the atmosphere occupied by E-layer (100-125 km). The amount of X-ray energy absorbed in this layer has been estimated to be 0.19 erg cm^{-2} sec^{-1}. The average rate of ion production in the E-region is 6.2×10^9 cm^{-2} sec^{-1} $column^{-1}$. This rate of ion production agrees with the value obtained from the formula (1) provided $\alpha = 6 \times 10^{-8}$ cm^3 sec^{-1} and $Ne = 2 \times 10^5$ cm^{-3}.

F-regions:

According to Havens, Friedman, and Hulburt (1954) F_1-layer is caused by solar radiations 100-200A and F_2-layer by He I (λ 584) and He II (λ 304) resonance lines together with other solar emissions in the region between 100 and 1000A. The energy of the solar emission lines of the spectrum between 100 and 1000 A obtained from rocket-borne spectrographs (Aerobee-Hi, June 4, 1958; March 30, 1959) was utilized for calculating the ionization rates from 120 to 350 km. The electron densities were then determined. The calculated rates of production of ions are given in Table 10 and electron density distribution with height is shown in Fig. 11 (Ghosh and Sharda Nand, 1961).

From Fig. 11 it follows that radiation $\lambda\lambda$ 100-200 can cause ionization of F_1-layer, although the height of calculated maximum ionization is lower than the

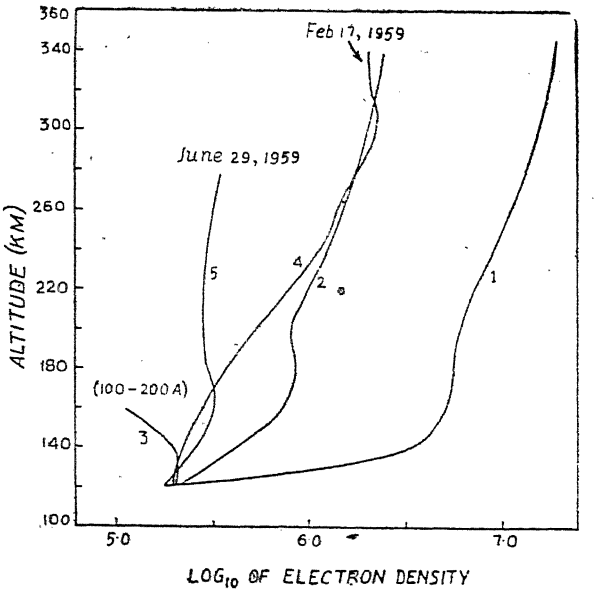

Fig. 11. Distribution of electron density with altitudes. Calculated distributions for radiations (100) 1000A), (He I and He II resonance lines), and (100-200A) are shown in curves 1, 2, and 3 respectively. Curve 4 (Jackson et al, 1958) and curve 5 (Nisbet, 1960) are obtained from rocket-borne experiments (Ghosh and Sharda Nand-Unpublished).

TABLE 10

Rate of ionization in F_1 and F_2 layers

Height	Ionization due to ultraviolet radiation				Ionization due to X-rays		Total rate of ionization
	O_2	O	N_2	N	O	N	
(km)	(cm^{-3} sec^{-1})	(cm^{-3} sec^{-1})	(cm^{-3} sec^{-1})	(cm^{-3} sec^{-1})	(cm^{-3} sec^{-1})	(cm^{-3} sec^{-1})	(cm^{-3} sec^{-1})
120	6.6×10	3.45×10^2	3.39×10^2	1.6	1.35×10^3	1.22×10^3	3.32×10^3
140	7.53×10^3	3.10×10^4	1.77×10^5	1.56×10^3	3.18×10^2	2.95×10^2	2.18×10^5
150	9.65×10^3	5.36×10^4	3.08×10^5	3.37×10^2	1.34×10^2	1.34×10^2	3.71×10^5
160	7.15×10^3	4.88×10^4	2.88×10^5	4.04×10^2	5.90×10	6.70×10	3.44×10^5
180	2.49×10^3	2.35×10^4	1.38×10^5	2.59×10^3	...	...	1.67×10^5
200	9.30×10^2	1.44×10^4	5.83×10^4	1.67×10^3	...	...	7.53×10^4
220	3.66×10^2	8.77×10^3	2.56×10^4	1.05×10^3	...	...	3.58×10^4
240	1.56×10^2	5.49×10^3	1.19×10^4	6.90×10^2	...	...	1.82×10^4
250	1.03×10^2	4.40×10^3	8.34×10^3	5.68×10^2	...	...	1.34×10^4
260	6.53×10	3.55×10^3	5.93×10^3	4.58×10^2	...	...	1.00×10^4
280	...	2.37×10^3	3.10×10^3	3.25×10^2	...	...	5.79×10^3
300	...	1.63×10^3	1.71×10^3	2.30×10^2	...	...	3.57×10^3
320	...	1.16×10^3	9.89×10^2	1.67×10^2	...	...	2.32×10^3
350	...	7.19×10^2	4.69×10^2	1.06×10^2	...	...	1.29×10^3

observed height The He resonance lines can explain the ionization of F_2-layer. However, the curve shows no maxima (curve 2). Furthermore, this radiation gives a maximum peak at 180 km in agreement with that given by Ratcliffe et al (1956) for F_1-layer. The question now arises what rôle other radiations between 200 and 1000A play. Ghosh and Sharda Nand (1961) assumed that the whole radiation ($\lambda\lambda$ 100-1000) is used in ionization and showed (curve 1) that it is hard to reconcile the big discrepancy between the observed and the calculated values of ionization.

(c) Distribution of neutral particles in the earth's atmosphere

Although the distribution of O_2 with height is well known, our knowledge of the distribution of N_2 and NO are meagre. These latter gases absorb solar energy in the extreme ultraviolet and X-ray regions. Therefore, from the amount of energy in these wavelength regions obtained from rocket-borne experiments at different altitudes, one can determine the distribution of these gases with height and is given below.

Distribution of N_2

The rocket data for X-ray energy measurements and their depths of penetration are collected in Table 11. Using these data, the rate of formation of O^+ ions by K-shell ionization due to absorption of solar X-rays, and also by valence shell ionization produced by electrons emanated from K-shell were calculated. The procedure was repeated for O_2 molecules and then assuming that the X-ray energy received from the sun is spent wholly in ionizing O_2, O, and N_2 molecules, the distribution of N_2 in the upper atmosphere was calculated by Ghosh and Sharma (1961) and is given in Table 12. The calculated distribution of N_2 was compared with other data (Table 13).

Distribution of NO:

It has been mentioned in Section 4. (b) that the normal D layer ionization is caused by photoionization of NO by Lyman-α radiation and the enhancement of ionization of this layer by X rays. The enhancement of ionization by radiations of wavelength less than 10A, which are emanated from the sun during solar activity, was discussed and its rate of ionization was estimated by Ghosh and Sharda Nand (1961). Assuming that the increment in the ionization of D-layer is equal to ten times the ionization of normal D-layer, the rate of photoionization of NO and hence the distribution of NO was determined as follows :

If β be the ionization cross-section for NO corresponding to frequency ν, $n(NO)$ the particle concentration per cm^3, $n(h\nu)_h$ the number of photons cm^{-2} sec^{-1} corresponding to frequency ν incident at a height h, the rate of production of ions is given by

$$q(NO^+) = \beta\, n(NO)\, n(h\nu)_h .$$

Therefore,

$$n(NO) = \frac{q(NO^+)}{\beta\, n(h\nu)_h} .$$

The photoionization of NO is mainly due to Lyman-α radiation. Taking the ionization cross-section of NO corresponding to Lyman-α as 2×10^{-18} cm^2 (Nicolet

TABLE* 11

Wavelength region (A)	Sun's condition	Incident energy (erg/cm²sec)	Altitude h for 95 absorption (km)	Number of O atoms above altitude h (/cm²column)	Number of O_2 molecules above altitude h (/cm²column)
6 – 10	160 minutes after class I flare	$10^{-4} - 10^{-3}$	95	$7{\cdot}0\times10^{18}$	$1{\cdot}8\times10^{18}$
Below 8	Late in class I flare	$5{\cdot}0\times10^{-3}$	95	$7{\cdot}0\times10^{18}$	$1{\cdot}8\times10^{18}$
8 – 12	Quiet	$3{\cdot}0\times10^{-3}$	100	$4{\cdot}9\times10^{18}$	$1{\cdot}5\times10^{17}$
8 – 18	High coronal activity	0·6	105	$2{\cdot}6\times10^{18}$	$1{\cdot}8\times10^{16}$
8 – 20	– do –	0·1	105	$2{\cdot}6\times10^{18}$	$1{\cdot}8\times10^{16}$
8 – 20	Quiet	$1{\cdot}5\times10^{-3}$	105	$2{\cdot}6\times10^{18}$	$1{\cdot}8\times10^{16}$
8 – 20	– do –	$1{\cdot}3\times10^{-3}$	105	$2{\cdot}6\times10^{18}$	$1{\cdot}8\times10^{16}$
8 – 20	– do –	$1{\cdot}2\times10^{-3}$	105	$2{\cdot}6\times10^{18}$	$1{\cdot}8\times10^{16}$
8 – 20	Minimum solar activity	$0{\cdot}4\times10^{-3}$	105	$2{\cdot}6\times10^{18}$	$1{\cdot}8\times10^{16}$
44 – 60	– do –	$1{\cdot}4\times10^{-2}$	110	$2{\cdot}3\times10^{17}$	$5{\cdot}2\times10^{15}$
44 – 100	– do –	$2{\cdot}9\times10^{-2}$	120	$5{\cdot}0\times10^{18}$	$2{\cdot}8\times10^{13}$
44 – 100	– do –	$3{\cdot}5\times10^{-2}$	120	$5{\cdot}0\times10^{16}$	$2{\cdot}8\times10^{13}$

TABLE 12

Rate of O^+ ion production above altitude h (/cm² col sec)	Rate of O_2^+ ion production above altitude h (/cm² col sec)	Rate of N_2^+ ion production above altitude h (/cm² col sec)	Number of calculated N_2 molecules above altitude h (/cm² col.)
$5{\cdot}3\times10^{6}$	$2{\cdot}7\times10^{6}$	$8{\cdot}5\times10^{6}$	$1{\cdot}1\times10^{19}$
$7{\cdot}3\times10^{6}$	$4{\cdot}4\times10^{6}$	$1{\cdot}6\times10^{6}$	$1{\cdot}5\times10^{20}$
$2{\cdot}8\times10^{7}$	$1{\cdot}9\times10^{6}$	$5{\cdot}3\times10^{7}$	$7{\cdot}7\times10^{18}$
$5{\cdot}7\times10^{9}$	$8{\cdot}7\times10^{7}$	$9{\cdot}7\times10^{9}$	$4{\cdot}3\times10^{18}$
$8{\cdot}9\times10^{8}$	$1{\cdot}4\times10^{7}$	$1{\cdot}6\times10^{9}$	$4{\cdot}3\times10^{18}$
$1{\cdot}1\times10^{7}$	$1{\cdot}7\times10^{5}$	$2{\cdot}3\times10^{7}$	$4{\cdot}4\times10^{18}$
$9{\cdot}4\times10^{6}$	$1{\cdot}5\times10^{5}$	$2{\cdot}0\times10^{7}$	$4{\cdot}3\times10^{18}$
$8{\cdot}7\times10^{6}$	$1{\cdot}3\times10^{5}$	$1{\cdot}8\times10^{7}$	$4{\cdot}3\times10^{18}$
$2{\cdot}9\times10^{6}$	$4{\cdot}5\times10^{4}$	$6{\cdot}0\times10^{6}$	$4{\cdot}3\times10^{18}$
$4{\cdot}0\times10^{7}$	$2{\cdot}1\times10^{5}$	$5{\cdot}2\times10^{8}$	$3{\cdot}4\times10^{18}$
$3{\cdot}5\times10^{7}$	$4{\cdot}6\times10^{4}$	$1{\cdot}1\times10^{9}$	$2{\cdot}0\times10^{18}$
$4{\cdot}0\times10^{7}$	$5{\cdot}4\times10^{4}$	$1{\cdot}4\times10^{9}$	$1{\cdot}9\times10^{18}$

*Ghosh, S. N., and Sharma, K. D. (1961).

TABLE 13

Number of molecular nitrogen in the atmosphere above the depth of penetration

Altitude (km)	Number of N_2 molecules above altitude h after White and Newell (1956) (/cm² column)	Number of N_2 molecules above altitude h after Miller (1957) (/cm² column)	Calculated number of N_2 molecules above altitude h after Ghosh and Sharma (1961) (/cm² column)
95	$4{\cdot}0\times10^{19}$	$3{\cdot}8\times10^{19}$	$1{\cdot}1\times10^{19}$
100	$1{\cdot}4\times10^{19}$	$1{\cdot}2\times10^{19}$	$7{\cdot}7\times10^{18}$
105	$8{\cdot}3\times10^{18}$	$7{\cdot}0\times10^{18}$	$4{\cdot}3\times10^{18}$
110	$3{\cdot}2\times10^{18}$	$2{\cdot}6\times10^{18}$	$3{\cdot}4\times10^{18}$
120	$9{\cdot}0\times10^{17}$	$7{\cdot}0\times10^{17}$	$1{\cdot}9\times10^{18}$

and Aikin, 1960) and the energy of Lyman-α at the top of the atmosphere equal to 6·3 erg cm^{-2} sec^{-1} (Byram et al, 1958), the distribution of NO with height was calculated by Ghosh and Sharda Nand (1961) from the above formula and is given in Table 14. The calculated values were compared with other available data given in Table 15.

TABLE 14

Calculated distribution of NO with height

Height (km)	Number of incident photons (cm^{-2} sec^{-1})	n(NO) (cm^{-3})
70	3.9×10^{10}	1.7×10^{8}
80	2.3×10^{11}	2.6×10^{7}
90	3.5×10^{11}	1.4×10^{7}
100	3.7×10^{11}	1.3×10^{7}

TABLE 15

The distribution of NO with height obtained by different investigators

Height (km)	n(NO) (cm^{-3})	Investigator
75	2×10^{11}	Bates and Seaton (1950)
90	4×10^{10}	
D-region	1×10^{12}	Mitra (1954)
70	1×10^{7}	Nicolet (1958)
80	2.2×10^{8}	
90	1.1×10^{7}	
100	2.7×10^{6}	
70	3.98×10^{8}	Miller (1957)
80	1.00×10^{8}	
90	1.58×10^{7}	
100	3.96×10^{6}	

5. SOME FUTURE PROBLEMS

1. In Section 2, we have mentioned the difficulties associated with photographing solar spectrum from a rocket. This is mainly due to the short time available for making such observation. The total time of flight of a rocket is only about five minutes of which only 3 minutes are available for taking observation, because during this period the rocket remains in the high altitude regions of the atmosphere. This difficulty can be eliminated if the observations are taken from satellites which stay aloft in the sky for days, months, and even years. Iu such case, it may even be possible to take X-ray spectrum of solar radiations which has not yet been photographed. Furthermore, if observations are taken from a satellite, it may be possible to use a spectrograph of high resolution requiring long time of exposure so that greater detail of the spectrum may be obtained.

2. The E-layer ionization is found to have an eleven-year variation. If this layer is caused by X-rays (Section 4-b), the radiations emitted from the sun should also vary with this period. Therefore, the observations should be made at least during a complete solar cycle from an altitude above the E-layer. Similar observations should also be made for extreme ultraviolet radiations from high altitudes.

3. More observations of the solar spectrum should be made under quiet sun conditions and also during flare time in order to clarify the cause of ionization of upper atmospheric layers.

4. It was mentioned before (Section 3-d) that radiations upto 0.6A was detected from a rocket-borne photon counter. Attempts should be made to obtain hard X-rays, if any, are emanated from the sun.

5. Observations in the extreme ultraviolet region below 1000A, in particular below 500A, are very meagre. Many lines were photographed by Violett and Rense (1959) in the region between Lyman-α and 550A. However, these lines were absent in the spectrum obtained by Purcell et al (1960). More observations should be taken in this region of the solar spectrum.

REFERENCES

1. Abound, A., Behring, W. E., and Rense, W. A. 1959, *Astrophys. J.*, **130**, 381.
2. Bates, D. R., and Seaton, M. J., 1950, *Proc. Phys. Soc. London*, **B63**, 129.
3. Baum, W. A., Johnson, F. S., Oberly, J. J., Rockwood, C. C., Strain, C. V., and Tousey, R., 1946, *Phys. Rev.*, **70**, 781.
4. Behring, W. E., McAllister, H., and Rense, W. A., 1958, *Astrophys. J.*, **127**, 676.
5. Byram, E. T., Chubb., T. A., and Friedman, H., 1954, *Rocket Exploration of the Upper Atmosphere Pergamon Press, Ltd., London, p.* 274.
6. Byram, E. T., Chubb, T. A., and Friedman, H., 1956, *J. Geophys. Res.*, **61**, 251.
7. Byram, E. T., Chubb, T. A., Friedman, H., and Gailar, N. 1953 *Phys. Rev.*, **91**, 1278.
8. Byram, E. T., Chubb, T. A., Friedman, H., and Kupperian, J E., Jr. 1956, *Astrophys. J.*, **124**, 480.
9. Byram, E. T., Chubb, T. A., Friedman, H., Kupperian J. E., Jr., and Kreplin, R. W., 1958, *Astrophys. J.*, **128**, 738.
10. Byram, E. T., Chubb, T. A., Friedman, H., and Lichtman, S. W., 1952, *J. Opt. Soc. Am.*, **42**, 876.
11. Chubb, T. A., Friedman, H., and Kreplin, R. W., 1960, *'Space Research' Edited by H. K. Kallmann Bijl, North-Holland Publishing Company-Amsterdam., p* 695.
12. Chubb, T. A., Friedman, H., Kreplin, R. W., and Kupperian, J. E., Jr. 1957, *J. Geophys. Res.*, **62**, 389.
13. Compton, A. H., and Allison, S. K., 1953, *X-ray in Thoory and Experiments, MacMillan and Company.*
14. de Jager, C., 1959, *Handbuch Der Physik. Published by Springer-Verlag, Berlin, Gottingen, Heidelberg.*
15. Durand, E., Oberly, J. J., and Tousey, R., 1949, *Astrophys. J.*, **109**, 1.
16. Friedman, H., 1959, *Proc. I. R. E.*, **47**, 272.
17. Friedman, H., and Chubb, T. A., 1955, *Physics of the Ionosphere, Physical Society, London, p.* 58.
18. Friedman, H., Lichtman, S. W., and Byram, E. T., 1951, *Phys. Rev.*, **83**, 1025.
19. Friedman, H., Lichtman, S. W., and Byram, E. T., 1953, *Phys. Rev.*, **91**, 1278.
20. Ghosh, S. N., and Sharda Nand, 1960. *Ind. J. Phys.*, **34**, 516.
21. Ghosh, S. N., and Sharda Nand, 1961, *Unpublished.*
22. Ghosh, S. N., and Sharma, K. D., 1961, *Planetary and Space Science.* **8**, 9.
23. Havens, R. J., Friedman, H., and Hulburt, E. O., 1954, *Physics of the Ionosphore, Physical Society, London*, p. 237.
24. Herzberg, G. 1950, *Spectra of Diatomic Molecules, D. Van Nostrand Co, Inc., New York*, p. 459.
25. Hopfield, J. J., and Clearman, H. E., 1948, *Phys. Rev.*, **73**, 877.
26. Hoyle, F., and Bates, D. R., 1948, *Terr. Mag.*, **53**, 51.
27. Hulburt, E. O., 1938, *Phys. Rev.*, **53**, 344.

28. Jackson, J. E., and Seddon, J. C., 1958, *J. Geophys. Res.*, **63**, 197.

29. Johnson, F. S., Purcell, J. D., and Tousey, R., 1954, *Phys. Rev.*, **95**, 621.

30. Johnson, F. S., Malitson, H. H. Purcell, J. D. and Tousey, R. 1954, *Astrophs J.* **127**, 80.

31. Jursa, A. S., Le Blanc, F. J., and Tanaka, Y. 1955, *J. Opt. Soc. Am.*, **45**, 1035.

32. Kallmann, H. K., White, W. B., and Newell, H. E., 1956, *J. Geophys. Res.*, **61**, 513.

33. Miller, L. E. 1957, *J Geophys. Res.*, **62**, 351.

34. Miller, S. C., Jr., Mercure, R., and Rense, W.A. 1956, *Astrophys. J.*, **124**, 580.

35. Mitra A. P., 1954, *J. Atmosph. Terr. Phys.*, **5**, 28.

36. Mitra, A. P., and Jones, R. E., 1954, *J. Geophys. Res.*, **59**, 391.

37. Nicolet, M. 1945, *Mem. Instit. Roy. Met., Belgium*, **19**, 1.

38. Nicolet, M. 1952, *Physics and Medicine of the Upper Atmosphere*, *The University of New Mexico Press*, p. 182.

39. Nicolet, M., 1954, *The Earth as a Planet, Edited by G. P., Kuiper, The University of Chicago Press, Chicago*, p. 644.

40. Nicolet, M. 1958, *Ionospheric Research, Scientific Report No* 102, *(April 1, 1958)*.

41. Nicolet, M., and Aikin, A. C, 1960, *J. Geophys. Res.*, 65, 1469.

42. Nisbet, J. S. 1960, *J Geophys. Res.* 65, 2597.

43. Purcell, J D., Packer, D. M., and Tousey, R. 1960, *'Space Research' Edited by H. K. Kallmann Bijl, North-Holland Publishing Company-Amsterdam*, p. 581.

44. Pietenpol, W. B., Rense, W. A, Walz, F. C, Stacey, D. S, and Jackson, J. M. 1953, *Phys. Rev.* **90**, 156,

45. Ratcliffe, J. A., Schmerling, E. R., Setty, C. S. G. K., and Thomas, J. O. 1956, *Phill. Trans. Roy. Soc. London*, **A248**, 621

46. Rense, W. A., 1953, *Phys. Rev.*, **91**, 299.

47. Tousey, R., 1953, *'The Sun' Edited by G. P. Kuiper, The University of Chicago Press, Chicago. Illinois.*, p. 658.

48. Tousey, R., Watanabe, K., and Purcell, J. D. 1951, *Phys. Rev.* **83**, 792.

49. Vegard, L. 1923, *Skr. Vid. Selsk, I, Nos.* 8, 9, and 10.

50. Vegard, L. 1938, *Geofhys. Public.*, **12**, 23, 2 *pls.*

51. Violett, T., and Rense, W A, 1959, *Astrophys. J.*, **130**, 954.

52. Watanabe, K., 1951, *Phys. Rev.* **83**, 781.

53. Watanabe, K. 1954, *J. Chem. Phys.*, **22**, 1564.

54. Watanabe, K, Marmo, F. F., and Inn, E. C. Y., 1953, *Phys. Rev.*, **91**, 1155.

55. Watanabe, K., Marmo, F. F, and Pressman, J. 1955. *J. Geophys. Res.*, **60**, 513.

56. Woolley, R.v.d.R., and Allen, C. W. 1950, *M. N.*, **110**, 358.

SPECTRA OF POLYATOMIC MOLECULES

By

NAND LAL SINGH

Banaras Hindu University

[Received on 7th April, 1962]

INTRODUCTION

Spectra of atoms and diatomic molecules are fairly well understood both from theoretical and experimental points of view; but the progress in the Spectroscopy of polyatomic molecules specially from its theoretical aspect has been very slow.

Earlier spectroscopic work on polyatomic molecules concern mainly with

(a) their absorption spectra in liquid or in solution, studied in the visible and in the ultraviolet regions and recently in infrared regions also.

and (b) their Raman spectra, also studied in liquid or solution phases. These studies have given information about the frequencies of such molecules in their ground state which are highly perturbed by intermolecular forces. We do not get information about free molecules.

The studies in gaseous phase are almost entirely free from inter-molecular forces. Attempts with fruitful results have been made recently to study the Raman and Infrared spectra of these molecules in gaseous phase.

Use of study of electronic spectra

The study of the electronic spectra of polyatomic molecules in vapour phase provides the following informations :—

1. The change of electronic energy of the free molecule, and
2. The normal vibrations of both the electronic states involved.

The selection rules governing the appearance of vibrations in the case of Electronic, Raman and Infrard spectra are not the same hence some vibrations which are not observed in Raman and I. R. spectra may appear in the electronic spectra.

3. Information regarding the structure, the normal vibrations and vibrational interactions and intra-molecular force-field of a molecule in its electronically excited states can be known.

4. Interactions between electronic and vibrational motions which play a prominent role in the electronic spectra of polyatomic molecules can be investigated.

5. Internal and external factors affecting the mean life of a molecule in its electronically excited states can be determined.

Electronic spectra in absorption give information mostly about their excited state; while their emission spectra give fuller informations about the ground state.

Emission spectra can be studied in fluorescence, phosphorescence and by electrical excitation. Emission in fluorescence and phosphorescence is too weak; while emission by electrical excitation is too difficult to manipulate without dissociation. All the same the emission studies are highly desireable not only for a full understanding of the ground state, but also in the development of the theory of spectra of polyatomic molecules which is still in its infancy. The only molecule of which the near U. V. spectrum has been understood to some degree of completeness is benzene.

According to the molecular orbital theory, benzene has got six mobile electrons, each carbon atom contributing one. These move in a field of hexagonal symmetry of the nuclear frame and the combined charge distribution has a node in the frame of the ring. Two of these electrons are accommodated in $l = 0$ and the remaining four are accommodated in $l = 1$. As such the ground state configuration is represented by $0^2\,1^4$. If one electron out of these is excited, the resulting configuration in the new state becomes

$$0^2\,1^3\,2$$

which is fourfold degenerate. Group theoretical considerations show that this four fold degenerate state splits into two non-degenerate states and a doubly degenerate state; but one can not know about the order of splitting or the measure of energy present in these states. We can only ascertain their symmetry types. This knowledge combined with the experimental data has proved that the 2600Å system in benzene arises out of $^1A_{1g} - {}^1B_{2u}$, which is a forbidden transition; but is made allowed due to a suitable non-totally symmetric vibration.

In the case of substituted benzenes, the symmetry is lowered and greater complexities arise due to these substituents leading to more and more uncertainty in arriving at definite conclusions. Their vibrational data are also not as comprehensive as that of benzene.

The symmetry of low lying levels in substituted benzenes can be obtained to a close approximation from those of benzene, when the D_{6h} correspond to certain types in D_{2h} or C_{2v} or C_{2v}*. Convenient illustrations of these transformations have been given by Langseth and Lord as shown in figure (1). Since the near U. V.

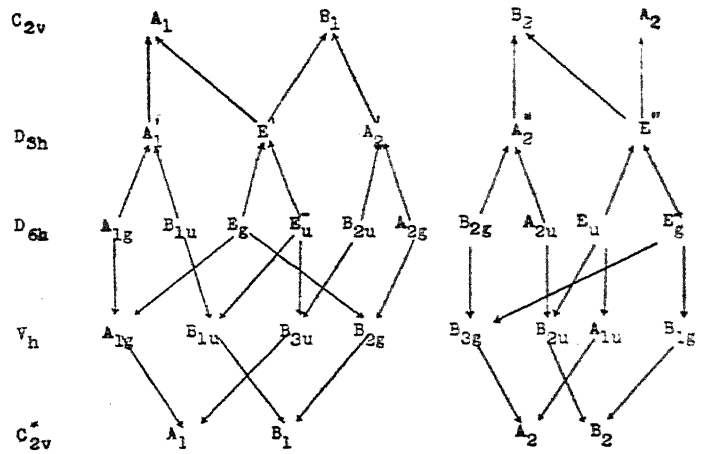

Fig. 1. Corresponding symmetry types obtained by substitutions.

absorption spectrum of benzene represents a transition $^1B_{2u}$—$^1A_{1g}$ the transitions for substituted benzenes are also shown in the same figure. These levels occur with multiplicities of one or three. Lewis and Kasha have observed such levels in their phosphorescence studies.

Because of rapid dissociation, the emission by electrical excitation is rather too difficult; yet Stewart *et al* and Schüler have succeded in exciting some of the polyatomic molecules and radicals in suitable discharge tubes. We, in the Department of Spectroscopy, Banaras Hindu University, have also succeeded in getting the emission spectra of some 30 molecules such as benzene, toulene, benzaldehyde, aniline, phenol, anisole, phenetole, benzonitrile, xylenes, cresols, di-cholorobenzene, fluorobenzene, benzotrifluoride, ethylbenxene, chlorophenol etc. The results obtained have already been reported to learned societies such as this on different occassions.

I shall present before you some of these results indicating the experimental manipulation in getting their characteristic emission spectra before dissociation.

The absorption spectra were taken in suitable tubes fitted with quartz windows joined through quartz to glass graded seal. A bulb containing the substance was attached in the middle to one side of the tube. The source of continuum has invariably been a Hydrogen bulb operated by a regulated power unit. The vapour pressure was regulated by suitably heating or cooling the bulb and sometimes the whole tube.

The emission spectra were obtained by exciting the substance in flowing vapour state with an uncondensed transformer discharge controlled by a variac or high frequency discharge. The discharge tube in the case of transformer excitation has always been of the conventional π type of length varying from 25 cm to 100 cms and diameter 2·5 cms. The ends were fitted with quartz windows joined by quartz to glass seals.

The electronic spectra of polyatomic molecules are very complicated because of a large number of vibrations involved in both the states and the superposition of different rotational transitions, Simpler symmetry considerations permit us to interpret the vibrational pattern of the band system and to decipher in favourable cases the nature of the electronic states involved. The transition probability between two states is proportional to

$$\int \psi'^{*}el \; M \; \psi''el \; dTel,$$

where M is the electric dipole moment of the system and $\psi'^{*}el$ and $\psi''el$ are the eigenfunctions of the two electronic states under consideration. $dTel$ indicates that the integration is to be carried over the whole electronic configuration. The transition will be allowed only if it remains unchanged under all symmetry operations or that the expression should be totally symmetric. It can be seen that this expression should be totally symmetric when the product $\psi'^{*}el \; \psi''el$ is of the same symmetry as that of M which in turn behaves as a translation. So we see, that the nature-forbidden or allowed—of a transition depends upon the product $\psi'^{*}el \; \psi''el$, which in turn depends upon the symmetry properties of the two states. It is likely that the product $\psi'^{*}el \; \psi''el$ does not behave as a translation (as in benzene) and the transition is forbidden but still it may be observable (again as in Benzene) by the perturbing influence of vibrations of proper symmetry. In such cases the presence of vibration changes the symmetry type of the Eigenfunction of one or of both the electronic states in such a manner that their product once again starts behaving as a translation and the product $\psi'^{*}el \; \psi''el \; dTel$, becomes totally symmetric. The perturbing influence of vibration is possible both in allowed and forbidden transition

as well, but in the case of allowed transition it is observed only weakly. However, when the transition is forbidden they are predominant.

A consideration of the symmetry types of the vibrational eigenfunctions indicates that the nature of vibrational pattern in the case of an allowed transition will follow the selection rules :—

1. A totally symmetric vibration may change by any number of quanta,

$$\triangle v = 0, 1, 2, 3...$$

2. A non-totally symmetric vibration may change by an even number of quanta,

$$\triangle v = 0, 2, 4...$$

3. No transition will take place from a state in which only totally symmetric vibrations are excited by several quanta to another state in which in addition one non-totally symmetric vibration with one quantum is present.

We expect in the case of an allowed transition one quantum progression of totally symmetric vibrations and their combination. We expect a two quanta progression of non-totally symmetric vibration to occur with weaker intensity and also combination bands of such vibrations as are allowed by the above selection rules.

In the case of forbidden transition, there being no zero band the above pattern starts from the band which involves the one quantum excitation of the vibration making the transition allowed.

(*a*) On the emission spectrum of mono-fluorobenzene

The emission spectrum of fluorobenzene excited by an uncondensed transformer and also by H. F. discharge through mixed vapour of fluorobenzene and *n*-hexane, were photographed on Hilger E_1 and E_2 Quartz Spectrographs by Dr. K. N. Upadhya. More than 100 sharp and red degraded bands have been recorded on the plate.

The emission spectrum consisting of more than 100 bands lies in the region 2577 – 2988Å. A continuum starts from 0, 0 band and covers faintly the entire spectrum without any sharp limit. The intensity of the continuum is maximum near about 2800Å and fades gradually on the longer wavelength side. Reproduction of a sample plate is given in fig. (2).

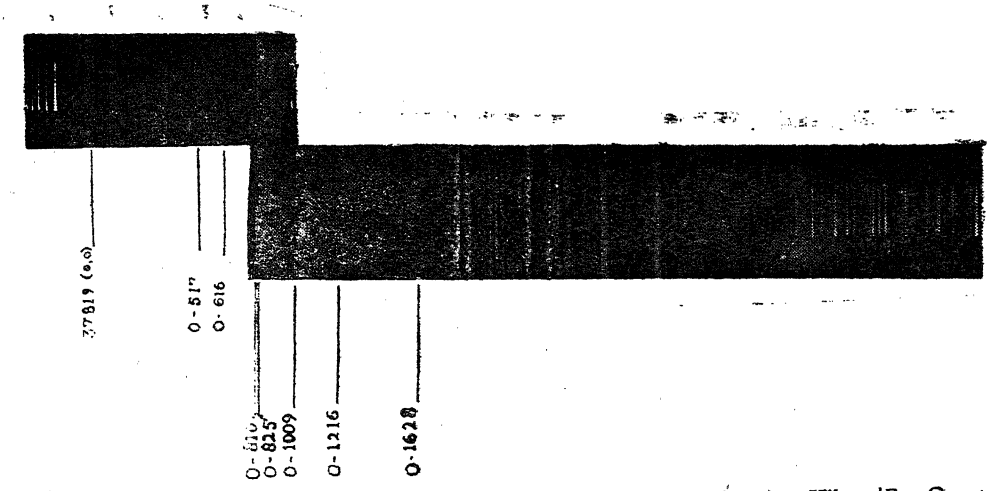

Fig. 2. Emission spectrum of mono-fluorobenzene; spectrogram taken on Hilger E_1 Quartz Spectrograph ; slit width 0.04 mm time 6 Hours.

The symmetry of mono-fluorobenzene molecule can be taken to belong to C_{2v} point-group to the first approximation and as such the electronic transition between $A_1 \leftarrow B_1$ states is an allowed transition. We expect totally symmetric vibrations to form progression. Vibrational analysis of the bands measured shows that out of four types of vibrations those of types a_1, b_1 and b_2 are observed. The position of 0, 0 band is observed at 37819 cm^{-1} which is close in agreement to fluorescence and absorption data. The following table gives the fundamental vibrations which are observed in the emission study. The symmetry as well as the probable modes of the fundamental vibrations are also included.

TABLE 2

Raman spectrum frequencies in cm^{-1}	Emission spectrum frequencies in cm^{-1}	Symmetry	Assignments
241	244	b_2	C-F cut of plane vibration.
407	418	b_1	
519	517	a_1	Totally symmetric part of E_g^+ (606 cm^{-1}) vibration of benzene.
612	616	b_1	Non-totally symmetric part of 606 cm^{-1} vibration.
759	758		
807	810	a_1	
831	825	a_1	
1010	1009	a_1	Ring breathing vibration.
1024	1025	a_1	Carbon vibration.
1157	1156	b_1	C—H bending.
1218	1220	a_1	C—F stretching.
1301	1303		
	1468		
3072	3068	a_1	C—H stretching.

Apart from these ground state frequencies the three frequencies 965, 910, 778 cm^{-1} are also observed involved in the bands lying towards shorter wavelenth side of the zero band (37819 cm^{-1}). Out of these 965 cm^{-1} is the excited state frequency corresponding to 1025 cm^{-1} ground state vibration. The other two excited state frequencies 910 and 778 cm^{-1} correspond to 1009 and 825 cm^{-1} ground state frequencies respectively.

The three difference frequencies 65, 44 and 24 cm^{-1} are observed in combination with other vibrations. Out of these 65 cm^{-1} appears to be involved in an intense band lying towards longer wave length side of the zero band.

(*b*) On the Emission Spectrum of Benzaldehyde

The emission bands of Benzaldehyde excited by transformer discharge were photographed on Hilger Large Quartz Spectrograph and on Fuess Spectrograph

by Garg S. N., and Singh I. S. Exposure time on Hilger Spectrograph was 10 hours with a slit width ·05 mm. and on Fuess it was 6 hours with a slit width of ·03 mm.

The spectrum lies in the region 3679-5933Å and consist of 325 bands. Some of the bands are very sharp and present a line like structure and some are diffuse and are degraded towards the red. A reproduction of the spectrum is given in fig. (3).

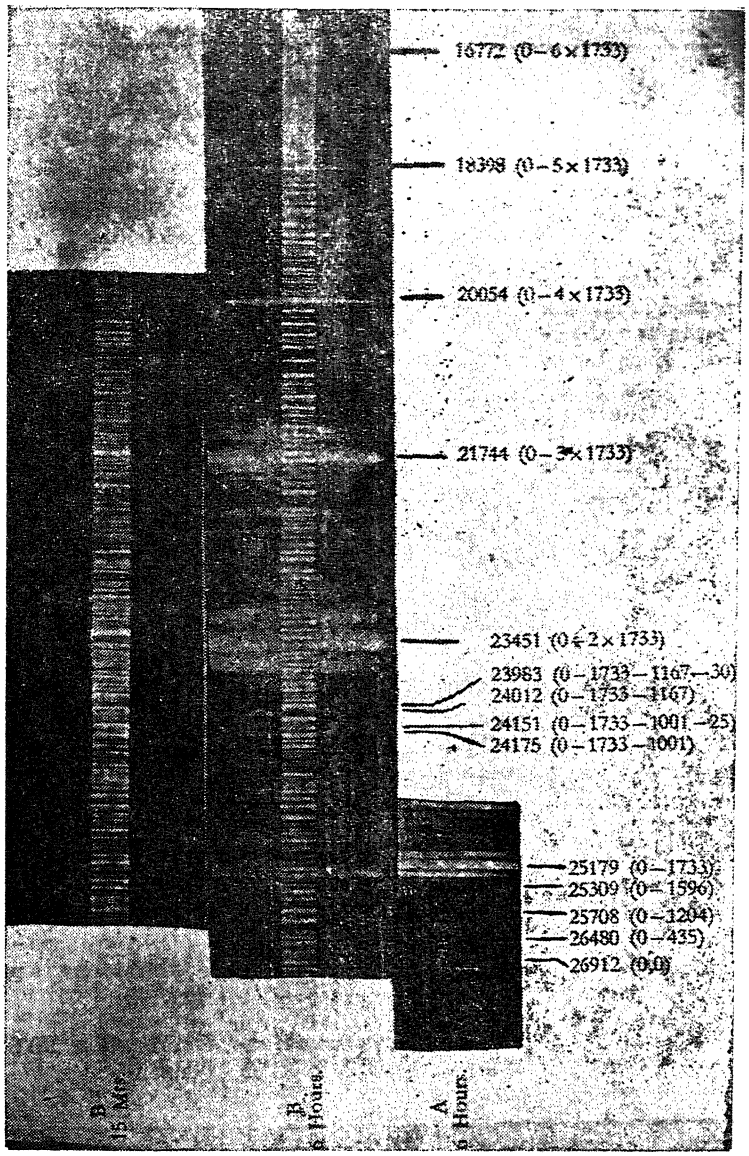

Fig. 3. Emission spectrum of benzaldehyde.
A. Spectrogram taken on Hilger medium quartz spectrograph, slit-width :—0,05 mm.
B. Spectrogram taken on Fuess glass spectrograph, slit-width :—0,03 mm.

It is possible to explain the grass structure of the spectrum on the basis of an allowed transition A_1—B_1 of the symmetry group C_{2v} but the finer details require a

lower symmetry C_s with the planes of CHO and C_6H_5 groups mutually perpendicular involving transition A′—A″. Probably the reduction of high symmetry D_{6h} to C_s takes place through the intermediary C_{2v} symmetry.

Analysis :

Band at	Separation	Raman line	Correlated with
26912 cm^{-1}	0-0	Corresponds to the zero band in absorption where the band at 26917 cm^{-1} is taken as (0,0) band. Robinson has taken 26914 cm^{-1} as zero band in emission.	
25179	1733	1700 cm^{-1} strongly polarised.	Assigned as the C=0 stretching frequency.
23451 S 21744 20054 18398 16772	This forms a progression and six quanta are observed. Each forms head of a group of bands arising out of other frequencies and their combinations.	...	...
25309 W	1603	1598 (depol. 0·88) totally symmetric freq. combines with various quanta of 1733 and other frequencies.	Corresponds to the ϵ_g^+ benzene freq. 1600 cm^{-1}.
23867 m. 20824 v.w.	3045 2 × 3045	3065 totally symmetric line. This also forms combinations with 1733 cm^{-1} (C = 0).	Magnitude of this freq. suggests it to be C—H stretching.
25708 w.	1204	1204 polarised ...	Corresponds to the ϵ_g^+ vibration of benzene.
24505 v.w.	2 × 1204	This also forms combinations with 1733 cm^{-1}.	Vibration 3047 cm^{-1}.
25909 v.w.	1003	1001 S. Polarised ...	Corresponds to breathing.
24908 v.w.	2 × 1001	Also forms combinations with 1733 & other freq.	Vibration 992 cm^{-1} of benzene.

Other ground frequencies observed in emission are 245, 430, 775, 828 and 1167. The Raman lines as recorded are 239, 439, 752, 828 and 1164. Of these 245 cm^{-1} and 828 are the non-totally symmetric and symmetric part respectively of the ϵ_g^- ben-

zene vibration 849 cm^{-1}. The 430 cm^{-1} frequency is the totally symmetric part of e_g^+ vibration of benzene at 606 cm^{-1}. The 1167 cm^{-1} is the totally symmetric part of e_g^+ benzene vibration at 1178 cm^{-1}.

Difference frequencies observed are 25, 30, 65 and 90 cm^{-1} which are probably due to 1 - 1 transitions of some suitable non-totally symmetric vibrations.

The upper state vibration frequencies responsible for some other bands are :—

140, 190, 245, 390, 500, 725, 860, 1175 and 1316 cm^{-1} of these 190 cm^{-1} combines very strongly with the 1733 cm^{-1} frequency and its multiples.

Observed Raman lines and vibrational frequencies of the ground state in the electronic spectrum :—

BENZALDEHYDE

Raman Lines		Vibration frequencies of the ground state
140 (w)d	...	140 (vw)
		215 (w)
245 (vw)d	...	245 (w)
		280 (vw)
440 (m)p	...	430 (w)
615 (w)d	...	620 (vw)
650 (vw)	...	650 (vw)
752 (vw)	...	775 (w)—?
828 (w)p	...	828 (mw)
1001 (s)p	...	1001 (m)
1023 (vw)	...	1020 (w)
1164 (m)p	...	1167 (m)
1204 (ms)p	...	1204 (m)
1395 (w)	...	1390 (w)
1458 (vw)	...	1456 (vw)
1495 (vw)	...	1500 (vw)
1598 (vs)d	...	1596 (w)
1701 (s)p	...	1733 (vs)—?
3065 (ms)p	...	3045 (ms)—?

Agreement :

In ground state frequencies :—1733 and its progressions, 215, 1003, 1167, 1596 and 3045 cm^{-1}. Also in the upper state frequency 190 cm^{-1}.

Difference :

The ground state frequency 452 cm^{-1} is correlated with 439 Raman Line by Robinson whereas we find it 433. He assumed ground state frequencies 538, 551 and 591 and correlated only 591 to Raman line 617, We explain the corresponding bands in another way. These frequencies are not proposed.

(c) On the emission spectrum of phenol.

In the general programme of our Laboratory to excite the organic molecules Shri B. R. Das obtained the emission bands of this molecule in an uncondensed transformer discharge under critical conditions. The discharge tube was longer in this case, of about 130 cm in length, and the discharge was maintained through the flowing vapour of the substance and it was found that a voltage of the order of 4 KV was suitable to get the emission bands. The Spectrum was photographed on the Hilger Medium Quartz Spectrograph having a dispersion of 13 Å/mm in the region of 2700 Å.

The complete spectrum lies between 2720-2940 Å and consists of red degraded bands which are not very sharp. A continuum is superposed over the entire spectrum and ends without sharp limit on the red side. About seventy bands have been measured on Hilger L76 Measuring Microscope having a least count of 0·001 mm. A reproduction of the spectrum is given in fig. (4).

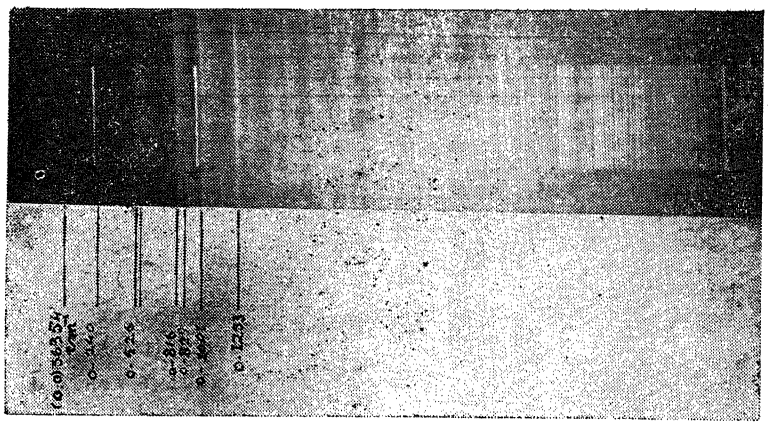

Fig. 4. Emission spectrum of phenol; spectrogram taken on Hilger E_2 Quartz Spectrograph.

Assuming OH radical to be one atom substituted in place of one H atom in benzene ring, the symmetry of phenol is reduced to C_{2v}. The bands are then attributed to the allowed transition $^1B_1 - {}^1A_1$.

The very weak band at 36354 Cm^{-1} is taken as the 0,0 band of the system. The weak intensity of the band, obviously due to self absorption by the unexcited vapour, is attributed to the very high oscillator strength of phenol and in some of the earlier plates, taken with discharge tube having window about 2 cm. away from the discharge (i.e. eleetrode), did not show this band; instead an absorption band in the continuum superposing the spectrum was observed in its place. This band agrees within experimental error with the 0,0 band in the absorption spectrum.

The bands lying at 36114, 35828, 35792, 35538, 35522, 35352 and 35099 are separated from the 0,0 band by 240 526, 625, 816, 832, 1002, and 1255 cm^{-1}. These are presumed to be the ground state frequencies and are correlated with Raman frequencies 242, 532, 617, 812, 429, 1001 and 1253.

A difference frequency 19 cm^{-1} has been found to be loaded on some of the above stronger bands and 2 to 3 quanta of it has been observed. This is the difference frequency due to $V' - V''$ transitions between low lying levels.

EMISSION SPECTRUM OF NiBr

By

N. SUNDARACHARY*

Department of Spectroscopy, Banaras Hindu University

[Received on 7th April, 1962]

1. INTRODUCTION

From empirical considerations it is expected that the diatomic nickel halide molecules should have electronic states with even multiplicities, but so far it is not definitely known whether the states involved in the emission of visible spectrum of NiBr are doublets or qaurtets or even both.

Kristnamurty (1952) excited the emission spectrum of NiBr in 2000 volts D. C. discharge and photographed it on a very low dispersion instrument such as Fuess Spectrograph. He analysed the spectrum in the region λλ 4000Å to 5000 Å into three systems designated as α, β and γ. Systems α and β were interpreted as due to transitions from two separate $^4\pi$ states to a common $^4\Sigma$ state, which has been assumed to be the ground state of the molecule.

Reddy and Rao (1960) excited the molecule again under 2000 volts D. C. discharge and photographed the spectrum on a grating spectrograph with a dispersion of 1.25 Å/mm. They analysed the bands in the region λ 4050 Å to λ 4700 Å into six brief systems and designated them as α_1, α_2 α_3, β_1, β_2 and γ, of which α_1, β_2 and γ were found to be double headed while the rest were single headed, but they failed to observe the heads of S and T and other satellite branches as reported by Kristnamurty. Instead the bands are either single headed or double headed. This leads one to think that the transitions between quartet states are improbable. Reddy and Rao's anaiysis of the spectrum also did not yield sufficient information regarding the multiplicity of the electronic states involved and the nature of the probable ground state of the molecule. It was, therefore, considered worthwhile to reinvestigate the spectrum of NiBr more systematically and under better conditions of excitation.

2. EXPERIMENTAL

The spectrum was excited using an anhydrous B. D. H. sample of $NiBr_2$ in a π form Pyrex tube with 9 mm bore. A 1 KW power transformer was used as a source of excitation and a strong heating of the discharge tube was found necessary to maintain sufficient vapour pressure of the substance. The NiBr bands were well developed when the colour of the discharge was blue. The spectrum was recorded on various low dispersion instruments such as Fuess Spectrograph and finally in the 2nd order of 21 ft. Concave Grating Spectrograph (Eagle Mounting) with an average dispersion of 1.25 Å/mm. Exposure of 2 to 3 hours was found sufficient to obtain good quality plates on the Grating Spectrograph.

3. STUDY OF PLATES AND ANALYSIS

The spectrum of NiBr extends from λ 5500 Å to λ 3800 Å and all bands are red degraded. Due to rapid decomposition of the substance there are number of

*Present address: Deptt. of Physics, Indian Institute of Technology, Kanpur.

atomic lines overlapping the spectrum and some times making it impossible to see some weak bands. Just as in the case of NiCl spectrum, band systems of NiBr exhibit very strong $\Delta v = 0$ sequences and weak ± 1 sequences while ± 2, ± 3 etc. sequences are not at all observed.

Comparatively stronger part of the spectrum in the region λ 4050 Å to λ 4500 Å has been analysed into five systems designated as A, B, C, D and E (shown in the Fig. (2).] The systems A, C, D and E correspond to systems α_1, α_3, β_1 and β_2 of Reddy and Rao, whose (0, 0) bands lie approximately at $\lambda\lambda$ 4112 Å (Q), 4204 Å (Q), 4354 Å and 4457 (Q) Å respectively. Our analysis of band systems A and D almost correspond to systems α_1 and β_1 of Reddy and Rao except for small differences in the value of vibrational constants. The points of disagreement are regarding the band systems α_3 and β_2.

Reddy and Rao reported the bands of system α_3 (present C) as single headed, but actually we find them clearly on our grating plates as double headed. Regarding system β_2 (present E), we could record the (1, 0), (2, 1) and (0, 1) bands on some over exposed plates on grating spectrograph. The only (1, 0) band (according to their analysis) which Reddy and Rao were able to measure on prism plates fits in our analysis as (2, 1) band. Thus, our present paper deals with the analysis and interpretation of three double headed and one single headed band systems. The wave-length and wave-number data of the bands of four systems with their vibrational quantum assignments are shown in the table Nos. 1, 3, 5 and 7. The derived vibrational constants ω_e, ω_e x_e and the ν_{00} in wave numbers are summarised in the table No. 9.

4. ISOTOPE EFFECT

More abundant isotopes of Nickel are having masses 58 and 60. Their natural abundances are 68% and 27% respectively. Bromine is having two isotopes of nearly equal abundance with masses 79 and 81. Therefore, in a natural mixture we expect four isotopic NiBr molecules namely $^{58}Ni\ ^{79}Br$, $^{58}Ni\ ^{81}Br$, $^{60}Ni\ ^{79}Br$, and $^{60}Ni\ ^{81}Br$ participating in the emission of the spectrum. In the spectrum as photographed in the 2nd order of grating spectrograph, we could observe the band heads of all four species with expected intensity ratio, namely 3 : 3 : 1 : 1, in $\Delta v = \pm 1$ sequences of all band systems. The wavenumber interval between the bands due to bromine isotopes is of the order 1 cm^{-1} while that of the bands due to nickel isotopes is of the order 3 cm^{-1}. The observed shifts of isotopic bands from the corresponding band head of $^{58}Ni\ ^{79}Br$ molecule are compared with the calculated shifts in the tables Nos. 2, 4, 6 and 8. Observation of isotope effect both due to nickel and bromine indicate the correctness of our analysis of the bands.

5. DISCUSSION

As shown in table No. 9 all the four systems show nearly equal values of first vibrational quanta in their upper states. The band systems A and C show nearly equal first vibrational quanta (307.2 cm^{-1}) and also vibrational frequencies (309.4 cm^{-1}) in their lower states, while the band systems D and E also show nearly equal first vibrational quanta of another value (320.5 cm^{-1}) in their lower states. This shows that these two pairs of band systems are having two different lower states with vibrational frequencies $\omega_e = 309.4$ cm^{-1} and $\omega_e = 322.6$ cm^{-1}.

An interval of 533 cm^{-1} occurs between the origins of first pair of band systems (A and C) and also between the origins of second pair of band systems (D and E). This observation leads us to suggest that these four systems probably arise out of transitions from a common doublet state with $\omega_e \approx 294$ cm^{-1} to two different lower

states with $\omega_e = 309{\cdot}4\ cm^{-1}$ and $\omega_e = 322{\cdot}6\ cm^{-1}$. If so, 533 cm^{-1} has to be taken as an electronic splitting of the upper common doublet state. Considering these observed facts following energy level diagram has been constructed representing the transitions giving rise to these four systems. The observed first vibrational quantum of each electronic states and the relative heights of the states are shown in the diagram. (Fig 1).

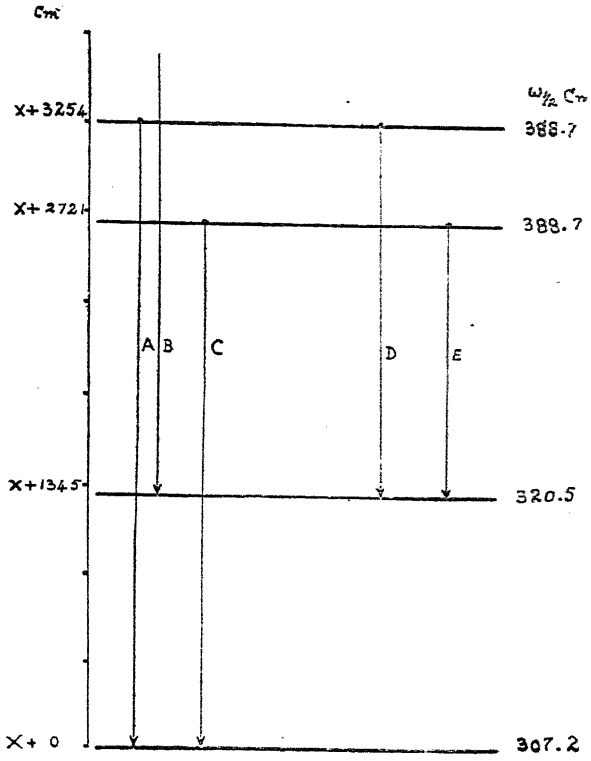

Fig. 1. Energy level diagram representing the transitions giving rise to the systems A, B, C, D and E of NiBr.

Thus, it is possible to interpret these four systems as due to transitions from a doublet electronic state with electronic multiplet splitting equal to 533 cm^{-1} to two different lower states with negligible electronic splittings such as $^2\Sigma$, $^2\Delta$ and $^2\pi$ (case b) states. The lowest of these two with $\omega_{1/2} = 307.2\ cm^{-1}$ or $w_e = 309{\cdot}4 cm^{-1}$ may probably be identified as the normal state of the molecule, but the evidence is not complete. Heimer (1937), Gaydon and Pearse (1935) analysed the fine structure of the NiH bands and determined $^2\Delta$ as the ground state of the molecule NiH. Diatomic halides and hydride of an atom in most of the definitely known cases show the same type of ground states. Therefore the ground state of the NiBr molecule may be assumed to be a $^2\Delta$ state with negligible electronic splitting.

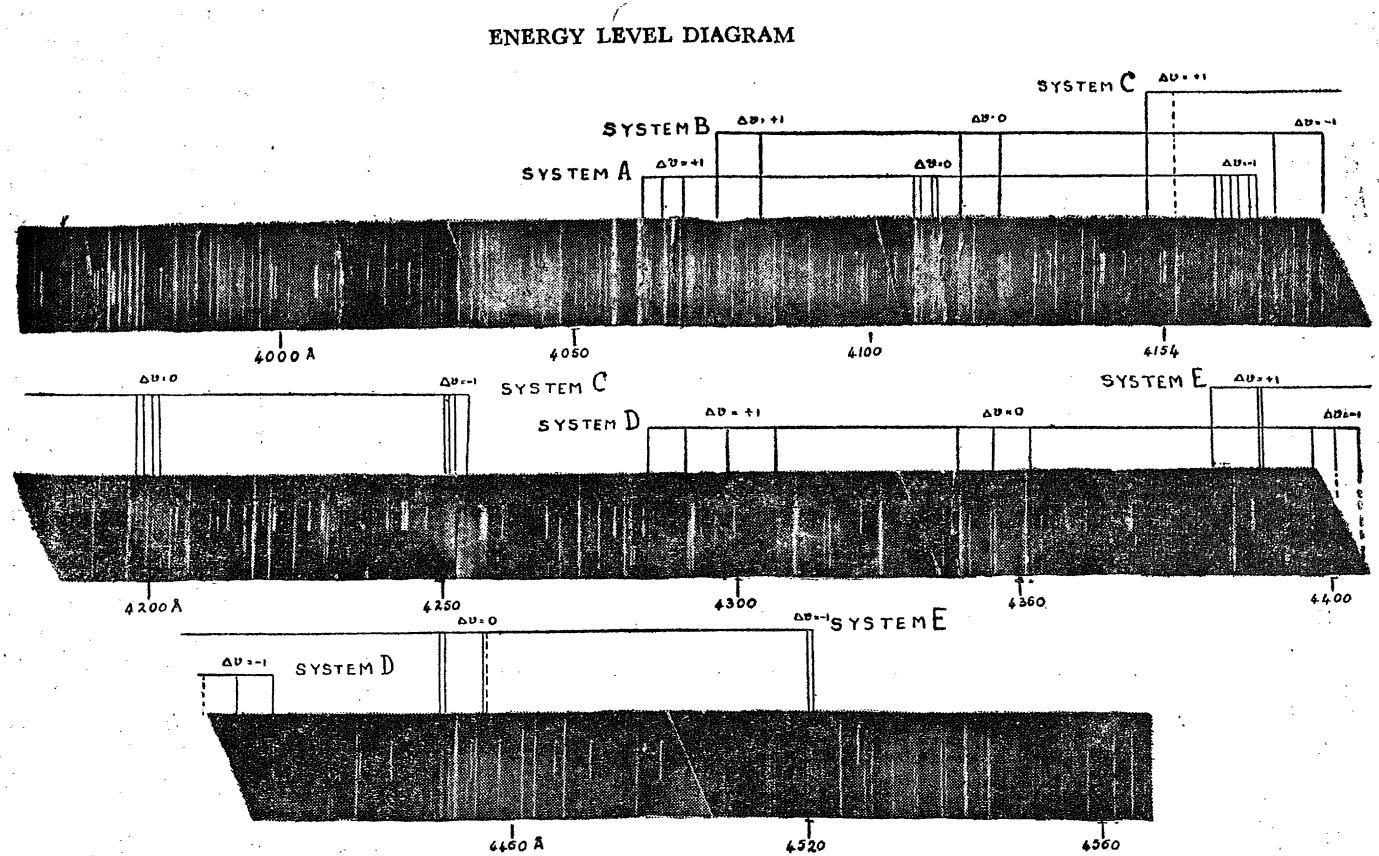

Fig. 2. Section of emission spec. mm. of NiBr in the region λ 4000 Å to λ 4550 as photographed in the 2nd order graphed classification of bands into systems A, B, C, D and E is shown.

TABLE No. 1

System – A

λ (Air) Å	I	k (Vac) cm^{-1}	V′,V″	Isotopic Emitter
4062·7	2	24607·2	(1,0) R	$^{58}Ni\ ^{79}Br$
4062·9	2	24606·0	(1,0) R	$^{58}Ni\ ^{81}Br$
4066·5	2	24584·2	(2,1) R	$^{60}Ni\ ^{79}Br$
4066·7	2	24583·0	(2,1) R	$^{60}Ni\ ^{81}Br$
4110·86	10	24318·97	(0,0) R	
4112·02	8	24312·12	(0,0) Q	
4114·00	6	24300·4	(1,1) R	
4115·04	4	24294·3	(1,1) Q	
4117·6	2	24279·16	(2,2) R	
4162·9	1	24014·9	(0,1) R	$^{60}Ni\ ^{81}Br$
4163·1	1	24013·8	(0,1) R	$^{60}Ni\ ^{79}Br$
4163·4	2	24012·1	(0,1) R	$^{58}Ni\ ^{81}Br$
4163·6	3	24010·9	(0,1) R	$^{58}Ni\ ^{79}Br$
–	–	–	(0,1) Q	$^{60}Ni\ ^{81}Br$
4164·2	1/2	24007·5	(0,1) Q	$^{60}Ni\ ^{79}Br$
4164·4	1	24006·3	(0,1) Q	$^{58}Ni\ ^{81}Br$
4164·65	1	24004·8	(0,1) Q	$^{58}Ni\ ^{79}Br$
4165·6	1	23999·4	(1,2) R	$^{60}Ni\ ^{81}Br$
4165·8	1	23998·2	(1,2) R	$^{60}Ni\ ^{79}Br$
4166·06	3	23996·7	(1,2) R	$^{58}Ni\ ^{81}Br$
4166·3	3	23995·4	(1,2) R	$^{58}Ni\ ^{79}Br$
–	–	–	(1,2) Q	
–	–	–	(2,3) R	$^{60}Ni\ ^{81}Br$
–	–	–	(2,3) R	$^{60}Ni\ ^{79}Br$
4169·5	3	23976·9	(2,3) R	$^{58}Ni\ ^{81}Br$
4169·8	3	23975·2	(2,3) R	$^{58}Ni\ ^{79}Br$
–	–	–	(2,3) Q	$^{60}Ni\ ^{81}Br$
–	–	–	(2,3) Q	$^{60}Ni\ ^{79}Br$
4170·5	2	23971·2	(2,3) Q	$^{58}Ni\ ^{81}Br$
4170·9	2	23968·9	(2,3) Q	$^{58}Ni\ ^{79}Br$

TABLE No. 2

Isotope Effect in System – A

Observed and calculated shifts

V′, V″	$^{58}Ni\ ^{79}Br - ^{58}Ni\ ^{81}Br$		$^{58}Ni\ ^{79}Br - ^{60}Ni\ ^{79}Br$	
	$\Delta\nu$ (Cal) cm^{-1}	$\Delta\nu$ (obs) cm^{-1}	$\Delta\nu$ (cal) cm^{-1}	$\Delta\nu$ (obs) cm^{-1}
(0, 1)R	1.6	1.3	3.05	2.9
(0, 1)Q	1.6	1.5	3.05	2.9
(1, 2)R	1.7	1.3	3.27	2.8
(1, 2)Q	–	–	–	–
(2, 3)R	1.8	1.7	–	–
(2, 3)Q	1.8	2.3	–	–

TABLE No. 3

System – C

λ (Air) Å	I	k (Vac) cm^{-1}	V′, V″
4152.6	1	24074.5	(1, 0)R
4153.0	1	24072.2	$(1, 0)R_i$
–	–	–	(1, 0)Q
4203.97	4	23786.02	(0, 0)R
4204.5	4	23777.4	(0, 0)Q
4206.1	2	23768.16	(1, 1)R
4207.5	2	23760.4	(1, 1)Q
4257.7	1	23480.3	$(0, 1)R_i$
4258.0	1	23478.6	(0, 1)R
4258.9	1	23475.6	$(0, 1)Q_i$
4259.2	1	23472.6	(0, 1)Q
4260.4	1	23465.4	$(1, 2)R_i$
4260.7	1	23463.7	(1, 2)R
–	–	–	(1, 2)Q
4262.2	1	23455.5	$(2, 3)R_i$
4262.5	1	23454.1	(2, 3)R
4263.7	1	23447.2	$(2, 3)Q_i$
4264.0	1	43445.6	(2, 3)Q

Band heads denoted by *i* are due to isotopic molecule $^{58}Ni\ ^{81}Br$.

TABLE No. 4

Isotope Effect in System – C

Calculated and observed shifts

(Due to Bromine only)

V′, V″	$\Delta\nu$ (Cal.) cm^{-1}	$\Delta\nu$(Obs.) cm^{-1}
(1, 0)R	−1.5	−2.3
(0, 1)R7	1.7	1.7
(0, 1)Q	1.7	1.6
(1, 2)R	1.7	1.7
(2, 3)R	1.8	1.4
(2, 3)Q	1.8	1.6

TABLE No 5

System – D

λ (Air) Å	I	k (Vac) cm^{-1}	V′,V″	Isotopic Emitter
4300.07	1	23248.9	(1, 0)	$^{58}Ni\ ^{79}Br$
4300.3	1	23247.5	(1, 0)	$^{58}Ni\ ^{81}Br$
4300.6	½	23246.16	(1, 0)	$^{60}Ni\ ^{79}Br$
4300.8	½	23244.9	(1, 0)	$^{60}Ni\ ^{81}Br$
4306.83	1	23212.4	(2, 1)	$^{58}Ni\ ^{79}Br$
4307.03	1	23211.35	(2, 1)	$^{58}Ni\ ^{81}Br$
4314.2	1	23172.7	(3, 2)	$^{58}Ni\ ^{79}Br$
4314.34	1	23172.07	(3, 2)	$^{58}Ni\ ^{81}Br$
4322.38	1	23128.9	(4, 3)	$^{58}Ni\ ^{79}Br$
4322.56	1	23128.5	(4 3)	$^{58}Ni\ ^{81}Br$
4330.0	½	23088.2	(5, 4)	
4354.08	6	22960.5	(0, 0)	
4360.15	4	22928.5	(1, 1)	
4366.74	2	22893.8	(2, 2)	
4373.76	1	22857.2	(3, 3)	
4415.42	1	22641.56	(0, 1)	$^{58}Ni\ ^{81}Br$
4415.72	1	22640.0	(0, 1)	$^{58}Ni\ ^{79}Br$
4420.77	½	22614.98	(1, 2)	$^{60}Ni\ ^{81}Br$
4420.95	½	22613.25	(1, 2)	$^{60}Ni\ ^{79}Br$
4421.28	1	22611.55	(1, 2)	$^{58}Ni\ ^{81}Br$
4421.6	1	22609.9	(1, 2)	$^{58}Ni\ ^{79}Br$
4426.92	0	22582.75	(2, 3)	$^{60}Ni\ ^{81}Br$
4427.18	0	22581.4	(2, 3)	$^{60}Ni\ ^{79}Br$
4427.6	1	22579.3	(2, 3)	$^{58}Ni\ ^{81}Br$
4428.05	1	22577.2	(2, 3)	$^{58}Ni\ ^{79}Br$
4434.5	1	22544.1	(3, 4)	$^{58}Ni\ ^{81}Br$
4434.94	1	22541.9	(3, 4)	$^{58}Ni\ ^{79}Br$

TABLE No. 6

Isotope effect in System—D

Observed and calculated shifts

V′, V″	$^{58}Ni\ ^{79}Br$ — $^{58}Ni\ ^{81}Br$		$^{58}Ni\ ^{79}Br$ — $^{60}Ni\ ^{79}Br$	
	$\Delta\nu$ (Cal) cm^{-1}	$\Delta\nu$ (obs) cm^{-1}	$\Delta\nu$ (cal) cm^{-1}	$\Delta\nu$ (obs) cm^{-1}
(1,0)	−1·4	−1·4	...	−2·72
(2,1)	−1·2	−1·1	...	...
(3,2)	−0·9	−0·7	...	...
(4,3)	−0·6	−0·5	...	...
(0,1)	1·8	1·5	...	...
(1,2)	1·9	1·6	...	3·3
(2,3)	2·1	2·1	...	...
(3,4)	2·4	2·2	...	...

TABLE No. 7

System—E

λ (Air) Å	I	k (Vac) cm^{-1}	V′,V″	Isotopic Emitter
4399·6	1	22722·9	(1,0) R	— Over lapped by an Atomic line
4406·3	1	22688·4	(2,1) R	$^{58}Ni\ ^{79}Br$
4406·5	1	22687·4	(2,1) R	$^{58}Ni\ ^{81}Br$
4407·4	1	22682·7	(2,1) Q	$^{58}Ni\ ^{79}Br$
4407·6	1	22681·7	(2,1) Q	$^{58}Ni\ ^{81}Br$
4456·27	4	22434·0	(0,0) R	
4457·62	4	22427·22	(0,0) Q	
4462·45	2	22402·94	(1,1) R	
4463·78	2	22396·12	(1,1) Q	
4520·61	1	22114·77	(0,1) R	$^{58}Ni\ ^{81}Br$
4520·89	1	22113·3	(0,1) R	$^{58}Ni\ ^{79}Br$
4521·43	0	22110·72	(0,1) Q	$^{60}Ni\ ^{81}Br$
4521·87	0	22108·56	(0,1) Q	$^{60}Ni\ ^{79}Br$
4522·23	1	22106·8	(0,1) Q	$^{58}Ni\ ^{81}Br$
4522·52	1	22105·3	(0,1) Q	$^{58}Ni\ ^{79}Br$

TABLE No 8

Isotope Effect in System—E

Calculated and observed shifts

(Due to Bromine only)

V′,V″	(Cal) cm^{-1}	(obs.) cm^{-1}
(1,0) R	–	–
(2,1) R	−1·2	−1·0
(2,1) Q	−1·2	−1·0
(0,1) R	1·8	1·4
(0,1) Q	1·8	1·5

TABLE No. 9

Summary of vibrational constants and first vibrational quanta

System	$\nu_{00}cm^{-1}$	$\omega'_{1/2}cm^{-1}$	$\omega'_e cm^{-1}$	$\omega'_e x'_e cm^{-1}$	$\omega''_{1/2}cm^{-1}$	$\omega''_e cm^{-1}$	$\omega''_e x_e cm^{-1}$
A	24318·97	288·9	294·0	2·55	307·43	309·5	1·03
C	23777·4	289·06	–	–	306·9	389·34	1·22
D	22960·5	288·45	294·03	2·78	320·4	322·82	1·21
E	22427·22	288·7	–	–	320·9	–	–

REFERENCES

1. V. G. Krishnamurty, *Ind. J. Phys.* (1952), **26** 429.
2. S. P. Reddy and P. T. Rao, *Proc. Phys. Soc. London* (1960) **75**, 275.
3. A. Heimer, *Z. Physik*, (1934), **105**, 56.
4. A. G. Gaydon and R. W. B. Pearse, *Proc. Roy. Soc. London* (1935), **148**, 312.

X-RAY SATELLITES AND THEIR ORIGIN —A GENERAL SURVEY

By

G. B. DEODHAR

Physics Department, Allahabad University, Allahabad

[Received on 7th April, 1962]

I. INTRODUCTION

After the introduction of the fundamental idea of the K, L series in X-ray emission and the intimate relation between X-ray emission and absorption discontinuities by Barkla, not long after the discovery of X-rays by Röntgen, the subject of X-ray spectroscopy was placed on a firm footing by von Laue, Bragg, M. de Broglie, Siegbahn and their associates. Various problems in X-ray spectroscopy such as accurate measurements of X-ray wave-lengths, determination of short wave-length limit of the continuous spectrum, the line widths, measurement of relative intensities of spectral lines, etc., were widely studied. Special spectrographs like the bent crystal X-ray spectrograph were developed to study weak lines such as usually occur in satellite spectra.

The subject of satellite spectra is perhaps the most intricate problem in the entire field of X-ray spectroscopy. Ever since their first discovery in 1916 by Siegbahn and Stenström[1] extensive work on the various aspects of their general characteristic features and theories of their origin has been published. The field of X-ray satellites on the experimental side does not seem to be exhausted and the theories regarding their origin do not appear to have as yet reached a final decisive stage. A number of surveys of satellite spectra have been published from time to time the last of these is that by F. R. Hirsh Jr.[2] in 1942. This survey gives a good picture of the satellite position at that time but is now out of date in many respects in view of recent investigations in this field of X-ray spectroscopy. The present article is an attempt to present an overall up-to-date picture of satellites. The author does not claim to have included in this account all the existing publications nor does he intend to give all details of data about them. All that is desired is to help the reader in locating a particular aspect of X-ray satellites in the literature through the references listed in the end of this article.

II. GENERAL SURVEY OF SATELLITE LINES

(A) K-Satellites :

Siegbahn and Stenström[1] were the first to report the existence of some weak lines on the high frequency side of $K\alpha_1$ of elements from $Z=11$ (Na) to $Z=30$ (Zn). These weak lines were designated as X-ray satellites due to the fact that they lie in the region close to the usual X-ray dipole lines. The discovery of X-ray satellite spectra in 1916 opened a new field of research in X-ray spectroscopy which

has steadily widened till to date. The simple character of satellite spectra in these early stages of their study is demonstrated in a figure, qualitatively.

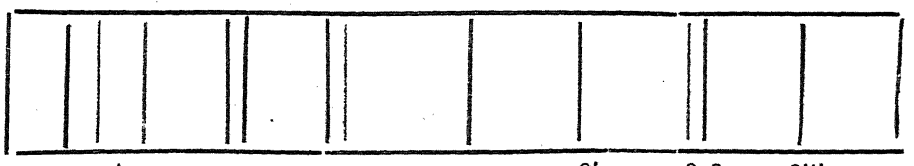

K—Satellites.

A careful survey of K-series satellite lines was made by O.R. Ford[3] in 1932. He reported in addition to the lines shown in the figure a satellite α_3' and also a number of $K\beta_1$ satellites designated by $\beta\eta$, β', β'', β^{IV}, β''' and β^{V} for elements $12 \leq Z \leq 32$. In 1936 Parratt[4], using ionisation method, showed that the $K\alpha_{3,4}$ satellites are not simple but consist of 5 components for $16 \leq Z \leq 28$ and four components $29 \leq Z \leq 32$. Later Shaw and Parratt[5] extended the work and reported the following satellites : 4 components $\alpha_{3,4}$, α_3' and α' for $30 \leqq Z \leqq 33$; 3 components $\alpha_3, \alpha_4, \alpha_3'$ for $34 \leq Z \leq 40$; 2 components α_4', α_3' for $41 \leqq Z \leq 46$.

The data regarding wave-lengths of X-ray satellites discovered up to 1947 have been collected by Y. Cauchois and H. Hulubei in their wave-length tables.[6]

In 1948 Hulubei, Cauchois and Manescu[7] observed weak lines in the X-ray spectra of elements $Z=33$ to 44. They reported two lines of wave-length less than β_2 designated by the symbols β_{11}'' and β'''. The latter is not of the same type for all the atoms in this group. Other lines reported are β_0, β_6, β_7 and β_8.

In 1947, using high frequency excitation method for the first time, Groven[8] studied the K-spectrum of As (33) in the vapour form with a Cauchois spectrograph. He found new lines α_s' and α_s on the long wave-length side of $K\alpha_2$. He also discovered many other weak lines both on the long and short wave-length side of $K\alpha$ and $K\beta$ and confirmed the measurements of Shaw and Parratt and Cauchois and Hulubei for α_3' α_3, α_3' and α_4 short wavelength satellites of $K\alpha$ and that of Hulubei for α_s long wavelength satellite of $K\alpha$. Adopting the same method Morlet[9] studied that K-spectrum of selenium both in the vapour and solid forms in 1949 and that of Br (35) in 1950[10]. He also reported a number of short and long wavelength satellites of $K\alpha$ and $K\beta$.

In 1951 Groven and Morlet[11] discovered many weak lines in the K-series using the high frequency excitation method of Groven refererred to above. The elements studied were Zn(30), As(33), Se (34), Br (35) and Kr(36). The lines were devided into five groups as follows :

TABLE I

Group I	α_s', α_s, α_s''	Long-wave-length satellites of $K\alpha$
Group II	α'', α', α_3, α_3', α_4, α'''	Short wave-length satellites of $K\alpha$
Group III	$X_1, X_2, \beta_s, \beta_0, \beta_1^{IV}, X_3, X_4$ $\beta_1', {}_{11}$	Long wave-length satellites of $K\beta_{1,3}$
Group IV	$\beta_{10}, \beta_7, \beta_9, \beta_6, \beta_5, \beta_8, X_5$	Short wave-length satellites of $K\beta_{1,3}$
Group V	β''', β_{11}''	Short wave-length side of $K\beta_2$

The work of Groven and Morlet is of importance as it opens the possibility of studying the effects of proximity of atoms in a solid on X-ray spectral emissions and thus holds promise of understanding the mechanism of emission of the weak lines referred to here.

In 1950 Edamato[12] carried out interesting experimental work using high resolution spectrograph for the elements. Z=25 to Z=30. He reports wave-lengths for α_3', α_4, α_3, α_3'', α_1' and α'' and a number of other lines on the longer wave-length side near the principal doublet. For some of the elements Edamato reports two lines α_0 and α_0'' of wave-lengths shorter than α_2'.

In 1952 Hayasi[13] investigated the satellites of $K\beta_1$ and $K\beta_5$ lines of Cu(29) which consist of five components and an emission line of wave-length shorter than the main absorption edge was found.

In 1955 Sawada[14] and others resolved the $K\beta\eta$ into two components and the longer wave-length was designated as $K\beta_i$. The spectrograph used was a Cauchois curved crystal one and the elements studied were Cr (24) to Zn (30). In view of this and the results quoted above for other authors especially those of Edamato, Groven and Morlet the picture given for $K\alpha$ and $K\beta$ satellites by A. Sandström[15] in Hand Buch der Physik should be considered as incomplete. The various $K\alpha$ satellites reported in this article are :

α'', α', α_3'', α_3, α_4, α_3', α_4', α_5, α_6 α_7 for elements Z=11 to Z=46 and β_0 (η), β', β_2, β_x, β^{IV}, β'', β''', β^{IV}, β_5, β_6, β_7, β_8, β_9, β_{10}, β_{11}'''', for elements Z=14 to Z=47.

In the soft X-ray region of 600 A. Bedo and Tomboulian[16] observed a K-satellite band for metallic Lithium. Calterall and Trolter[17] during their study of K-satellite band of Lithium and Beryllium found that the hole which occurs in the core level during the soft X-ray emission process does not appreciably affect the intensity of the spectra.

One of the most interesting aspects of X-ray satellite emission is the question regarding their excitation by fluorescence. Recent experiments go to show that satellites do appear in X-ray fluorescence spectra. In this connection the work of Tsutsumi[18] in 1959 is most noteworthy. This author studied the $K\beta'$ satellite of some compounds of iron group by fluorescent spectra. We shall return to this aspect in another section. Appearance of satellites in fluorescence spectra contradicts the assertion made by A. Sandström on Page 85 of his article in the Hand Buch der Physik.[15]

(B) L-Satellites :

From their very first detection and measurement by Druyvesteyn[19] in 1928 it was noted that the L-series satellites are much more numerous than those of the K-series. In 1929 F.K. Richtmyer and R. D. Richtmyer made a careful survey[20] of the satellites of $L\alpha_1$, $L\beta_1$, and $L\beta_2$. A satellite structure accompanying these X-ray diagram lines was investigated for the elements Rb (37) to Sn (50). This structure was much more complex than what was previously assumed. The following L-satellite lines were reported.

TABLE 2

8 Lα satellites when Z=42

5 Lα satellites when 37 ≤Z≤49

4 $L\beta_1$ satellites when 42 ≤Z≤48

3 $L\beta_1$ satellites when 48 ≤Z≤50

5 $L\beta_2$ satellites when 42 ≤Z≤50

In 1936, Parratt[21] reported Lα satellites of Ag (47). Later on Cauchois[22] discovered Lα satellites of heavy elements from U(92) to Sm (62) and reported four satellites over this range of elements. Since then investigations in L-spectra made a steady progress. The position of these spectra in 1947 can be visualised by referring to the excellent wave-length tables compiled by Cauchois and Hulubei[6]. Table 3 gives an on overall picture of the L-satellites known up to 1947.

TABLE 3

Number of Satellites	Satellites			
	$L\alpha_1$	$L\beta_1$	$L\beta_2$	Lγ
1	Z=64, 76, 77	Z=60, 62→68	Z=59, 62→67 71, 84	Z=40, 44, 46, 48→51 64→71, 74, 81
2	Z=62, 68, 70→72	—	Z=55, 56, 58, 60 68, 70, 72, 92	Z=41, 42, 45, 47 63, 72, 77, 83
3	Z=66, 74	Z=48→50	Z=51, 52, 53, 73	Z=58, 59, 60, 62 73, 75, 76, 78, 80, 82
4	Z=47, 55, 75, 88	—	Z=42	—
5	Z=45, 46, 48, 81, 92	—	Z=44→50, 81	Z=78
6	Z=41, 50, 52, 73, 90	—	Z=75, 77, 88	Z=55
7	Z=44, 47, 49, 51, 53, 78, 83	—	Z=82	Z=56
8	Z=42, 45, 46, 48, 56, 79	—	Z=83, 90	—
9	Z=42, 80	—	Z=79	—

The lines repo ted are :

Lα satellites :

α_2', α_3, α_4, α_5, α_5', α_6, α_7, α_8, α_9, α_9', α_{10}, when 26≤Z≤ 56

α_0, α_s, α_{111}, α_{11}^z, α_1^z, α^y, α', α^{iv}, α_{11}^x, α^x, α^l when 57 ≤Z≤ 92

Lβ satellites :

$L\beta_1$ ... β_1', β_1'', β_1''', β_1^{iv}

$L\beta_2$ ... β_{14}, β_2^a, β_2', β_2^5, β_2'', β_2^6, β_2^{iv}, β_2^v, β_2^{vi}, β_2^{vii}

$L\beta_5$ ... β_5', β_5'', β_5'''

Lγ satellites :

$L\gamma_1'$ ... γ_2' γ_2'', γ_{23}', γ_5, γ_9, γ_{10}

In 1949 L. Groven and A. Lagasse[23], using high frequency excitation method, found as many as 20 weak lines on the long wave-length side of $L\alpha_1$—of Hg (80). Of these only two viz. α_o and α_s were identified. They also found as many as 15 weak lines on the short wave-length side of $L\alpha_1$ of this element. Of these α', α^y, α^{ix}, α^{x}_{iii}, α^x, α^a and η were identified. In the $L\beta$ spectrum of this element they found as many as five weak lines on the long wave-length side of $L\beta_1$ and as many as ten weak lines on its short wave-length side. Of these β_2', β_5'', β_2^{iv}, β_2^v, β_2^{vi}, and β_2^{vii} were identified. In the $L\gamma$ spectrum of mercury they found three weak lines of which $L\gamma_1'$ was identified.

In 1951 Barrere[24] using 400 KV i.e. nearly 40 times the excitation voltage for $L\gamma_1$ of W (74) found the satellite $L\gamma_1'$ of $\lambda 1090.5 \times U$. It is worthy to note that for Hg (80) Barrere reports no K-satellites although the excitation—voltage used by him was 140 KV, nearly one and a half times the excitation voltage necessary for the emission of K-series. Only the dipole lines $K\alpha_1$, $K\alpha_2$, $K\beta_5$ and $K\beta_2$ were reported by him.

In 1953 Sakellaridis[25] reported γ_8, γ_{10}, γ_9 and β_{14} satellites in the L-spectrum of the rare earths Eu (63), Gd (64), Tb (65), Ho (67) and Γa (69).

In 1957 G. P. Borovikova and Mikorsunkii[26] reported $L\alpha_{12}$ and $L\beta_1$ satellites in the L-spectrum of Ge (32).

(C) M-Satellites :

The occurrence of satellites in the M-series seems to have been reported by Stenström[27] for the first time in the year 1918. Later Hjalmar[28] made an extensive study of these lines and reported two satellites of $M\alpha$ viz $M\alpha'$ and $M\alpha''$ for elements γ_b (70) to U (92), three satellites β', β'' and β''' of $M\beta_1$ for U(92) and one satellite of $M\beta$ for elements Z=67 (Ho) to Z=92 (U). He also reported one satellite γ' of $M\gamma$ for elements renging from Z=74 (W) to Z=92 (U) Beuthe[29] reported a few M_α satellites of Re (75). Lindberg[30] found two satellites of M_α for elements ranging from Z=71 (C_p) to Z=92 (U) and one satellite of M_β for elements ranging from Z=71 (Cp) to Z=92 (U). In 1931 Hirsh, Jr[31] studied the M-series satellites of various elements and gave wave-lengths for three satellites of $M\beta$ and four satellites of $M\alpha_1$. He did not find any satellite of $M\gamma$. Much later in 1950 by careful analysis of density plots Hirsh[32] showed that for the elements studied, viz. Pt (78), AU (79), TI (81), Pb (82), Bi (83), Th (90) and U (92), six distinct satellites were discovered. On the other hand study of Micro-photometer records of the spectrograms showed complete absence of sharp $M\alpha$ satellite maxima. Hirsh attributed this to Auger broadening of the satellites, while in the case of $M\beta$ satellites Hirsh[33] shows that Auger effect is impossible.

Table 4 based on the wave-length tables of Cauchois and Hulubei demonstrates the number of M_{α}, M_{β} and M_{γ} satellites for a number of elements.

TABLE 4—M-Satellites

	Number of Satellites	Satellites		
		M_{α}	M_{β}	M_{γ}
1	(αII)	Z=67→69	β_{II} Z=64→69 Z=71, 76	γ_1' Z=74,
2	(αIV, αII)	Z=70, 76	β_{II}, β_{III} Z=70	81→83, 90, 92
3	(αI, αII, αIV)	Z=71→74 Z=77, 78, 90, 92	β_I, β_{II}, β_{III} Z=72→74 Z=77→79 Z=81→83 Z=90, 92	— — —
4	(αI, αII, αIII, αIV)	Z=79, 80→83	—	

A perusal of this general survey of X-ray satellites brings out the fact that not only the number of satellite lines in the various series has considerably increased since their first discovery in 1916 but their original simplicity is replaced by intricate complexity. Moreover, another important feature of satellite spectrum is that during recent years satellite lines on the low frequency side of the principal dipole lines have also been observed for a number of elements. In another section we will review theoretical ideas about the origin of the low and high frequency satellite lines.

III. CHARACTERISTICS OF SATELLITES

As discussed by F. Wisshak[34] as early as 1937 a satisfactory theory of the origin of X-ray satellite spectra required detailed study of the following characteristics of these lines :

(1) Exact frequencies of the lines. (2) Their widths. (3) Minimum excitation potential. (4) Minimum photon energy if excited in fluorescence.

(5) Intensity variation with atomic number of the anticathode, potential and current in the X-ray tube.

(6) Relative intensities of a satellite and its socalled parent line.

From time to time work on these lines has been published and the reader may reach the original papers in this connection to get an idea of the progress made up to 1943 or so[35]. In the year 1948 H. Hulubei, Y. Cauchois and Manescu observed new weak lines in the Kβ spectrum of elements Z=33 to 44. They found that increase in excitation potential generally favours the appearance of satellities. In 1951 Barrare[24] using excitation voltage nearly equal to forty times the excitation voltage for $L\gamma_1$ of W(74) obtained the satellite $L\gamma_1'$ of λ1090.5

X. U. In their study of satellites of Gold, Lead and Bismuth L. Salgusiro and M. H. Blanc[36] found that the satellites of $L\beta_2$ disappear when the applied potential decreases below the ionisation potential of the L_1 electrons. The intensity ratios of the two components $K\beta_3$ and $K\beta_2$ of $K\beta_\eta$ to the $K\alpha_1$ line for elements $Z=24\rightarrow30$ reported in the previous section were both estimated to be of the order 10^{-4}. The significance of this work in the theory of the origin of satellites will be considered in the next section. Vainshtein, Bril and Staryi[37] showed that several regularities in the relative intensities of $K\beta''$ and $K\beta_2$ for certain titanates exist. It is thought that they throw light on the electronic structures of the substances studied. Vainshtein and Ya N. Vasilév[38] obtained interesting results about the effect of carbon content in Titanium on the intensity of $K\beta''$ line. For carbon content of 9-24% the spectral location of the $K\beta$ lines remains constant but the relative intensities of the lines change. For $K\beta''$ the relative intensity of this line increases with the carbon content. The influence of the Auger effect and atomic number on the line width and relative intensity of satellite bands were the subject of study by J. Gomes Ferreira[39] for elements $Z=30$ to 72. With the help of a specially developed grain technique they measured the intensity of the higher frequency $L\alpha_1$ satellite band as a fraction of the intensity of the $L\alpha_2$ line. It was found that this fraction rose steadily from 15 percent for Ta (73) to 64 percent for Tl (81), dropping to 40 percent for Bi (83), then decreasing slowly to 36 percent for U (92). The lower frequency satellite band gave a similar curve. The hitherto unmeasured $L\alpha_2$ line widths were given from $Z=T_a$ (73)$\rightarrow$Bi (83) and also for Th (90).

Excitation by Fluorescence : Excitation of X-ray spectral lines and ejection of photo electrons, K, L, etc., by incident X-radiation has been known for long. The question arose whether the satellite lines can be produced by an incident X-ray photon of suitable energy. Dauvillier[40] made an attempt to excite (26) Fe $K\alpha_{3,4}$ lines by $K\alpha_1$ radiation of 29 (Cu). Later on in 1927, Coster and Druyvesteyn[41] succeded in exciting Fe $K\alpha_{3,4}$ by Cu K radiation. Hirsh and Richtmyer[42] excited Zr (40), Mo (42) and Ru (44) and Ag (47) by 20 KV Ag-radiation. It was found that the intensity of $L\alpha$ satellite relative to the parent line diminished. In 1953, H. Herglotz[43] using photometric and grain counting methods found that the ratio of the intensities of $K\alpha_3$ satellite of Cr (24), primary and secondary excited, was 2.5 ± 20 percent. The results are considered to support the views of Druyvesteyn[44] given in section IV of this article.

In 1959, K. Tsustumi[45] studied by fluorescent method the nondiagram lines $K\alpha_{3,4}$ and $K\beta'$ of some compounds of the iron group. The λ values and relative intensities of $K\alpha_{3,4}$ of metallic iron and $K\beta'$ of Cr_2O_3, $Cr_2(SO_4)_3$, M_nO_2, $MnSO_4$. $4H_2O$, Fe_2O_3 and $Fe(NH_4)_2(SO_4)_2\,6H_2O$ were measured by the fluorescent method using two different characteristic X-rays. The $K\alpha_{3,4}$ lines did not appear when an iron atom was excited by N_i K-rays but were clearly observed when excited by Cu K-rays. This agrees with the idea that $K\alpha_{3,4}$ lines arise from the transition KL—LL (see section IV of this article) In the casse of $K\beta'$ line it did not matter whether it was excited by photons of energy lower or higher than K(Z) + L(Z+1) which is necessary to remove simultaneously a K and an L−electron of an atom Z. It is concluded that $K\beta'$ line is due not to the double but to the single ionisation process. The author derived it from the difference of the exchange interactions of the states of total spins $(S+\frac{1}{2})$ and $(S-\frac{1}{2})$, where S is the total spin of the incomplete $3d$ shell and $\frac{1}{2}$ that of the incomplete $3p$ shell in the final state. The energy separation of the $K\beta_1$ and $K\beta'$ lines calculated from these exchange energies were shown by Tsutsumi to agree with experimental results.

IV. ORIGIN OF X-RAY SATELLITES

A. High frequency satellites.

It is well known that complete X-ray energy level diagrams have been constructed which describe the transitions giving rise to the strong lines in the various X-ray spectral series. Certain selection rules for these transitions have been framed. The pre-requisite condition for such emission is the expulsion of an electron from one of the shells of the atom. Thus for the K-series an electron should first be expelled from the K-shell. In re-arrangement K-series lines are emitted.

As mentioned in section II of this article Siegbahn and Stenström observed weak lines on the high frequency side of the strong lines, the frequencies of the latter being given by the energy level diagram as the difference of frequencies of two terms. It was soon realised that the frequencies of these faint lines could not be obtained from the energy level diagrams even after violating the selection rules. It is customary therefore to call them nondiagram lines although frequently they are called satellite lines because they lie not far from the strong diagram lines.

Wentzel[46] made the first attempt to explain the origin of high frequency satellites. It was natural for Wentzel to assume that the satellite spectra are the result of single electron jumps in atoms in which two or more eletrons have been removed from the inner shells The multiplicity of X-ray levels was not taken into account in the early form of the theory of X-ray satellites. Researches on excitation potentials showed that excitation voltage for a satellite is decidedly somewhat greater than that for the diagram line associated with it. It was found that the energy of excitation of a K-satellite is equal to the sum of the energies required to eject one K-electron and one L electron. The initial state of the atom for the emission of the K satellites is represented by the symbol K^1L^1 other atomic states are represented by K^2, K^1M^1, L^1M^1, etc. In table 5 below are given the assignments of initial and final states for some satellites in the K-series, according to Wentzel. The indices give the number of electrons removed from a shell.

TABLE 5

Satellite	Initial State	Final State
α^1	K^1M^1	L^1M^1
α_3	K^1L^1	L^2
α_4	K^2	K^1L^1
α_5	K^1L^2	L^3
α_6	K^2L^1	K^1L^2

Druyvesteyn[47] modified Wentzel's theory in such a way that there is no necessity for supposing that two electrons from the same level are ejected. He showed that there is a good agreement between his theoretical calculations and experimental data for the satellites of the diagram lines $K\beta_1$, $K\beta_2$, $L\gamma_1$ and $L\gamma_{2,3}$. For $K\beta'''$ he

gives K^1L^1 and L^1M^1 as the initial and final states, For the $K\alpha$ group of satellites, Druyvesteyn gave the assignments in Table 6 but he did not present data to support these.

TABLE 6

Satellite	Initial state	Final state
$K\alpha^1$	$K^1L_1^1$	$L_1^1\ L_{2,3}^1$
$K\alpha_{3,4}$	$K^1L_{2,3}^1$	$L_{2,3}^2$
$K\alpha_{5,6}$	$K^1L_{2,3}^2$	$L_{2,3}^3$

B. B Ray[48] introduced the opitical spectroscopic interpretation of the $K\alpha$ satellites taking into account the multiplicity of levels and explained the emission of the five $K\alpha$ satellites, α_3, α_4, α_5, α_6 and α_x. Langer[49] using optical spectroscopic natations proposed that the five $K\alpha$ satellites α', α_3, α_4, α_5, and α_6 may arise from the transitions $1s\ 2s \rightarrow 2s\ 2p^5$ and $1s\ 2p^5 \rightarrow p^4$. He assumed Russel-Saunders Coupling in calculating the terms. Wolfe[50] mode some improvements in Langer's assignments and showed very satisfactory agreement between the calculated and the observed ν/R values for the satellites of the $K\alpha$ group. In Table 7 are given the

TABLE 7

Satellite	Langer	Wolfe
$K\alpha'$	$^1S \rightarrow {}^1P$	$^1P \rightarrow {}^1S$
	$1s\ 2s \rightarrow 2s\ 2p^5$	$1s\ 2p^5 \rightarrow 2p^4$
$K\alpha_3$	$^3P \rightarrow {}^3P$	$^3S \rightarrow {}^3P$
	$1s\ 2p^5 \rightarrow 2p^4$	$1s\ 2s \rightarrow 1s\ 2p^5$
$K\alpha_4$	$^3S \rightarrow {}^1S$	$^1S \rightarrow {}^1P$
	$1s\ 2s \rightarrow 2s\ 2p^5$	$1s\ 2s^5 \rightarrow 2s\ 2p^5$
$K\alpha_5$	$^1P \rightarrow {}^1S$	$^3P \rightarrow {}^3P$
	$1s\ 2p^5 \rightarrow 2p^4$	$1s\ 2p^5 \rightarrow 2p^4$
$K\alpha_6$	$^1P \rightarrow {}^1D$	$^1P \rightarrow {}^1D$
	$1s\ 2p^5 \rightarrow 2p^4$	$1s\ 2p^5 \rightarrow 2p^4$

assignments made by Langer and Wolfe for comparison. Sawada[51] made assignments of the $K\beta$ group satellites extending Langer's idea. Kennard and Ramberg[52] discussed the origin of $K\alpha$ satellites making use of the idea of Hartree self consistent field. They found excellent agreement with observed frequency differences. No doubt seems to have been left that the $K\alpha$ satellites are due to KL ionised state of an atom. It should be noted that the basic idea of multiple ionisation of atoms is supported by wave mechanical considerations as discussed by Richtmyer and Ramberg[53]. D. J. Candlin[54] calculated the expected structure of satellite lines due to $K^{-1}L^{-1} \rightarrow L^{-2}$ transitions for 11 elements, $Z=19$ to $Z=42$, using first order perturba-

tion theory and Hydrogenlike wave-functions. The agreement with experimental values is good and perhaps goes to show the correctness of the approach. It is desirable to extend their work to other elements and to the L and M series satellites.

The question of the intensity of satellite lines is of considerable value in the development of a theory of X-ray satellites. The probability of KL ionization was discussed by R.D. Richtmyer.[55] He found that the relative intensities of the $K\alpha_{3,4}$ satellite and the principal diagram line $K\alpha_1$ is given by $A/(Z-b)^3$, where A and b are constants. This relation, however, was not borne out by the intensity measurements of Shaw and Parratt.[5]

The study of $\Delta\nu/R$ values of a satellite line with respect to its principal diagram line is of considerable value in theoretical interpretation of the satellite spectra. It was known that the square root of $\Delta\nu/R$ varies linearly with atomic number; in other words satellite lines obey what may be called semi-Moseley graphs. Based on this behaviour of satellites Richtmyer[56] introduced the idea of double jump of electron. Consider an atom having lost one electron in an inner shell and one is an outer shell. In the rearrangement of the atom the inner vacancy will be filled by an electron from one of the inner shells and the outer vacancy from the valence electron. The emitted quantum is given by

$$h\nu_s = h\nu_i + h\nu_0$$

From this we have the observed relation, $\sqrt{\nu_s - \nu_i} = \sqrt{\nu_0} = \alpha Z$.

This is Richtmyer's hypothesis of double jump for explaining the origin of the satellite spectra. Richtmyer's double jump theory readily explains the presence of the continuous spectrum in the region of X-ray satellites, Idei[57] has concluded that $(\nu_s - \nu_i) \propto Z$. This throws some doubt on the real significance of the linear relationship pointed out by Richtmyer.

In an important article discussing the probability of double jumps in X-ray spectra E. G. Ramberg[58] questions the validity of Richtmyer's double jump hypothesis. He points out that the intensity of $K\alpha_3$, $K\alpha_4$ satellite-doublet relative to the intensity of $K\alpha_{1,2}$ lines for Na (11) is

$$\frac{I\alpha_3}{I\alpha_{1,2}} = \frac{1}{170} \text{ and } \frac{I\alpha_4}{I\alpha_{1,2}} = \frac{1}{320}$$

Their calculated relative intensitites are very much smaller than the observed values. Another objection raised by Ramberg against Richtmyer's hypothesis was that long wave-length satellites which may possibly arise due to subtraction of energy corresponding to the ionisation energy of the semi-optical shell electron from the X-ray quantum were not observed. As pointed out in section II of this article long wavelength satellites are now observed and the force of Rambergs contention, at least on this ground, is lost.

Another interesting relation between $\delta(\nu/R)$ and Z was for the first time found by Deodhar and Abidi.[59] This was later on extended to a number of elements and a large number of satellites by Deodhar and Padalia.[59] If for a particular satellite, say $K\alpha'$, $\delta(\nu/R) = (\nu/R)_{Z+1} - (\nu/R)_Z$ values are plotted against atomic number a linear relation $\delta(\nu/R) = 1{\cdot}55\,(Z-1)$ is obtained. The range of elements covered is $Z = 11 \rightarrow 35$. Similarly, for the $L\alpha$ satellites the relation $\delta(\nu/R) = 0{\cdot}25\,(Z-4)$ holds over the range $Z = 33$ to 42 and $\delta(\nu/R) = 0{\cdot}25\,(Z-3)$ over the range of elements $Z = 44$ to 53. Interpretation of these now relationships is that satellites arise

due to single electron jumps in multiply ionised atomps, supporting the basic idea of the Wentzel Druyvesteyn theory of X-ray high frequency satellites. Although there is a considerable amount of evidence in favour of the basic idea of Wentzel and Druyvesteyn regarding the theory of X-ray high frequency satellite spectral emission, other lines of reasoning are not ruled out. Bloch[60] finds that the $K\alpha_{3,4}$ doublet of Cu (29) could be attributed to double electron transitions. His calculated relative intensities agree satisfactorilly with the experimental results. T. I. Kakuschadse[61] has extended Bloch's theory of satellite spectra to give a satisfactory explanation of the origin of $K\alpha_3$ and $K\beta'$ lines in terms of electron interaction with thermal vibrations of the lattice. The extended theory also gives an explanation of the observed asymmetry of $K\alpha_1$ and $K\alpha_2$ lines.

As given in Section II of this article Sawada, Tsustumi and Shiraiwa[62] succeeded in resolving $K\beta\eta$ for elements $Z=24\rightarrow30$ into two lines $K\beta n$ and $K\beta_L$. They ascribe the origin of these two lines to the two electron jumps obeying the Heisenberg selection rule first proposed by one of the authors. Accordingly the line $K\beta n$ originates from the transition $KL_{II} \rightarrow L_1M_1$ and $K\beta_L$ from the transition $KL_{III}\rightarrow L_1M_1$.

The adoption of Wentzel-Druyvesteyn conception to explain the origin of L and M satellites in the same way as the K-series satellites was retarded due to certain peculiar and anomalous behaviour of the intensity character of the L and M series satellites. Assuming that double ionisation takes place due to the single impact of a cathode ray electron the intensity of satellites relative to the accompanying diagram line should decrease continuously with atomic number. Although this is found to be so far the K series satellites it is not so far the L and M ones. Take the case of $L\alpha$ satellites as an example. Experiments show that the intensity of $L\alpha$ satellites decreases abruptly as the atomic number increases from 47 to 50 and their intensity increases suddenly at $Z=75$ Between $Z=50$ and $Z=75$ the intensity of $L\alpha$ satellites is so low that they are hardly observable.

This difficulty was solved by the important work of coster and Kronig[63] who showed that the doubly ionised state of atom, first singly ionised, can result from radiationless transition in singly ionised atoms, the phenomenon established first by Auger[64] and called Auger effect. The theory put forward by Coster and kroning gives a very satisfactory picture of the L-series satellites.

Hirsh[65] has discussed the Auger effect in the M-series and gives the probable origin of the $M\alpha_1$ and $M\beta$ satellites. He has pointed out that $N_{4,5}$ electron is ejected due to the radiationless transition $M_3\rightarrow M_5$ which gives rise to the transition $M_5N_{4,5}\rightarrow N_7,N_{4,5}$. In the same way, $M\beta$ satellites are due to the radiationless transition M_3M_4 resulting in the ultimate transition $M_4N_{4,5}\rightarrow N_6N_{4,5}$ Hirsh[66] has done some further work on the intensity maximum for the $M\alpha_1$ satellites confirming the theoretical explanation af Coster and Kronig applied to M-series satellites. The material available in the literature goes to show convincingly that the Auger effect theory of Coster and Kronig is well established.

Inspite of these successes of the Wentzel-Dryvesteyn theory and the refinements made thereon it must be admitted that the theory of X-ray satellites has not yet reached the final quantitative stage. There may be some atomic processes other than those considered heretofore which may cause the emission of some satellite lines. Besides this there is the unsettled question regarding the origin of the low frequency satellites.

S. M. Karl'nak and S. B. Nyzhnyk[67] have discussed the emission of satellite lines on the basis of what is called the external screening. They consider the case of the iron group. It is thought that this conception opens the possibility of arriving at a unified approach in accounting for the origin of X-ray satellites.

B. Low Frequency Satellites

We reviewed above the existing theoretical ideas regarding the origin of the high frequency satellites. In a systemetic study of the elements As (33) to Br (35) and that of the elements from Rb (37) to Mo (42) Hulubei[63] reported for the first time a line α_s on the long wave-length side of α_1 α_2. L Groven and J. Morlet by high frequency excitation method observed three lines α_s'', α_s and α_s' on the long wave-length side of α_1 α_2. For the Kβ spectra also for these elements Groven and Morlet[11] observed a number of lines on the long wave-length side of β_1 and β_3. Y. Cauchois, J. Manescu and H. Hulubei also reported some lines of this group. Much earlier in 1922, D. Coster has observed in his study of the L-spectra of elements Rb 37) to Lu(71) lines lying on the long wave-length side of γ_2 (L_1 N_2), γ_1 (L_1 N_4) and β_2 (L_3N_5) called by him γ_{10}, γ_9 and β_{14} respectively. P. Sakelaridis[79] has reported these lines for Eu, Ga, Te, Ho. The number of the low frequency satellites in the various series is not as large as that of the high frequency ones. Generally an element in gaseous form give more of the low frequency satellite lines.

Hulubei proposed two mechanisms of the emission of the low frequency satellites: (1) A partial Auger effect. According to this a dipole transition $K\alpha_1$ or $K\alpha_2$ undergoes partial internal conversion by ionising the outer electron shells. The remaining energy comes out as a radiation of longer wave-length.

Groven points out that the difference of frequencies of a satellite and the dipole line does not give the ionisation energy of an external shell. This disagreement seems to be more or less a general one and so after Groven we may rule out the validity of this mechinism.

(2) According to the second mechanism proposed by Hulubei a radiationless forbidden transition K—L_1 takes place. Satellite lines corresponding to this forbidden transition will arise. To this forbidden transition is to be added the additional ionisation of the L shell. Groven and Morlet making use of the function of the self-consistent field of Hartree calculated the values of $(\nu_p - \nu_s)$ for Zn (30) and As (33). Although agreement with the experimental values was fair, we have yet to see whether this conception of Hulubei has reached a decisive stage.

Taking the data for the K-low frequency satellites for the elements X=33 to Z=42 the values of $\delta(\nu/R) = (\nu/R)_{2+1} - \nu/R_2$ for a particular satellite can be calculated. If these are plotted against atomic number as in the case of high frequency satellites a linear relation is obtained. Deodhar[59] in collaboration with his students has shown that the relation $\delta(\nu/R) = 1.53\ (Z-1)$ is obeyed. It, therefore, appears that the low frequency satellites arise in the same way as the high frequency ones by single electron transfers in the multliply ionised atoms.

The interesting liner relationships discussed above bring into prominence the unsuitability of the term 'Satellite' although I have used it freely in this article. It will be more in the fitness of things if these spectra are described as the spectra of the second and higher kind according to the degree of ionisation, the spectra of first kind being the usual X-ray spectra corresponding to the transition in singly ionised

states. Construction of energy level diagrams for multliply ionised states has however not yet been achieved. In concluding this general survey of X-ray non-diagram lines, we cannot help remarking that the theory of these spectra has not yet reached a final decisive quantitative stage.

In conclusion I have to offer my hearty thanks to Mr. B. D. Padalia M. Sc. my research fellow for his assistance in collecting references and preparing abstracts of recent papers published on the topic of X-ray spark lines discussed in this article. I am also thankful to the organiser of the symposium, Prof. S. N. Ghosh for giving me an oppertunity to lay before the interested worker a connected account of the recent developments in this field of X-ray spectroscopy with appropriate references which I hope will be of value to the interested readers in locating the various aspects of X-ray spark lines in the literature.

REFERENCES

1. M. Siegbahn and W. Stenström, *Physik. Zeits*, **17**, 48 and 318 (1916).
2. F. R. Hirsh Jr, *Rev. Mod. Phys.*, Vol. **14**, 45 (1942).
3. O. R. Ford, *Phys Rev.*, **41**, 577 (1932).
4. L. G. Parratt, *Phys. Rev.*, **49**, 132 (1936).
5. C. H. Shaw and L. G. Parratt, *Phys. Rev.*, **50**, 1006 (1936).
6. Cauchois, Y. and Hulubei, H., *Longueurs d'onde des emissions X et des discontinuites d'absorption X. Paris*, 1947.
7. Hulubei, H. Cauchois, Y., and Manescu, J., *C. R. Acad. Sci. (Paris)* **226**, 764 (1948).
8. Groven, L., *Ann. Phys. Paris*, **4**, 62 (1949).
9. Morlet, J., *Ann. Phys. Paris*, (1949).
10. Morlet, J., *C. R. Acad. Sci. Paris*, **230**, 942 (1950).
11. L. Groven and L. Morlet. (5 Serie Tome XXXVII), *Extrait du Bulletin de L Academie Royaledes Belgique (classes des Scinces)*, p. 630 (1951).
12. I. Eadamoto, *Sci. Rep. Res. Institute, Tohoku University*, A, **2**, 561 (1950).
13. T. Hayasi, *Sci. Rep. Tohoku University*, **36**, 225 (1952).
14. Masao Sawada, Kenjiro Tsutsumi, Toshio Shairaiwa, *J. Phys. Soc. of Japan*, Vol. 10, 64 (1955).
15. Handbuch der Physik, Vol. XXX (1957).
16. D. E. Bedo and D. H. Tomboulian, *Phy. Rev.*, Vol. **109**, 35 (1958)
17. J. A. Calterall and Trolter, J., *Phil. Mag.*, Vol. **3**, 1424 (1958).
18. K Tsutsumi, *J. Phys. Soc. Japan*, **14**, 1696 (1959).
19. M. J. Druyvesteyn, *Dissertation (Groningen) on Roentgen Spectra of the Second Kind.*, (1928).
20. F. K. Richtmyer and R. D. Richtmyer, *Phys. Rev.*, **34**, 574 (1929).
21. L. G. Parratt, *Phys. Rev.*, **50**, 598 (1936).
22. Y. Cauchois, *C. R. Acad. (Paris)*, **202**, 169 (1936) ; **205**, 519 (1937).
23. L. Groven and A Lagasse *C. R. Acad. (Paris)*, **228**, 1642-44 (1949).
24. Barrere, *C. R. Acad. (Paris)*, **233**, 376 (1951).
25. M. Paul Sakellaridis, *C. R. Acad. (Paris)*. **236**, (1953) and 1767.

26. G. P. Borovikova and Mikorsunkii, *Dokl. Akad Nauk S. S. S. R.*, Vol. **115**, No. 1, 75-7 (1957).
27. W. Stenstrom, *Ann. d. Phys.*, **57**, 347 (1918).
28. E. Hjalmar, *Zeits F. Physik*, **1**, 439 (1920).
29. H. Beuthe, *Zeits F. Physik*, **50**, 762 (1928).
30. E. Lindberg, *Zeits F. Physik*, **50**, 82 (1928).
31. F. R. Hirsh Jr., *Phys. Riv.*, **38**, 914 (1931).
32. F. R. Hirsh Jr., *Letter in Physica*, **16**, 377-3 (1950).
33. F. R. Hirsh Jr., *Phys Rev.* **62**, 137 (1942).
34. F. Wisshak, *Ann. d. Phys.*, **28**, 71 (1937).
35. J. N. Cooper, *Phys. Rev.* **61**, 234, (1942).
J. H. Humier, J. A. Bearden, and C. H. Shaw, *Phys. Rev.* **58**, 537 (1940).
F. K. Richtmyer and R. D. Richtmyer, *Phys. Rev.* **34**, 574 (1929).
J. W. Dumond and A. Hoyt, *Phys. Rev.* **36**, 799 (1930).
F. K. Richtmyer and L. S. Taylor, *Phys. Rev.* **36**, 1044 (1930).
F. R. Horish and F. K. Richtyer, *Phys. Rev.* **44**, 955 (1933).
Mrs. A. W. Pearsall, *Phys. Rev.* **46**, 694 (1934).
M. Valadares, *La Ricerea Sci.* **18**, 270 (1940),
C. A. Randall and L. G. Parratt, *Phys. Rev.* 57, 766 (1940).
L. Pincherle, *Phys. Rev.* **61**, 225 (1942).
D. Coster, *Phil. Mag.* **44**, 546 (1922).
E. Bäcklin, *Zeits. f. Physik* **27**, 30 (1924).
J. W. Dumond and A. Hoyt., *Phys. Rev.* **36**, 799 (1930).
D. Coster and W. J. Thijssen, *Zeits f. Physik* **24**, 686 (1933).
D. Coster, H. H. Kuipers and W. J. Huizinga, *Physika* **2**, 870 (1935).
L. G. Parratt, *Phys. Rev.* **49**, 132 (1936).
Phys. Rev. **49**, 502 (1936).
M. A. Dauvillier, *C. R.* **177**, 167 (1923).
D. Coster and M. J. Druyvesteyn, *Zeits. f. Physik* **40**, 765 (1927).
F. R. Hirsh and F. R. Richtmyer, *Phys. Rev.* **44**, 955 (1933).
36. L. Salgusiro and M. H. Blanc De Sausa, *Portugal Phys.*, **3**, 95-9 (1959).
37. E. E. Vainshtein, M. N. Bril and I. B. Staryi, *Dokl. Acad. Nauk, S. S. S. R.*, **117**, 597-600 (1957).
38. E. Vainshtein and Yu. N. Vasilev, *Dokl. Acad. Nauk, S. S. S. R.*, **114**, 741-4 (1957)
39. J. Gomes Ferreira, *C. R. Acad. Paris*, **241**, 1929-32 (1955).
40. M. A. Dauvillier, *C. R.*, **177**, 167 (1923).
41. D. Coster and M. J. Druyvesteyn, *Zeits F. Physik*, **40**, 765 (1927).
42. F. R. Hirsh Jr. and F. K. Richtmyer, *Phys. Rev.*, **44**, 955 (1933).
43. H. Herglotz, *Accad Wissla*, **162**, 235-52 (1953).
44. M. J. Druyvesteyn, *Zeit. F. Phys.*, **43**, 711 (1927).
45. K. Tsutsumi, *J. Phys. Soc. Japan*, **14**, 1696-1704 (1959).
46. G. Wentzel, *Ann. d. Physik*, **66**, 437 (1921); *Zeit. F. Physih*, **31**, 445 (1925).
47. M. J. Druyvesteyn, *Zeit F. Physik*, **43**, 707 (1927).
48. B. B. Ray, *Phil. Mag.*, **8**, 772 (1929).
49. R. M. Langer, *Phys. Rev.*, **37**, 457 (1931).
50. H. C. Wolfe, *Phys. Rev.*, **43**, 221 (1933).
51. M. Sawada, *Kyoto Coll. Sci. Mens.*, **15**, 43 (1932).
52. E. H. Kennard and E. G. Ramberg, *Phys. Rev.* **46**, 1040 (1934).

53. F. K. Richtmyer and E. G. Ramberg, *Phys. Rev.*, **51**, 925, (1937).
54. D. J. Candlin, *Proc. Phys. Soc*, **63A**, 322 (1955).
55. R. D. Richtmyer, *Phys. Rev.*, **49**. 1 (1936).
56. F. K. Richtmyer, *J. Frankl. Inst.*, 203, 325 (1927).
57. Idei., S., *Sci. Rep. Tohoku University*, 19, 551, (1930).
58. E. G. Ramberg, *Phys. Rev.*, **45**, 389 (1934).
59. (1) Deodhar, G. B and Abidi, S. T. H. *Naturwiss.*, **47**, **319**, (196).
(2) Deodhar, G.B. and Padalia, B. D., *J. Sci. Industr. Res. India*, Vol. **21B**, 4-7 (1962).
(3) Deodhar, G. B. and Padalia. B. D., *Z. Physik* (Germany), Vol. 168 (1962) page 343-48.
60. F. Bloch, *Phys. Rev*, **48**, 187 (1935).
61. T. I. Kakuschadse, *Ann. d. Phys*, **3**, 352-9 (1959).
62. Masao Sawada, Kenjiro Tsutsumi, Toshio Shiraiwa, *J. Phys. Soc. Japan*, 8, 647 (1955).
63. Coster and Kronig. *Physica*, **2**, 13 (1935)
64. Auger, P., *C. R.*, **180**, 65 (1925).
65. Hirsh, F. R. Jr., *Phys. Rev*, **50**, 593 (1936).
66. F. R. Hirsh Jr., *Phys. Rev.*, **57**, 662 (1940).
67. S. M. Karlnak and S. B. Nyzlnyk *Ukraiyin Fiz. Zh.*, **2**, 333-7 (1957).
68. H. Hulubei, *C. R.* **224**, 770 (1947).
69. D. Coster, *Phil. Mag.*, **44**, 545 1922).
70. P. Sakellaridis, *J. de Phys. et la Rad.* **16**, 422 (1955).

SPECTRA OF DIATOMIC MOLECULES COMPOSED OF I GROUP ELEMENTS

By

K. MAJUMDAR

Allahabad

[Received on 7th April, 1962]

A perusal of the existing spectroscopic literature reveals that our knowledge regarding the diatomic molecules, which are composed of atoms both belonging to I group of the periodic table, is still inadequate. If we leave aside H-since hydrides might better be considered separately—and Fr (87), a rare element, there are eight other elements in this group, five belonging to Ia subgroup and three belonging to Ib sub-group. These elements combining with one another could form altogether thirty-six diatomic molecules. So far only seventeen of these molecules have been spectroscopically established, twelve of which arise from combinations among the elements of Ia sub-group and five from combinations among elements of Ib sub-group. It has not yet been possible to record the spectra of the remaining four molecules of such combinations, i. e., those which could be formed out of atoms belonging to the same sub-group, three of Ia sub-group and AuAg of Ib sub-group. None of the fifteen molecules that could be formed from a combination of an atom of Ib sub-group with an atom of Ib sub-group has been spectroscopically observed. These evidently need full investigation. It may be mentioned here that while Ia-Ia sub-group molecules were known much earlier, investigation regarding Ib-Ib sub-group molecules were taken up only recently.

The work carried out on these molecules has been mainly confined to the study of their electronic spectra and the determination of their vibrational constants. The spectra have been observed mostly in absorption in the visible and ultraviolet regions. The dissociation energies have been calculated in most of the cases by using ω_e and $\omega_e x_e$ values. Excepting for the molecules Li_2, Na_2 and K_2, no rotational analyses have been made. Ruamps has, however, reported a rotational structure in the 0,2 band of system A of Au_2 molecule. Practically no infrared spectra have been observed for these molecules. A brief account of the results obtained regarding the different molecules of the two sub-groups have been shown in tables I and II. These indicate the various electronic states observed together with their T_e and ω_e values.

One of the reasons why the spectra of Ib-Ib sub-group molecules could not be observed earlier is the difficulty of their formation at lower temperatures. With the comparatively high melting and boiling points of elements of Ib sub-group, the necessary amount of vapour could not be obtained at the usual temperatures of the experiment. The recent workers have employed graphite tube resistance furnace to obtain very high temperatures and thereby have been successfull in recording the spectra of Ib-Ib sub-group molecules either in absorption or in thermal emission. Ruamps and Kleeman and others employed King type of furnace, while workers in this laboratory employed the furnace originally used by Saha and his co-workers for work on thermal ionisation and absorption spectra. This furnace essentially consists of a tube of pure graphite held in a horizontal position, which is heated by a very heavy alternating current obtained from a 10 kw step-

down transformer. The furnace tube is kept inside a chamber which consists of three parts, separable from one another, the top, the middle portion and the bottom. Each portion is double walled and is cooled by passage of water through it. The chamber is evacuated and can be filled with any gas whenever necessary. Temperatures as high as 2500°C could be obtained with this furnace. The source of continuum used for absorption work in the visible region was either a 200 watts pointolite lamp or a ribbon filament lamp with intensity control or a 200 watt straight filament lamp. For the ultraviolet region, a vitreosil quartz hydrogen lamp, supplied by Messrs. Thermal Syndicate London, was used.

I_b-I_b Group

	Cu				Ag				Au			
	State	T_e	ω_e	Des.	State	T_e	ω_e	Des.	State	T_e	ω_e	Des.
Cu									D	23672·0	182	D→X
									C	22173	231	C→X
	B	21747·5	245·8	B→X					B	20661·4	257	B→X
	A	20396·0	194·9	A→X	A	25851·6	178·5	A→X	A	20220	$\Delta G_{\frac{1}{2}}$ = 195·7	A→X
	X	0	266·1		X	0	231·8		X	0	250	
Ag					E	40159·1	146·08	E↔X				
					D	39023·7	166·7	D↔X				
					C	37626·9	172·9	C↔X				
					B	35827·3	151·3	B↔X				
					A	22996·4	154·6	A↔X				
					X	0	192·4					
Au									B	25686·0	179·85	B→X
									A	19668·1	142·3	A→X
									X	0	190·9	

Plate I

Ia - Ia Group

	Li	Na	K	Rb	Cs
Li	D_0 = 1.03 ev Reaction C $^1\Sigma_u^+$ 30553.5 231.5 C↔X B $^1\pi_u$ 20431.4 267.69 B↔X A $^1\Sigma_u^+$ 8.048 255.45 A↔X X $^1\Sigma_g^+$ 0 351.43		B (17578) (569) B↔X X $^1\Sigma$ 0 (607)	B (12562) (681) B↔X X $^1\Sigma$ 0 (655)	B (11477) (771) B↔X X $^1\Sigma^+$ 0 (767)
Na		D_0 = 0.75 ev Reaction E 33205.1 109.5 E↔X D $^1\Pi$ 31934.1 112 D↔X C $^1\Sigma_u^+$ 21342.1 119.33 C↔X B $^1\pi_u$ 20329.2 123.79 B↔X A $^1\Sigma_u^+$ 16680.4 147.6 A↔X X $^1\Sigma_g^+$ 0 159.23	D_0 = 0.62 ev E $^1\Sigma^+$ 25228 95.85 E↔X D $^1\Pi$ 20090.6 82.17 D↔X C $^1\pi$ 16791.4 77.68 C↔X A $^1\Sigma^+$ 12439.7 77.85 A↔X X $^1\Sigma^+$ 0 125.29	D_0 = (0.57) ev A $^1\pi$ 11686.8 63.49 A↔X X $^1\Sigma^+$ 0 106.44	C (29870) (62) C↔X B (12250) (66) B↔X X $^1\Sigma^+$ 0 (98)
K			D_0 = 0.514 ev Reaction G 28091 64.9 G↔X F 27571 62.2 F↔X E 26495 63.09 E↔X D ($^1\pi_u$) 24627.7 61.68 D↔X C ($^1\Sigma_u^+$) 22970.0 60.60 C↔X B $^1\pi_u$ 15378.8 75.00 B↔X A $^1\Sigma_u^+$ 11682.6 69.69 A↔X X $^1\Sigma_g^+$ 0 93.64		
Rb				D_0 = 0.49 ev C 32771.5 48.62 C↔X B 20885.1 56.46 B↔X A $^1\pi_u$ 14612.6 48.05 A↔X X $^1\Sigma_g^+$ 0 57.38	A 15747.2 58.44 A↔X X $^1\Sigma^+$ 0 49.41
Cs					D_0^0 = 0.45 ev D 16775.8 27.34 D↔X C 14061.0 29.58 C↔X B ($^1\pi_u$) 13043.7 31.23 B↔X A ($^1\Sigma_u^+$) ? ? A↔X X $^1\Sigma_g^+$ 0 41.99

Plate II

Below is given a brief account of the spectra of Ib-Ib sub-group molecules. The spectra of Ia-Ia sub-group molecules have been well reported in standard books and journals and are not therefore described here.

Cu_2—Singh, N. L. (1946) found some bands in emission in the red region in the flame spectrum of copper and ascribed them to Cu_2 molecule. He proposed a vibrational analysis for the same the value of the ground state vibrational frequency being 160 cm^{-1}. More recently Kleman and Lindkvist (1954) and Ruamps (1954) investigated the spectra of Cu_2 molecule. Two systems of bands were observed in the visible region with a common ground state vibrational frequency of value 266.1 cm^{-1}. The analyses have been substanciated by the presence of isotope shift of right order of magnitude. Ruamps re-

ported some bands also in the ultraviolet region λλ 2900-2300. These, however, have not been analysed. The general feature of the bands shows well marked sequences and sharp heads. The molecule appears to be quite stable and the energy of dissociation has been computed to be 2.1 e. V. No work in absorption has so far been reported.

Ag_2—Ruamps (1954) was the first to report the band system due to Ag_2 molecule. He observed them in thermal emission by heating silver in a King's furnace. The bands occur in the region λλ 5050—4120 and were classified into two systems. The value of the ground state vibrational frequency was found to be 190 cm^{-1}. M. M. Joshi (1958) made a more complete study of these bands. He photographed them both in thermal emission and in absorption and obtained a large number of new bands in absorption in the ultraviolet region λλ 2940—2725. Fragments of one more system were also obtained nearabout λ 2600. A close examination of the emission spectrum revealed existence of self reversal of the bands, indicating thereby that the lower electronic state involved is the ground state. Predissociation has been noticed in the visible system. Vibrational isotope shift has also been found, which confirms the identity of the molecule. Very recently Ruamps has observed more band systems for the Ag_2 molecule in the ultraviolet region. The heat of dissociation has been found to be 1.8 e.V.

Au_2—Kleman, Lindkvist and Selin (1954) reported the presence of discrete bands in thermal emission in the visible region from gold heated in a King's furnace and analysed them. The vibrational isotope shift could not possibly be observed in this case but the remarkable similarity in the general structure of these bands with those of the molecules Cu_2 and Ag_2 led them to infer that these are due to Au_2 molecule. Ruamps (1960) observed three more band systems of Au_2 molecule in the ultraviolet region nearabout λ 2210, λ 2130, and λ 2090 respectively, which however have not been analysed. A rotational structure of the 0,2 band of system A has been reported by Ruamps. The heat of dissociation of this molecule has been found to be 2.7 e.v.

CuAg—This molecule has recently beea established spectroscopically in this laboratory. Details of the investigation will be published elsewhere in a short time. (K. C. Joshi and K. Majumdar). A large number of bands were observed in theremission in the region λλ 4090-3790 when a mixture of copper and silver were strongly heated in the vacuum graphite tube furnace. The bands are quite sharp and well marked sequences occur. It was found that careful manipulation of experimental conditions is necessary for observation of the bands, as their production is very susceptible to changes in the temperature of the furnace and the pressure of nitrogen introduced in it. The bands were best developed at a temperature of about 1800°C and with a pressure of nitrogen of 60 cm. of murcury. No vibrational isotope effect was observed but on a comparison of the vibrational constants and the general features of these bands with those of other molecules of this group, one can very well conclude that the emitter is CuAg molecule.

CuAu—When a copper-gold alloy was heated in a King's furnace a large number of emission bands in the visible region were observed by

Ruamps (1954). He classified these into four systems and ascribed them to the molecule CuAu. The ground state vibrational frequency was found to be 250 cm^{-1}. The bands are sharp and they show well marked sequences. Vibrational isotope shift has also been observed.

AgAu—The spectrum of this molecule has not yet been reported.

DISCUSSIONS

The common characteristics of the band spectra of Ib-Ib diatomic molecules are well marked sequences and the occurance of comparatively large number of bands in the individual systems. Besides, the bands of these molecules are all degraded to the red and their general appearance is very similar. The vibrational analyses of the bands studied have been substantiated by the presence of isotope shift of right order of magnitude in all cases except for the molecule CuAg where no such shift was observed and for Au_2 where it is not expected.

The ground state vibrational frequencies of the molecules Cu_2, Ag_2 and Au_2 have been found to be 266.1 cm^{-1}, 192.4 cm^{-1} and 190.7 cm^{-1} respectively. These values require a closer scrutiny. As far as Cu_2 and Ag_2 are concerned the ω_e'' values seem to be reasonably correct. Since the spectrum of Ag_2 has been investigated both in emission and in absorption it is almost certain that the lowest state involved is the ground state and the value of 192.4 cm^{-1} which is substantiated by the observed isotope shift is in all probability the correct value of ω_e''. Regarding Cu_2 molecule, simple consideration of the masses of the vibrating nuclei would require that its vibrational frequency should be higher than that of Ag_2. The observed value 266.1 cm^{-1} for ω''_e which is also confirmed by the presence of isotope shift appears to be correctly determined. Similar considerations for Au_2 molecule would require a lower frequency for the ground state than the obserbed one. Since Au_2 molecule is much heavier than Ag_2 it is not expected that the value of its ground state frequency would be of the same order of magnitude as that of Ag_2 molecule.

Further, if we calculate the heat of dissociation by using the relation $D_o = \omega_e''^2/4\omega_e'' x_e''$, the respective values for the molecules Cu_2, Ag_2 and Au_2 come out to be 2.1 e. v., 1.8 e. v. and 2.7 e. v. respectively. These values suggest that the molecule Au_2 is the most stable out of the three, which is doubtful. It, therefore, appears that the value of ω_e'' viz. 190.7^{-1}, has not been properly determined for Au_2. In the investigation with gold the general features of the bands no doubt resemble those of the molecules Cu_2 and Ag_2 but in the absence of isotope effect and of absorption data one cannot feel certain of the emitter of the bands and of the value of the vibrational frequency of the ground state. A more complete information is expected to be obtained in this respect when the absorption spectrum is studied.

As regards CuAg molecule although no observations of the absorption spectrum has been made, other considerations hold that the value of ω_e'' determined is not incorrect. In a paper published in 1954 Majumdar and Varshni studied the relation of the vibration frequencies of the diatomic molecules XY with the vibration frequencies of the diatomic molecules XX and YY where X and Y belong to the same group of the periodic table. It was shown that if ω_e'' .^{65} for XY be represented by ϕ (XY), etc. then

$$\phi(XY) = \tfrac{1}{2}[\phi(XX) + \phi(YY)]$$

The relation was found to hold good for a large number of molecules. On applying it to CuAg molecule the value of ω_e'' comes out to be 228 cm^{-1}. The observed value of 231.8 cm^{-1} for ground state frequency being in close agreement to this, one is reasonably certain of the same. However, absorption data for this molecule are also necessary to confirm the results. It may be mentioned here that the above relation does not hold good for the molecule CuAu. This shows that ω_e'' has not been determined properly for either Au_2 or CuAu. It thus appears that further studies regarding these molecules are necessary for more complete information.

The author is thankful to Dr. M. M. Joshi and Dr. K. C. Joshi for help rendered in the preparation of this paper and to Mr. R. Yamdagni for making the charts.

REFERENCES

G. Herzberg, Molecular Spectra and Molecular Structure, Vol. I, 1950.

B. Rosen, Tables De Constantes et donnees numeriques, Constantes Selectionne'es, Donnees Spectrocopiques Concernant les Molecules diatomiques, 1951.

R. W. B. Pearse and A. G. Gaydon, Indentification of Molecular Spectra, 1950.

N. L. Singh, *Proc. Ind. Acad.* 25 A, I (1946).

B. Kleman, S. Lindkvist and L. E. Selin, *Ark. Fys.*, 8, paper 50, 505 (1951).

J. Ruamps, C. *R. Acad. Sci. (Paris)* 238, 1481 (1954).

J. Ruamps, *C. R. Acad. Sci. Paris)* 238 1489 (1954).

J. Ruamps, C. *R. Acad Sci (Paris)* 239, 1200 (1954).

B. Kleman, and S. Lindkvist, *Ark. Fys.*, 8, paper 32, 333 (1954).

B. Kleman and S. Lindkvist, *Ark Fys.* 9, paper 26, 385 (1955).

M. M. Joshi, D. Phil. Thesis, University of Allahabad, (1958).

K. C. Joshi and K. Majumdar, *Proc. Phys. Soc.*, (Under publication)

Majumdar and Varshni, *Ind. Journ. Phys.* 28, 209 (1954).

Published by Dr. R. K. Saksena, for the National Academy of Sciences, India, Allahabad
and Printed by M. Sarwat Husain at The Mission Press, Allahabad

Secretary, Editorial Board—Dr. R. K. Saksena